University of Alberta

Application of Advanced Oxidation Processes for Treatment of Naphthenic Acids in Oil Sands Process Water

by

Atefeh Afzal

A thesis submitted to the Faculty of Graduate Studies and Research
in partial fulfillment of the requirements for the degree of

Doctor of Philosophy
in
Environmental Engineering

Department of Civil and Environmental Engineering

©Atefeh Afzal
Fall 2013
Edmonton, Alberta

DEDICATION

This work is dedicated to my lovely mother, Zohreh Izadi, who had a great influence on my life, and taught me everything with her hard work, and was always there for me when I needed her. She encouraged me to start this education, but unfortunately is not here now to see my achievement.

ABSTRACT

The large volume of oil sands process-affected water (OSPW) produced by the oil sands industries in Northern Alberta, Canada, is an environmental concern. The toxicity of OSPW has been attributed to a complex mixture of naturally occurring acids, including naphthenic acids (NAs). NAs are a broad range of alicyclic and aliphatic compounds that are persistent in the environment. This work focused on the application of advanced oxidation processes (AOPs): UV/H_2O_2 and O_3/H_2O_2 for degradation of model NA compounds and OSPW NAs. Cyclohexanoic acid (CHA) was selected as a simple model naphthenic acid, and its oxidation and byproduct formation in the UV/H_2O_2 and ozonation processes was studied. The results indicated that in the UV/H_2O_2 process, the pH had no significant effect on the degradation, nor on the formation and degradation of byproducts in ultrapure water. A real OSPW matrix had a significant impact by decreasing the CHA degradation rate up to 82% relative to that in ultrapure water. Relative rate measurements using binary mixtures of model NA compounds confirmed that reactivity favoured compounds with more carbons, and also favoured NAs with one saturated ring, relative to the corresponding linear NA. However, for model compound with three rings, no increased reactivity was observed relative to mono-cyclic NA. The mechanism of ozonation of CHA was different at pH 3 and pH 9. At pH 9, oxo-CHA and hydroxy-CHA were both detected by LC-MS/MS, confirming the hydroxyl radical (•OH) pathway in which superoxide CHA radical is a possible intermediate. The results of the O_3/H_2O_2 advanced oxidation process of OSPW NAs showed that in a semi-batch system, approximately 90% of extractable organic acids of OSPW were removed using O_3/H_2O_2 process with 85 mg/L of O_3 and O_3 to H_2O_2 ratio of 0.3.

ACKNOWLEDGMENT

TABLE OF CONTENT

LIST OF TABLES

LIST OF FIGURES

LIST OF SYMBOLS

AOP	advanced oxidation process
COD	chemical oxygen demand
DCM	dichloremethane
DOC	dissolved organic carbon
EPL	end pit lake
EOA	extractable organic acid
ESI-MS	electrospray ionization-mass spectrometry
FT-IR	Fourier transform infrared
GC-MS	gas chromatography-mass spectrometry
H	hydrogen
HPLC	high-performance liquid chromatography
H_2O_2	hydrogen peroxide
MW	molecular weight
NAs	naphthenic acids
O_3	ozone
ODF	ozone-demand free
•OH	hydroxyl radical
OSPW	oil sands process-affected water
PAHs	polycyclic aromatic hydrocarbons
pK_a	acid dissociation constant
TBA	*tert*-butyl alcohol

TDS	total dissolved solids
TOC	total organic carbon
UPLC-HRMS	ultra-pressure liquid chromatography-high resolution mass spectrometry
UV	ultraviolet light
VUV	vacuum-ultraviolet
West in-Pit	WIP

1 GENERAL INTRODUCTION

1.1 Background

The oil sands in northern Alberta, Canada, represent one of the world largest oil deposits that reserves 174 billion barrels of bitumen (Alberta Energy and Utilities Board, 2005). Oil sands is a mixture of 6-16 %wt bitumen, 80-87 %wt mineral solids (in the form of sand or clay, and silt), and 1-7 %wt water (Liu et al., 2005). Bitumen is an unconventional fossil fuel which is more costly to process and recover than the conventional oil and gas (Allen, 2008). In the past decades, due to the low price of crude oil, and high costs of extraction, the oil sands development was not economically attractive. However, because of an increased demand for oil throughout the world and increasing price, the oil sands industry has grown rapidly.

Bitumen is either extracted from the sand after surface-mining or brought to the surface by *in situ* methods such as steam-assisted gravity drainage (Smith et al., 2008). Both techniques consume large volumes of water; on average three barrels of water to produce one barrel of synthetic crude oil (Syncrude Canada Limited, 2005; Suncor Energy Incorporated, 2005; Shell Canada, 2005). In 2006, it was approved to divert 370 million m^3 of the fresh water per year from the Athabasca River for oil sands mining projects (National Energy Board, 2006). Most of the water is consumed in the hot water extraction process in which caustic hot water is used to separate bitumen from the sand and clay. The resulting oil sand process-affected water (OSPW) is slightly alkaline,

1

highly saline, and acutely toxic to aquatic organisms due to the high concentrations of organic compounds leaching from bitumen during the extraction process (Leung et al., 2003). Oil sand producers store OSPW and tailings on-site (Rogers et al., 2002; Clemente and Fedorak, 2005; Quagraine et al., 2005) which leads to the construction of more than 70 km^2 of tailing ponds (Dominski, 2007). As a result, an estimated one billion m^3 of OSPW will be accumulated in the Athabasca oil sands region by 2025 (Herman et al., 1994). This can be compared with approximately 150 million m^3 of wastewater that a wastewater treatment plant can treat per year (for a city with population of 1.5 million).

1.2 Characteristics of OSPW

The characteristics of OSPW depend on several parameters including extraction process, ore quality, source, and age (Kannel and Gan, 2012). Typically, the pH of OSPW is between 7.8 and 8.5 (Mikula et al., 1996) and OSPW is a relatively hard water with calcium and magnesium concentrations in the range of 15-25 mg/L and 5-10 mg/L, respectively (Allen, 2008). The total dissolved solids (TDS) in OSPW are between 2000 to 2500 mg/L and are dominated by bicarbonate (~800–1000 mg/L), sodium (~500 to 700 mg/L), chloride (~75 to 550 mg/L), and sulphate (~200 to 300 mg/L) ions (Allen, 2008). The concentration of ammonia in OSPW is about 3 mg/L which is higher than in the Athabasca River (0.6 mg/L) (MacKinnon and Boerger, 1986). The organic compounds detected in tailings pond water include bitumen, benzene, toluene, creosols, phenols, phthalates, asphaltenes, polycyclic aromatic hydrocarbons (PAHs), humic and fulvic

2

acids, and naphthenic acids (NAs) (Madill et al., 2001; Rogers et al., 2002; Allen, 2008). Organic and inorganic chemistry of OSPW from different oil sand facilities has been stated in an extensive review by Allen (2008). As an specific recently published example (Pourrezaei et al., 2011), the selected characteristics of OSPW collected in October 2009 from the West in-Pit (WIP) tailing pond located at the Syncrude Canada Ltd. in Fort McMurray, Alberta are shown in Table 1-1.

Table 1-1. Characteristics of OSPW (adapted from Pourrezaei et al., 2011)

Parameter	Average Value
TOC	51 mg/L
COD	240 mg/L
NAs	23.6 mg/L
Oxidized-NAs	31.6 mg/L
Extractable Organic Acids	70.0 mg/L
pH	8.5
Turbidity	180 NTU
Alkalinity	630 mg/L
Conductivity	3750 μS/cm
Ammonium	22 mg/L
Chloride	515 mg/L
Sulfate	513 mg/L
Sodium	827 mg/L
Aluminum	8.5 mg/L
Iron	3.3 mg/L
Barium	0.35 mg/L
Vanadium	0.018 mg/L

1.3 Naphthenic acids

Naphthenic acids are natural constituents of petroleum (Seifert et al., 1969; Fan, 1991) and bitumen (Headley and McMartin, 2004). These organic acids are solubilized and concentrated in tailings during the extraction processes in the oil sand industry. In Athabasca oil sands, approximately 2 % (by weight) of the total bitumen content are NAs. These acids may enter surface waters naturally through the groundwater mixing and erosion of oil deposits of riverbank (Headley and McMartin, 2004). The concentration of NAs in northern Alberta rivers is normally less than 100 μg/L (Ross et al., 2012); however, the reported range of the extractable organic acids (EOA) concentration in tailings ponds is 40-125 mg/L [as measured by the Fourier transform infrared (FT-IR) spectroscopy] (Allen, 2008).

1.3.1 Chemical properties of NAs

NAs comprise a complex mixture of alicyclic and cycloaliphatic carboxylic acids that may have alkyl substitution. The general chemical formula of NAs is $C_nH_{2n+Z}O_2$ where n indicates the carbon number and Z is zero or a negative even integer number that represents the number of hydrogen (H) atoms that are lost from ring formation (e.g., Z = 0, no rings; Z = -2, one ring; Z = -4, two rings) (Rogers et al., 2002). Molecular weight (MW) of NAs changes by 2 mass units (H_2) between Z series and by 14 mass units (CH_2) between n series. Some hypothetical examples of NAs structure identified in OSPW are shown in Figure 1-1-a (West et al., 2013). Headley et al. (2011) reported that OSPW

4

contain N- and S-species according to the results for high resolution MS. Thus, the broader acid extractable organics with other functional groups, nitrogen (N) and sulphur (S) atoms, along with unsaturated groups can be described in Figure 1-1-b (Mohamed et al., 2013). Ring structures may not be fully saturated in the figure.
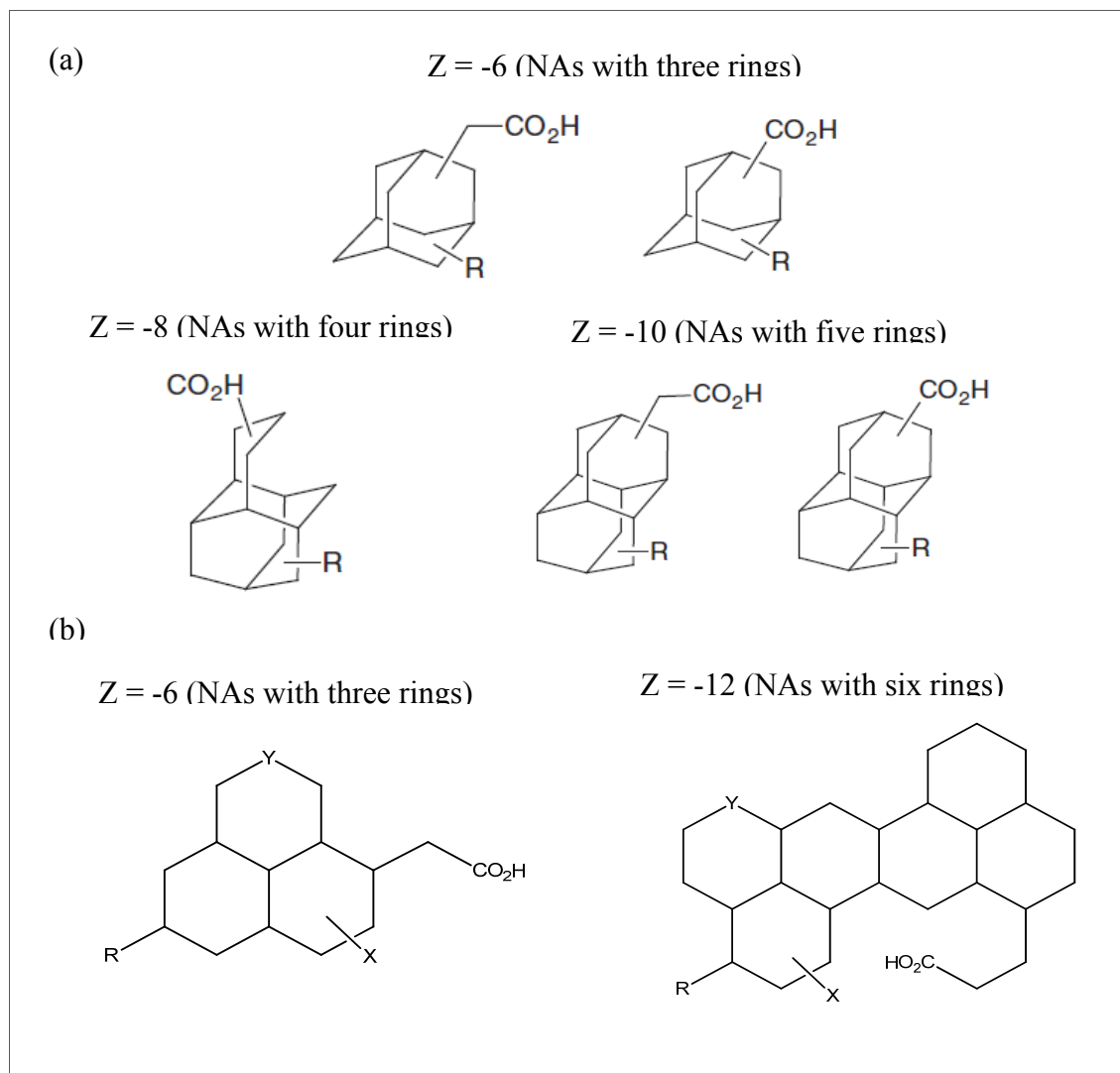
Figure 1-1. (a): Sample of chemical structure of NAs (adapted from West et al., 2013); (b): sample structure of naphthenic acid fraction components in OSPW. R = alkyl group, X = COOH, R, OH, SOx, NOx, SH and Y = C, S, N (adapted from Mohamed et al., 2013).

NAs are non-volatile, chemically stable compounds that work similar to surfactants during the extraction process (Headley and McMartin, 2004). With increasing the MW, the non-polarity and non-volatility of NAs increases. This results in different chemical, toxicological, and physical properties of individual NAs (Headley et al., 2002; Clemente et al., 2003).

The solubility of NAs in water is pH dependent; however, they are completely soluble in organic solvents (Quagraine et al., 2005). Because of the alkaline pH of OSPW, in the tailings ponds NAs exist in the form of water soluble salts. However, based on the structure, the water solubility of NAs varies from soluble in the case of the low MW NAs (fewer cyclic rings) to insoluble (high MW or highly cyclic) (Quagraine et al., 2005). The acid dissociation constant of NAs is in the range of 10^{-5} to 10^{-6} (pK_a = 5-6) which makes them weaker acids compared to low MW carboxylic acids such as acetic acid (pK_a = 4.7); however, their dissociation constants are close to those of fatty acids (Kanicky et al., 2000).

1.3.2 Toxicity of NAs

NAs are quite soluble in slightly alkaline waters. As such, dissolved naphthenates present in waters may impose a toxic hazard to aquatic organisms (Dokholyan and Magomedov, 1983). It was shown in different reports that NAs had inhibitory or toxic effects on a variety of organisms including fish, plants, zooplankton, rats, and luminescent bacteria (Clemente and Fedorak, 2005). The Microtox bioassay performed

by Herman et al. (1994) showed that sodium salts of NAs (100 mg/L) are acutely toxic to micro-organisms with an EC50 value (the percentage required to produce a 50% loss of bioluminescence of the organism) of 30% (v/v).

Rogers et al. (2002) studied the effect of NAs toxicity on rats. The authors believed that the liver was the primary affected organ. The latest study by Garcia-Garcia et al. (2011) showed that the organic fraction of OSPW and commercial NAs caused immunotoxic effects that may impair the ability of an exposed host to defend against infectious disease. The authors also concluded that commercial NAs should not be used as a direct surrogate for the immunotoxic chemical species in OSPW.

For monocarboxyl NA-like surrogates, toxicity increased with increasing MW; however, with adding a second carboxylic acid moiety, the toxicity was significantly reduced (with similar MW). In higher molecular weight NAs, the acute toxicity of OSPW decreases as the relative abundance of smaller NAs (C number 13-16) decreases (Holowenko et al., 2002). As reported by Headley et al. (2004), the toxicity of NAs is mostly associated with their surfactant-like characteristics.

1.3.3 Analysis of NAs

There are several analytical techniques for the analysis of NAs in aqueous solutions that were explained in detail by Headley at al. (2004) and Clemete and Fedorak (2005). These methods mainly include gas chromatography-mass spectrometry (GC-MS), negative ion electrospray ionization-mass spectrometry (ESI-MS), and high performance

liquid chromatography (HPLC). All these methods give an approximate response that can be corresponded to NAs concentration, if there are no interferences. However, because of the complexity of NAs, at present there is no specific method for detailed identification or quantification of individual acids in the mixture. The current ultra-pressure liquid chromatography high resolution mass spectrometry (UPLC-HRMS) analytical method treat NAs as a group or sub-groups based on n and Z numbers. In this method, the structures of components in a complex mixture can be presented in a meaningful way which sorts the n number along the X-axis and the Z number along the Y-axis in a 3D plot in which the Z-axis represents the intensity.

The former standard method for NAs quantification in OSPW was FT-IR spectroscopy. In this method, the organic fraction in OSPW is extracted by dichloremethane (DCM) and the concentrated sample is then analyzed by measuring the absorbance of the dimeric form of carboxylic groups at 1743 and 1706 cm^{-1} (Scott et al., 2008). The FT-IR method was believed to determine the NAs concentration; however, recent studies have shown that along with NAs, other compounds with a carboxylate group such as oxidized NAs can also be measured and the reported number is an overestimated concentration for NAs. Therefore, throughout the thesis, EOA (extractable organic acids) is used to describe the results obtained from the FT-IR analysis.

1.4 Options of OSPW treatment

As explained earlier, OSPW is currently accumulated in the tailings ponds near the oil sands sites, and the volume of OSPW is continuously increasing (Mohamed et al., 2011). There is a concern of contaminants leaching onto Athabasca River due to the close proximity of tailings ponds to the river which may endanger the aquatic environment (Allen, 2008; Grewer et al., 2010). In the future, all oil sands companies have to remediate OSPW for a safe discharge into the environment because all the lands used for the oil sands operations, including tailings ponds, should be eventually reclaimed (Allen, 2008).

The quality of the treated OSPW should meet the standard guidelines in order to discharge the treated water to the environment; therefore, the removal of the organic compounds including NAs should be considered as the highest treatment priority (Allen, 2008). In order to remove all the contaminants such as dissolved and suspended solids, dissolved organic compounds, and insoluble hydrocarbons, a series of sequential treatment processes is needed (Zubot, 2010). The applicability of various treatment options for OSPW remediation has been investigated. These methods includeed coagulation/flocculation/sedimentation (CFS), adsorption, biological treatment, membrane filtration, advanced oxidation, and constructed wetlands (Herman et al., 1994; Knight et al., 1999; Madill et al., 2001; Peng et al., 2004; Quagraine et al., 2005; Del Rio et al., 2006; Scott et al., 2008; Headley et al., 2010; Martin et al., 2010; Gamal El-Din et al., 2011; Liang et al., 2011; Mohamed et al., 2011; Pourrezaei et al., 2011; Golby et al.,

2012; Small et al., 2012; Zubot et al., 2012).Yet, there is significant work to be done in order to develop feasible and effective treatment technologies for OSPW remediation.

Even though natural microbial remediation is one of the options for OSPW treatment, it is still not a practical option because of its very low degradation rate and also inadequate removal of the organic compounds (Quagraine et al., 2005; Allen, 2008). It was shown that natural biodegradation decreased the NAs concentration in the tailings ponds by 16% per year during the first five years, and insignificant natural biodegradation was observed in the following years (Allen, 2008).

A treatment option for the OSPW remediation is biological process that has been investigated for the oil refinery produced waters (Del Rio et al., 2006; Allen, 2008; Golby et al., 2012). Although microbial degradation processes are low cost treatments compared to other processes, they are not considered as an effective remediation methods which can achieve complete biodegradation of NAs (Quagraine et al., 2005; Headley et al., 2010). Cyclic, branched and large MW NAs are more recalcitrant to biodegradation (Smith et al., 2008); thus, biological treatments should be considered as a treatment following the removal of recalcitrant NAs (Martin et al., 2010).

Effective removal of inorganic and organic compounds from oil refinery produced waters using membrane filtration was studied by several researchers (Zaidi et al., 1992; Peng et al., 2004; Kim et al., 2011). Nanofiltration was shown to be capable of removing 95% of NAs, and high removal of anions (sulphate, chloride, and bicarbonate) and cations (calcium, sodium, and magnesium) from OSPW (Peng et al., 2004) was also

observed. Cost and durability of the process as well as membrane fouling have been considered as the main concerns affecting the large-scale membrane applications (Farnand and Krug, 1989; Allen, 2008). Currently, there is no viable practical and economical technology to treat the huge amount of generated OSPW on the industrial scale (Quagraine et al., 2005).

A long-term proposed solution for reclamation of toxic tailings involves human-made water bodies termed end pit lake (EPL) (The Royal Society of Canada, 2010). In this method, OSPW along with soft tailings placed at the bottom of a pit which then capped with ground and surface water from surrounding reclaimed landscapes. EPLs will be expected to develop into a biologically active community with a self-sustaining aquatic ecosystem. To date, approximately 27 EPLs have been planned within the Athabasca oil sands region. The ultimate intention is that the EPLs will connect with the regional aquatic ecosystem and thus discharge into the environment. However, there are some risks associated with the EPLs. Potentially toxic chemicals may enter the EPL through the soft tailings at the bottom of the EPL, or through surface runoff from disturbed lands. Seepage or discharge from tailings ponds could also introduce toxic chemicals into the EPL which may later build up in both the sediments and the cap water. Some concerns also have been raised regarding the physical, chemical, and biological processes that will occur while establishing EPLs (The Royal Society of Canada, 2010).

1.5   Ozonation and advanced oxidation Processes

Advanced oxidation processes (AOPs) have been studied extensively in water and wastewater treatment and have been found very effective for the removal of organic pollutants (Parsons, 2004). AOPs rely on the formation of reactive and short-lived oxidizing agents, such as hydroxyl radicals ($\bullet$OH). Some of the main advanced oxidation processes include ozonation at alkaline pH, photolysis of hydrogen peroxide (H_2O_2) using ultraviolet (UV) light at 254 nm (UV/H_2O_2), ozone (O_3)/H_2O_2, photolysis of ozone at 254 nm (UV/O_3), and UV/O_3/H_2O_2. The $\bullet$OH generated in all of these processes, is a powerful oxidizing agent that reacts with inorganic and organic substances. $\bullet$OH can abstract hydrogen atoms from almost any organic compound, add to alkenes or aromatic compounds and so on. However, the rates of reaction change from compound to compound (Prousek, 1996). The dissolved organic carbon in OSPW (other than NAs) may affect the decomposition of NAs as other constituents would compete for the $\bullet$OH. Additionally, the presence of high amount of inorganic anions in OSPW, such as chloride and carbonate/bicarbonate ions, could act as significant $\bullet$OH scavengers in OSPW, further slowing degradation of NAs.

The degradation of NAs using photolysis, ozonation, and AOPs has been investigated in a number of studies (McMartin et al., 2004; Scott et al., 2008; Headley et al., 2009; Drzewicz et al., 2010; Martin et al., 2010; El-Din et al., 2011; Liang et al., 2011; Perez-Estrada et al., 2011). NAs do not absorb light in the solar wavelength region; therefore, direct photolysis using both artificial and natural sunlight is not an effective

12

process for NA degradation. In experiments using natural water, the estimated half-life of *trans-* and *cis-* isomers of NAs exposed to ultraviolet (UV) light at 254 nm and solar light was in the range of tens of hours to thousands of hours, respectively. The presence of organic and inorganic constituents in natural water results in the indirect photolysis of NAs due to the possible formation of radicals (McMartin et al., 2004). It was shown that UV/H_2O_2 and vacuum-UV (VUV) are effective AOPs for the degradation of a model NA compound, cyclohexanoic acid (Drzewicz et al., 2010).

Ozonation of OSPW was investigated through a number of studies and has been shown to be a promising OSPW reclamation strategy (Scott et al., 2008; Martin et al., 2010; El-Din et al., 2011; Perez-Estrada et al., 2011). Ozonation experiments were performed in both batch and semi-batch systems. In a semi-batch method, ozone gas is directly bubbled into the solution, where in a batch system; the ozone stock solution is added to the reactor containing the solution to be treated. Gamal El-Din et al. (2011) showed that using a semi-batch ozonation system at a utilized ozone dose of 150 mg/L, more than 76% of the EOA was removed. Martin et al. (2011) proved that the major OSPW ozonation byproducts included oxidized NAs such as hydroxy- and/or keto- (oxo-) NAs, which are similar to the byproducts generated during the biodegradation of NAs. Scott et al. (2008) also showed that NAs in OSPW could be removed by O_3, but a fraction of NAs remained unoxidized. It was shown by Perez-Estrada et al. (2011) that during ozonation process at alkaline pH (pH = 8), in which both ozone and •OH are involved, model NA compounds and NAs in OSPW with more rings and more carbon atoms

underwent faster degradation. However, it is still unknown whether the reaction of NAs with O_3 is mainly through the molecular ozone or •OH pathway.

1.6   Research objectives and scope of the research

To date, little research on the efficiency of AOPs with respect to the treatment of OSPW has been done (Allen, 2008b). As discussed earlier, ozonation has shown to be a promising treatment process to degrade OSPW NAs. However, studies have shown that although ozonation did not fully mineralize the parent NAs (Gamal El-Din et al., 2011; Scott et al., 2008b), the subsequent microbial biodegradability of NAs increased and the toxicity towards specific test organisms decreased (Martin et al., 2010; Scott et al., 2008a). There are significant research gaps with respect to the applicability and effectiveness of the advanced treatment technologies for the OSPW remediation at the industrial scale.

Based on these needs, the present research focused on studying the applicability of three types of advanced oxidation processes: UV/H_2O_2, ozonation at alkaline pH, and O_3/H_2O_2 for the removal of NAs from aqueous solutions and elucidation of the reaction mechanisms. In the first phase of this research, the effect of different system parameters, including H_2O_2 concentration, the power of the UV lamp, pH, presence of radical scavengers and OSPW constituents (organic and inorganic content) on the reactivity of a one-ring NA model compound, cyclohexanoic acid (CHA) in the UV/H_2O_2 AOP was investigated. The byproducts formed during this reaction were also determined.

In the second phase of the research, the structure-reactivity of model NA compounds in the UV/H_2O_2 advanced oxidation process was studied. Several model NAs compounds were selected and their reactivities in the UV/H_2O_2 AOP were compared. Then, the OSPW was treated using UV/H_2O_2 for the structure-reactivity study. The third phase of the research was focused on the elucidation of mechanism of CHA ozonation at different conditions including pH and presence of radical scavengers. The last part of this study was related to the treatability of OSPW NAs using the O_3/H_2O_2 process. This study was conducted using batch and semi-batch ozonation systems and the batch systems.

The objectives during the first phase were as follows:

- To assess the reactivity of CHA in the UV/H_2O_2 process and to identify the formed byproducts.

- To study the effect of H_2O_2 concentration on CHA reactivity and to optimize the amount of H_2O_2 added to the process.

- To investigate the effect of solution pH on CHA reactivity and on byproducts formation.

- To study the effect of UV lamp irradiance on CHA degradation and byproduct formation.

- To study the effect of carbonate and chloride ions as radical scavengers on CHA reactivity in ultrapure water, along with assessment of byproduct formation.

- To evaluate the effect of the OSPW matrix on the rate of CHA decomposition.

For the second phase, the main objective was to assess the relative structure-reactivity of pure model NAs and of a complex mixture of OSPW NAs toward •OH in the UV/H_2O_2 AOP. Based on previous knowledge with respect to the ozonation of NAs, it was hypothesized that an increase in the number of carbon atoms and rings, as well as increasing alkyl branching in the NA molecular structure would lead to more reactivity towards •OH. Based on this, the detailed objectives were as follows:

- To study the effect of carbon number on the reactivity of model cyclic and linear NA compounds in the UV/H_2O_2 AOP using relative kinetics method and comparing it with theoretical rates using models previously developed in two studies, and also comparing the structure reactivity in UV/H_2O_2 process with the ozonation.

- To study the effect of the number of rings (0, 1, and 3 saturated rings) on the reactivity of model NA compounds in the UV/H_2O_2 AOP using relative kinetics method and comparing it with theoretical rates using two models and also comparing with ozonation.

- To investigate the effect of branching in linear model NA compounds in addition to the effect of tertiary carbon on the reactivity of cyclic model NA compounds in the UV/H_2O_2 AOP using relative kinetics method and comparing it with theoretical rates using two models and also comparing with ozonation.

- To evaluate the structure-reactivity of the complex and undefined mixture of NAs in OSPW by UV/H_2O_2.

16

The objective of the third phase was to investigate the mechanism of CHA degradation and byproducts formation during the ozonation process. The effect of inorganic constituents such as carbonate and the impacts of organic radical scavengers such as *tert*-butyl alcohol (TBA) and tetranitromethane (TNM) on the performance of the ozonation treatment were also studied by using the stoichiometric analysis.

The main objectives of the fourth phase were as follows:

- To assess the reactivity of CHA in the O_3/H_2O_2 process by using the stoichiometric analysis approach.

- To study the effect of O_3 to H_2O_2 ratio on CHA reactivity and to optimize the process.

- To investigate the effect of solution pH on CHA reactivity in the O_3/H_2O_2 process.

- To investigate the removal of OSPW NAs using the O_3/H_2O_2 process with different ratios in a batch ozonation system.

- To investigate the removal of EOA in OSPW using the O_3/H_2O_2 process with different oxidant ratios in a semi-batch ozonation system.

The successful execution of this project will provide fundamental and practical knowledge not only in terms of the reaction mechanisms and pathways but also in terms of the applicability of the AOPs for the treatment of high volumes of OSPW.

17

1.7 References

Afzal A, Drzewicz P, Martin JW, Gamal El-Din M. Decomposition of cyclohexanoic acid by the UV/H_2O_2 process under various conditions. Sci Total Environ 2012; 426:387-392.

Alberta Energy and Utilities Board. Alberta's reserves 2004 and supply/demand outlook 2005-2014. Report no. ST98-2005. AFRD. Alberta Energy and Utilities Board 2005. Calgary, Alberta, Canada.

Allen EW. Process water treatment in canada's oil sands industry: I. Target pollutants and treatment objectives. J Environ Eng Sci 2008a;7:123-138.

Allen, E. W. (2008b). Process water treatment in canada's oil sands industry: II. A review of emerging technologies. J Environ Eng Sci 2008b; 7:499-524.

Clemente JS, Fedorak PM. A review of the occurrence, analyses, toxicity, and biodegradation of naphthenic acids. Chemosphere 2005;60:585-600.

Clemente JS, Prasad NGN, MacKinnon MD, Fedorak PM. A statistical comparison of naphthenic acids characterized by gas chromatography-mass spectrometry. Chemosphere 2003;50:1265-1274.

Del Rio LF, Hadwin AKM, Pinto LJ, MacKinnon MD, Moore MM. Degradation of naphthenic acids by sediment microorganisms. J Appl Microbiol 2006;101:1049-1061.

Dokholyan BK, Magomedov AK. Effect of sodium naphthenate on survival and some physiological–biochemical parameters of some fishes. J Ichthyology 1983;23:125-132.

Dominski M. Surface mined oil sand: tailings practices, performance, and projections. Alberta Energy and Utilities Board 2007. *In* Proceedings of the 3rd International Heavy Oil Conference, March 5-7, 2007, Calgary, Alberta. Alberta Energy and Utilities Board.

Drzewicz P, Afzal A, Gamal El-Din M, Martin JW. Degradation of a model naphthenic Acid, cyclohexanoic acid, by vacuum UV (172 nm) and UV (254 nm)/H_2O_2. J Phys Chem A 2010;114:12067-74.

Fan TP. Characterization of naphthenic acids in petroleum by fast-atom-bombardment mass-spectrometry. Energ Fuel 1991;5:371-375.

Farnand BA, Krug TA.Oil removal from oilfield-produced water by cross flow ultrafiltration. J Can Petrol Technol 1989;28:18-24.

Frank RA, Kavanagh R, Burnison BK, Arsenault G, Headley JV, Peru KM, Van Der Kraak G, Solomon KR. Toxicity assessment of collected fractions from an extracted naphthenic acid mixture. Chemosphere 2008;72:1309-1314.

Gamal El-Din M, Fu HJ, Wang N, Chelme-Ayala P, Perez-Estrada L, Drzewicz P, Martin JW, Zubot W, Smith DW. Naphthenic acids speciation and removal during

petroleum-coke adsorption and ozonation of oil sands process-affected water. Sci Total Environ 2011;40:5119-25.

Garcia-Garcia E, Pun J, Pérez-Estrada LA, Gamal El-Din M, Smith DW, Martin JW, Belosevic M. Commercial naphthenic acids and the organic fraction of oil sands process water downregulate pro-inflammatory gene expression and macrophage antimicrobial responses. Toxicol Lett 2011;203:62-73.

Golby S, Ceri H, Gieg LM, Chatterjee I, Marques LLR, Turner RJ. Evaluation of microbial biofilm communities from an alberta oil sands tailings pond. Fems Microbiol Ecol 2012; 79:240-250.

Grewer DM, Young RF, Whittal RM, Fedorak PM. Naphthenic acids and other acid-extractables in water samples from Alberta: What is being measured? Sci Total Environ 2010 408:5997-6010.

Headley JV, Du JL, Peru KM, McMartin DW. Electrospray ionization mass spectrometry of the photodegradation of naphthenic acids mixtures irradiated with titanium dioxide. J Environ Sci Heal A 2009;44:591-597.

Headley JV, McMartin DW. A review of the occurrence and fate of naphthenic acids in aquatic environments. J Environ Sci Heal A 2004;39:1989-2010.

Headley JV, Peru KM, Adenugba AA, Du JL, McMartin DW. Dissipation of naphthenic acids mixtures by lake biofilms. J Environ Sci Heal A 2010;45:1027-1036.

Headley JV, Peru KM, McMartin DW, Winkler M. Determination of dissolved naphthenic acids in natural waters by using negative-ion electrospray mass spectrometry. J Aoac Int 2002;85:182-187.

Headley JV, Barrow MP, Peru KM, Derrick PJ. Salting-out effects on the haracterization of naphthenic acids from Athabasca oil sands using electrospray ionization. J Environ Sci Heal A 2011;46:844-854.

Herman DC, Fedorak PM, Mackinnon MD, Costerton JW. Biodegradation of naphthenic acids by microbial-populations indigenous to oil sands tailings. Can J Microbiol 1994;40:467-477.

Kanicky JR, Poniatowski AF, Mehta NR, Shah DO. Cooperativity among molecules at interfaces in relation to various technological processes: Effect of chain length on the pK_a of fatty acid salt solutions. Langmuir 2000;16:172-177.

Kannel, PR, Gan TY. Naphthenic acids degradation and toxicity mitigation in tailings wastewater systems and aquatic environments: A review. J Environ Sci Heal A 2012;47:1-21.

Kim ES, Liu Y, Gamal El-Din M. The effects of pretreatment on nanofiltration and reverse osmosis membrane filtration for desalination of oil sands process-affected water. Sep Purif Technol 2011;81:418-428.

Knight RL, Kadlec RH, Ohlendorf HM. The use of treatment wetlands for petroleum industry effluents. Environ Sci Technol 1999;33:973-980.

Leung SS, MacKinnon MD, Smith REH. The ecological effects of naphthenic acids and salts on phytoplankton from the Athabasca oil sands region. Aquat Toxicol 2003;62:11-26.

Liang XM, Zhu XD, Butler EC. Comparison of four advanced oxidation processes for the removal of naphthenic acids from model oil sands process water. J Hazard Mater 2011;190:168-176.

Liu JJ, Xu ZH, Masliyah J. Processability of oil sand ores in Alberta. Energ Fuel 2005;19:2056-2063.

MacKinnon MD, Boerger H. Description on two treated methods for detoxifying oil sands tailings ponds water. Water Pollut Res J Can 1986;21:496-512.

Madill REA, Orzechowski MT, Chen GS, Brownlee BG, Bunce NJ. Preliminary risk assessment of the wet landscape option for reclamation of oil sands mine tailings: Bioassays with mature fine tailings pore water. Environ Toxico 2001;16:197-208.

Martin JW, Barri T, Han XM, Fedorak PM, Gamal El-Din M, Pérez-Estrada L, Scott AC, Jiang JT. Ozonation of oil sands process-affected water accelerates microbial bioremediation. Environ Sci Technol 2010;44:8350-8356.

McMartin DW, Headley JV, Friesen DA, Peru KM, Gillies JA. Photolysis of naphthenic acids in natural surface water. J Environ Sci Heal A 2004;39:1361-1383.

Mikula RJ, Kasperski KL, Burns RD, MacKinnon MD. Nature and fate of oil sands fine tailings. Adv Chem Ser 1996;251:677-723.

Mohamed MH, Wilson LD, Headley JV,Peru KM. Sequestration of naphthenic acids from aqueous solution using beta-cyclodextrin-based polyurethanes. Phys Chem Chem Phys 2011;13:1112-1122.

Mohamed MH, Wilson LD, Peru KM, Headley JV. Colloidal properties of single component naphthenic acids and complex naphthenic acid mixtures. J Colloid Interf Sci 2013;395:104-110.

National Energy Board. Canada's oil sands opportunities and challenges to 2015: an update. The Publications Office National Energy Board 2006, Calgary, Alberta, Canada.

Parsons S. Advanced oxidation processes for water and wastewater treatment. IWA, London; 2004.

Peng H, Volchek K, MacKinnon M, Wong WP, Brown CE. Application of nanofiltration to water management options for oil sands operations. Desalination 2004;170:137-150.

Pérez-Estrada LA, Han XM, Drzewicz P, Gamal El-Din M, Fedorak PM, Martin JW. Structure-reactivity of naphthenic acids in the ozonation process. Environ Sci Technol 2011;45:7431-7437.

Pourrezaei P, Drzewicz P, Wang YN, Gamal El-Din M, Pérez-Estrada LA, Martin JW, Anderson J, Wiseman S, Liber K, Giesy JP. The impact of metallic coagulants on

the removal of organic compounds from oil sands process-affected water. Environ Sci Technol 2011;45:8452-8459.

Prousek J. Advanced oxidation processes for water treatment: Photochemical processes. Chem Listy 1996;90:307-15.

Quagraine EK, Peterson HJ, Headley JV. *In situ* bioremediation of naphthenic acids contaminated tailing pond waters in the athabasca oil sands region-demonstrated field studies and plausible options: A review. J Environ Sci Heal A 2005;40:685-722.

Rogers VV, Liber K, MacKinnon MD. Isolation and characterization of naphthenic acids from Athabasca oil sands tailings pond water. Chemosphere 2002;48:519-527.

Rogers VV, Wickstrom M, Liber K, MacKinnon MD. Acute and subchronic mammalian toxicity of naphthenic acids from oil sands tailings. Toxicol Sci 2002;66:347-355.

Ross MS, Pereira A, Fennell J, Davies M, Johnson J, Sliva L, Martin JW. Quantitative and Qualitative Analysis of Naphthenic Acids in Natural Waters Surrounding the Canadian Oil Sands Industry. Environ Sci Technol 2012;46:12796-12805.

Scott AC, Young RF, Fedorak PM. Comparison of GC-MS and FT-IR methods for quantifying naphthenic acids in water samples. Chemosphere 2008a;73:1258-64.

Scott AC, Zubot W, MacKinnon MD, Smith DW, Fedorak PM. Ozonation of oil sands process water removes naphthenic acids and toxicity. Chemosphere 2008b;71:156-60.

Seifert WK, Teeter RM, Howells WG, Cantow MJR. Analysis of crude oil carboxylic acids after conversion to their corresponding hydrocarbons. Anal Chem 1969;41:1638.

Shell Canada. The Athabasca oil sands project 2004 Sustainability Report [online] 2005. Available from: http://www.shell.com/static//ca-en/downloads/responsible_energy/sd_reports/sd04.pdf [cited 18 July 2012].

Small CC, Hashisho Z, Ulrich AC. Preparation and characterization of activated carbon from oil sands coke. Fuel 2012;92:69-76.

Smith BE, Lewis CA, Belt ST, Whitby C, Rowland SJ. Effects of alkyl chain branching on the biotransformation of naphthenic acids. Environ Sci Technol 2008;42:9323-9328.

Smith DF, Schaub TM, Kim S, Rodgers RP, Rahimi P, Teclemariam A, Marshall AG. Characterization of acidic species in Athabasca bitumen and bitumen heavy vacuum gas oil by negative-ion ESI FT-ICR MS with and without acid-ion exchange resin prefractionation. Energ Fuel 2008;22:2372-2378.

Suncor Energy Incorporated. Suncor Energy 2005 Report on Sustainability [online] 2005. Available from http://www.suncor.com/pdf/ic-annualreport 2005-e.pdf [cited 18 July 2012].

Syncrude Canada Limited. Syncrude Canada Limited 2004 Sustainability Report [online] 2005. Available from:

http://sustainability.syncrude.ca/sustainability2004/download/SyncrudeSD2004.pdf [cited 18 July 2012].

The Royal Society of Canada. Environmental and health impacts of Canada's oil sands industry 2010. Expert panel reports, The Royal Society of Canada, Ottawa, Ontario, Canada.

West CE, Scarlett AG, Pureveen J, Tegelaar EW, Rowland SJ. Abundant naphthenic acids in oil sands process-affected water:studies by synthesis, derivatisation and two-dimensional gaschromatography/high-resolution mass spectrometry. Rapid Commun Mass Sp 2013;27:357-365.

Zaidi A, Simms K, Kok S. The use of micro/ultrafiltration for the removal of oil and suspended-solids from oil-field brines. Water Sci Technol 1992;25:163-176.

Zubot W, MacKinnon MD, Chelme-Ayala P, Smith DW, Gamal El-Din M. Petroleum coke adsorption as a water management option for oil sands process-affected water. Sci Total Environ 2012;427:364-372.

Zubot WA. Removal of naphthenic acids from oil sands process water using petroleum coke. M.Sc. Dissertation 2010. University of Alberta, Edmonton, Alberta, Canada.

2 DECOMPOSITION OF CYCLOHEXANOIC ACID BY THE UV/H₂O₂ ADVANCED OXIDATION PROCESS UNDER VARIOUS CONDITIONS[*]

2.1 Introduction

Naphthenic acids (NAs) are complex mixtures of alkyl-substituted aliphatic cyclic and non-cyclic carboxylic acids that are natural constituents of petroleum, including bitumen. In Northern Alberta, the surface mining oil sands industry extracts bitumen from the oil sands using hot process water (Masliyah et al., 2004). The soluble NA fraction of bitumen becomes concentrated in the resulting oil sands process affected water (OSPW), which is subsequently stored in large tailings ponds and continually recycled because of a zero discharge policy (Schramm et al., 2000). The concentration of NAs in tailing ponds depends on the specificity of the analytical method used (Martin et al., 2008), but the reported range is from 40 to 125 mg NA/L (Allen, 2008a) using Fourier transform infrared (FT-IR) spectroscopy.

The acute and chronic toxicity of fresh OSPW to aquatic organisms has been mainly attributed to NAs (Headley and McMartin, 2004; Scott et al., 2005). Thus, the removal of NAs from OSPW has been one of the targets of remediation studies since the

---

1980s (Allen, 2008a). The existing technologies for the treatment of OSPW have mostly relied on natural microbial degradation, but this is too slow to keep up with the fast expansion of the industry. Thus, decontamination and detoxification of OSPW are still major challenges currently facing the oil sands industry (Allen, 2008b).

Advanced oxidation processes (AOPs) have been studied extensively in water and wastewater treatment and have been proven to be very effective for the removal of organic pollutants (Parsons, 2004). AOPs rely on the formation of reactive and short-lived oxidizing agents, such as hydroxyl radicals (•OH). Photolysis of hydrogen peroxide (H_2O_2) using ultraviolet (UV) light at 254 nm is one of the AOPs in which •OH are generated as shown in reaction 2-1.

$$H_2O_2 + h\nu \longrightarrow 2 \cdot OH \qquad\qquad (2\text{-}1)$$

The •OH is a very powerful oxidizing agent that reacts non-selectively with organic and inorganic substances. •OH can abstract hydrogen atoms from virtually any organic compound, although the rates of reaction change from compound to compound (Prousek, 1996).Therefore, other dissolved organic carbon in OSPW (i.e. other than NAs) may affect the decomposition of NAs as they compete for the •OH. Furthermore, abundant inorganic anions in OSPW, such as chloride and carbonate/bicarbonate (Allen, 2008a), could act as significant hydroxyl radical scavengers in OSPW, further slowing the degradation of NAs.

28

To date, little investigation of the effect of AOPs on the treatment of OSPW has been carried out (Allen, 2008b). Recent studies showed that ozonation did not fully mineralize the parent NAs (Gamal El-Din et al., 2011; Scott et al., 2008b), but the subsequent microbial biodegradability and toxicity removal was increased (Martin et al., 2010; Scott et al., 2008a). It was also determined that the major intermediate byproducts of NA ozonation were oxidized NAs (Martin et al., 2010).

Cyclic structures are a prominent feature of NA structures in OSPW (Headley and McMartin, 2004), hence we previously selected cyclohexanoic acid (CHA) (Figure 2-1) as a simple model compound to study the mechanism of NA decomposition induced by •OH in ultrapure water (Drzewicz et al., 2010). It was shown that the principal byproducts formed during •OH induced decomposition of CHA were hydroxy-CHA, dihydroxy-CHA, and oxo-CHA. Heptadioic acid and other simple carboxylic acids were also observed (Drzewicz et al., 2010).
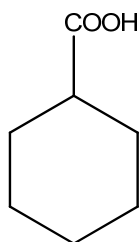
Figure 2-1. Chemical structure of cyclohexanoic acid.

The objective of this study was to assess the reactivity of CHA in the UV/H_2O_2 process under various conditions including the H_2O_2 concentration, pH of the solution,

and the presence of carbonate and chloride as radical scavengers. The changes in byproducts formation in presence of these scavengers in ultrapure water were studied. In addition, the effect of OSPW matrix on the rate of CHA decomposition was investigated.

2.2 Material and methods

2.2.1 Chemicals and sample preparation

Cyclohexanoic acid (CHA, > 99% purity) was purchased from TCI (Portland, OR, USA). A stock standard solution (2 mM) of CHA was prepared in ultrapure water and stored at 4 °C; working solutions were prepared daily from this stock solution. The pH of solutions was adjusted using 50% sodium hydroxide and 80% perchloric acid solutions (Fisher Scientific Co., Canada). Carbonate and chloride solutions were prepared using $NaHCO_3$ and NaCl (Fisher Scientific Co., Canada). An H_2O_2 stock solution (Fisher Scientific Co., Canada, 30% w/w) was used for the experiments, and catalase from bovine liver (Sigma-Aldrich, 2 950 units/mg solid) was used to quench any H_2O_2 residuals in the sample vials as needed. Ammonium acetate, acetic acid, and methanol (LC-MS grade) were purchased from Fisher Scientific. All other chemicals and reagents were of analytical grade and were used as received.

Ultrapure water (resistivity = 18 MΩ×cm and TOC < 0.1 mg/L) was obtained from a Millipore and Elga system equipped with an Elix UV lamp. To investigate the effect of water matrices on CHA degradation, two other types of water were used: a sample of OSPW, supplied by Syncrude Canada Ltd., and the same OSPW sample after

30

adsorption by commercial powder activated carbon (PAC) (5% PAC by mass for 3 h). The OSPW was filtered through a 0.45 μm filter and kept at 4 °C until use.

2.2.2 Analytical methods

A high performance liquid chromatograph (HPLC) coupled to an ion trap mass spectrometer (Varian 500-MS) was used for the analysis of CHA and its degradation byproducts. A Phenomenex, C8, 5 μm, 250 mm × 3 mm column was used for separations. The chromatographic conditions were: A, 100% methanol, and B, 4 mM aqueous ammonium acetate with 0.01% acetic acid, gradient elution from 30% to 70% A over 30 min, flow 200 μL/min, injected volume 20 μL. Using these conditions, the detection limit of CHA was 20 μg/L (4 ng), and the retention time of CHA was around 40 min.

Fourier transform infrared (FT-IR) spectroscopy was used (Scott et al., 2008a) to determine the concentration of the extractable organic acids in the OSPW before and after PAC adsorption (details are presented in Appendix A). Chemical oxygen demand (COD) and alkalinity were measured following standard methods (Clesceri et al., 2005). The H_2O_2 was measured using the iodine method (Klassen et al., 1994) (Appendix A). In addition, the concentration of the H_2O_2 stock solution was controlled using UV-vis spectrometer before the preparation of the solutions. Chloride and carbonate were measured only for OSPW by ion chromatography and titrimetric method, respectively.

2.2.3 UV/H$_2$O$_2$ experiments

A UV collimated beam apparatus (Calgon Carbon Corporation, Pittsburg, PA, USA) equipped with a 10 W low-pressure UV lamp (Calgon Carbon Corporation) was used. The light source had a monochromatic emission, predominantly at 253.7 (~254) nm, with irradiance at the sample position of 0.11 mW/cm^2. For the experiments on study of radical scavengers and real OSPW another UV lamp with slightly higher irradiance (0.20 mW/cm^2) was used. A control experiment was carried out and it was shown that with changing the UV lamp, no change in the system was observed except the change in decomposition rates. A calibrated radiometer (International Light Inc. Model IL 1400A) equipped with a UV detector (International Light Inc. Model SED240) and a neutral density filter (Model QNDS2) was used to measure the irradiance at the sample surface (details are presented in Appendix A).

For the treatment optimization and byproduct investigation, 10 mg/L of CHA was used in UV/H$_2$O$_2$ AOP. This optimization was verified for higher concentrations of CHA (up to 80 mg/L). However, for further studies, the CHA concentration was increased from 10 to 50 mg/L in order to be in the same range as the NAs concentration in OSPW.

The CHA solutions (15 mL) in glass Petri dishes (60 mm diameter) were exposed to UV light under a completely mixed condition without turbulence using a small magnetic stir bar, at room temperature (21 ± 2 °C). Hydrogen peroxide was added to the CHA solutions right before the UV exposure. Samples (200 μL) were taken at intervals

of 10–20 min over 2 h for CHA and byproduct analyses. The experiments were performed in triplicate.

2.3   Results and discussion

2.3.1   Effect of H_2O_2 concentration on CHA decomposition and byproduct formation

The degradation of CHA by the UV/H_2O_2 process was studied in ultrapure water at various H_2O_2 concentrations. The efficiency of the UV/H_2O_2 process in degradation of organic pollutants depends on the concentration of H_2O_2 at the beginning of the process, such that sufficient hydroxyl radicals are produced over the entire process. Furthermore, the decomposition of CHA involves sequential reactions with •OH (Drzewicz et al., 2010); therefore, optimizing the H_2O_2 concentration was studied.

The initial CHA concentration was 10 mg/L in all experiments, and the pseudo-first order degradation rate constant (k_1) was determined over 80 min of UV exposure with H_2O_2 concentrations of 0, 20, 40, 60, and 80 mg/L. In a control study it was determined that H_2O_2 alone (80 mg/L), without UV exposure, caused no CHA degradation. Similarly, in the absence of H_2O_2, CHA degradation was not observed (Figure 2-2), likely because CHA does not absorb UV at 253.7 nm. The fact that NAs do not undergo significant photolysis by direct UV at 254 nm had been previously confirmed (Headley et al., 2009; McMartin et al., 2004).
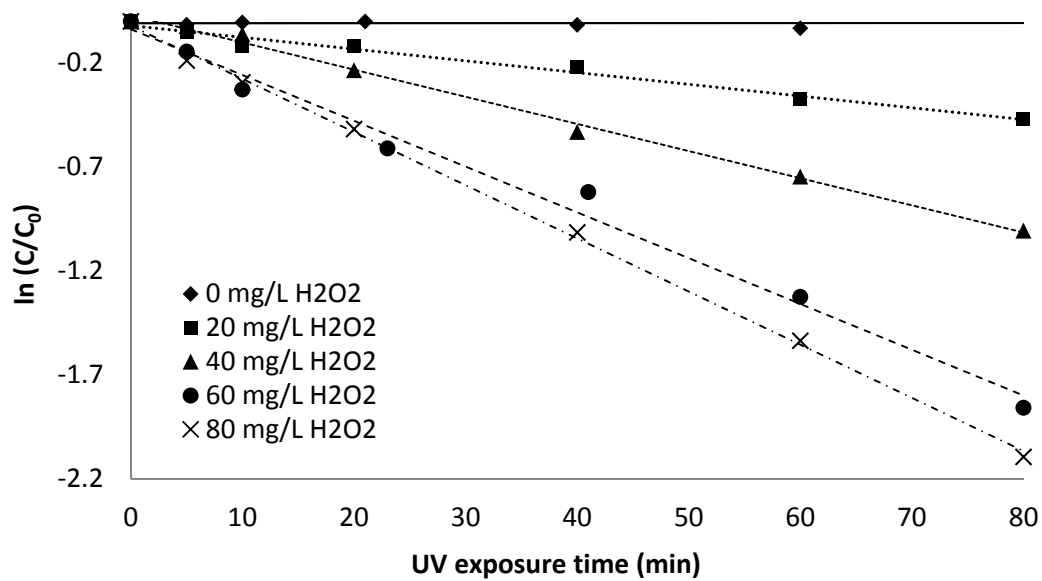
Figure 2-2. Decomposition of cyclohexanoic acid with and without H_2O_2 at pH 9 ($[CHA]_0 = 10$ mg/L).

Using the combined addition of H_2O_2 and UV exposure, significant removal of CHA was observed. Pseudo-first order degradation rate constants increased with increasing H_2O_2 concentrations, up to 60 mg/L (Table 2-1). In this H_2O_2 concentration range (i.e. 20-60 mg/L), the fraction of UV absorbed leading to the production of •OH must have increased, leading to a higher CHA degradation rate. At 80 mg/L H_2O_2, the rate of degradation was slightly faster but was not statistically different from that at 60 mg/L H_2O_2 (based on the t-test analysis with 95% confidence interval that was carried out). The optimal concentration of H_2O_2 for the degradation of 10 mg/L of CHA appears to be 60 mg/L, consequently, the optimal molar ratio of H_2O_2 to CHA in the treatment

34

was established to be 23. This ratio was verified for the CHA concentrations up to 80 mg/L.

The likely explanation for why, at high H_2O_2 concentrations (i.e. 80 mg/L), the reaction rate no longer increases proportionately is that H_2O_2 can also act as an •OH scavenger, producing the HO_2• radical and water (reaction 2-2) (Buxton et al., 1988).

$$H_2O_2 + \bullet OH \longrightarrow HO_2\bullet + H_2O \qquad k_{OH} = 2.7 \times 10^7 \, M^{-1} \, s^{-1} \qquad (2\text{-}2)$$

The HO_2• radical is much less reactive than •OH, and it decays quickly to non-radical products (Bielski et al., 1985), often without reacting with organic compounds. Similar results were observed during decomposition by the UV/H_2O_2 process for other organic compounds, such as parathion and anatoxin-a (Wu and Linden, 2008; Afzal et al., 2010).

Using the irradiance of the UV lamp at 253.7 nm, photon efficiency (mole of CHA degraded / mole of photon entering the solution) depending on H_2O_2 concentration was calculated (Table 2-1). These data indicate that increasing the H_2O_2 concentration, the degradation efficiency of the CHA increased, while maintaining the same amount of the photon entering the solution. See Appendix B for detailed photon efficiency calculations.
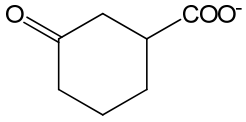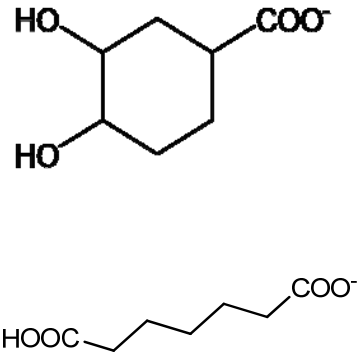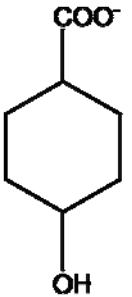
Table 2-1. Pseudo-first-order degradation rate constant of CHA decomposition and estimated photon efficiency (mole of CHA degraded/mole of photon entering the solution) at different concentrations of H_2O_2 at pH 9 ($[CHA]_0 = 10$ mg/L); UV lamp irradiance = 0.11 mW/cm^2.

H_2O_2 concentration (mg/L)	Pseudo-first-order rate constant (min^{-1})	photon efficiency
20	$5.65 \times 10^{-3} \pm 0.0009$	0.92
40	$1.30 \times 10^{-2} \pm 0.001$	1.58
60	$2.2 \times 10^{-2} \pm 0.003$	2.05
80	$2.5 \times 10^{-2} \pm 0.001$	2.15

Based on a previous study, the principal CHA byproducts in the UV/H_2O_2 process are oxo-CHA, hydroxy-CHA, and dihydroxy-CHA (Table 2-2). Among them, oxo-CHA was the principal byproduct; here the 4-oxo-CHA isomer was monitored. The next important byproduct, hydroxy-CHA isomers, elute at retention times of 9.5, 11.0, 12.2, 13.7, 14.6, 22.2, and 24 min. However, the signal of cis-4-hydroxy-CHA (retention time = 13.7 min) was the highest compared to the signals of the other isomers. The changes of all the hydroxy isomers were similar to the changes of cis-4-hydroxy-CHA throughout the treatment. The oxo- and hydroxy- isomers of CHA are the products of the same reaction of bimolecular decomposition of peroxy-CHA, which occurs during the hydroxyl radical induced decomposition of CHA (Drzewicz et al., 2010). The highest peak of dihydroxy-CHA (the third most prominent byproduct) with the most notable change of magnitude over time was observed at 17 min. However, several isomers of dihydroxy-

CHA eluting at retention times of 7.8, 11.0, 12.0, 17.0, 24.5, and 25.3 min were observed as well, but with very low signal changes over time.

Table 2-2. Chemical formulae and proposed structures of major byproducts formed during UV/H_2O_2 at m/z 141, 159, and 143 at pH 9 ([CHA]$_0$ = 10 mg/L), 60 mg/L H_2O_2).

compound	oxo-CHA	dihydroxy-CHA	hydroxy-CHA
Mass (*m/z*)	141	159	143
Empirical Formula	$C_7H_9O_3^-$	$C_7H_{11}O_4^-$	$C_7H_{11}O_3^-$
Proposed structures			

The temporal trends for removal of CHA and formation/removal of these byproducts during the UV/H_2O_2 treatment are shown in Figure 2-3. At the beginning of the experiment, the concentration of byproducts is high; however after some time, the

concentration of the byproducts along, with the CHA, starts decreasing due to the high reactivity toward •OH radicals.
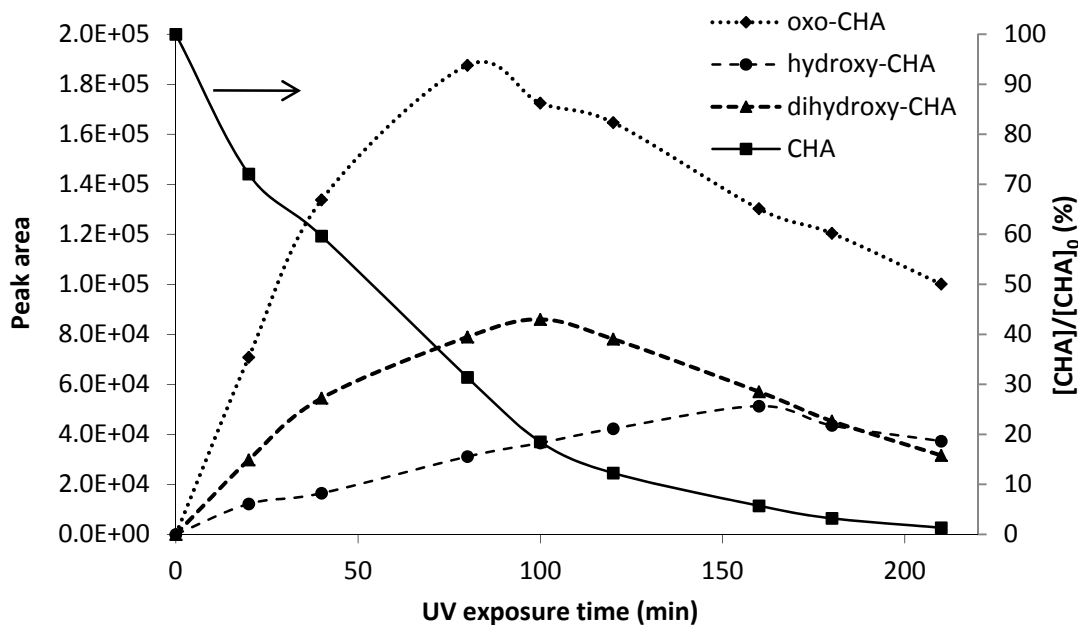
Figure 2-3. Formation of three major byproducts during UV/H_2O_2 degradation of cyclohexanoic acid at pH 9 ([CHA]$_0$ = 10 mg/L), 60 mg/L H_2O_2); retention times: 4-oxo-CHA 12 min; dihydroxy-CHA 17 min; cis-4-hydroxy-CHA 13 min.

2.3.2 Effect of UV lamp irradiance on the rate of CHA decomposition and byproduct formation

A study using two UV lamps with different irradiances was performed. The results showed that changing the UV lamp to high irradiance one, just shortens the time of the process proportional to the increase of lamp irradiance (i.e., decreasing the pseudo-first order rate), and does not affect the type of byproducts formed. For example, when

38

the UV lamp with irradiance of 0.11 mW/cm^{-2} was used, the pseudo-first order rate constant of the CHA degradation was 0.02, whereas when the lamp with irradiance of 0.2 mW/cm^{-2} was used, the pseudo-first order rate constant changed to 0.04 (see Figure 2-4).
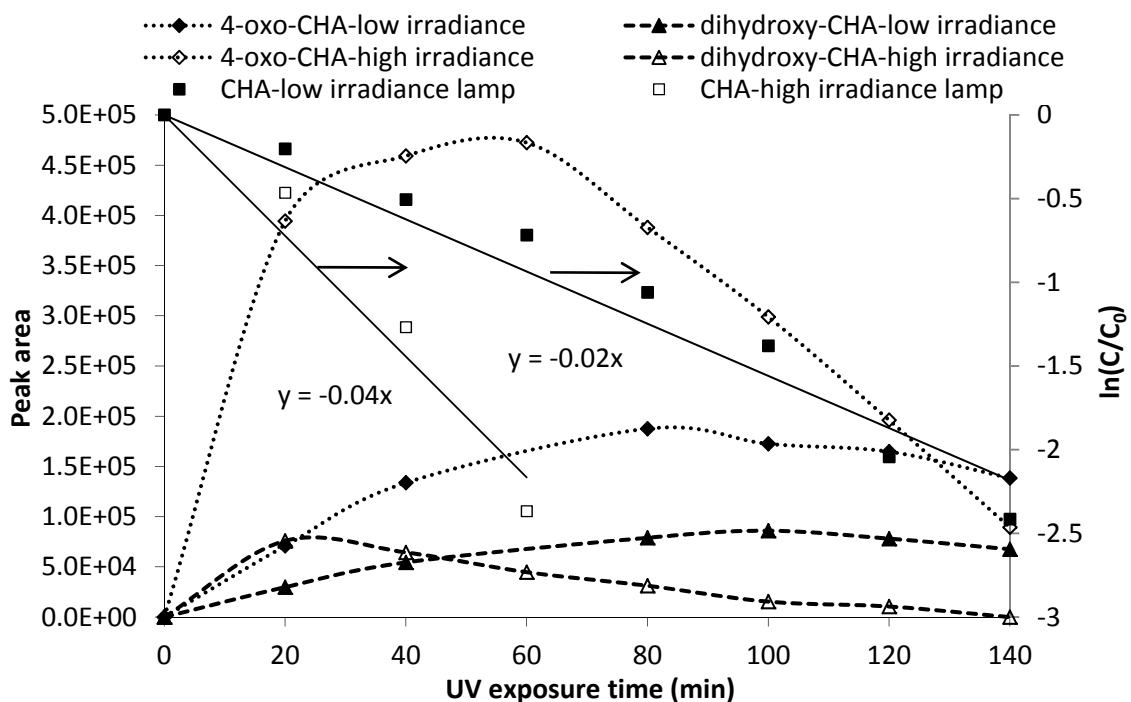
Figure 2-4. Degradation of CHA and byproducts formation using two UV lamp with low and high irradiance.

2.3.3 Effect of pH on the decomposition of CHA and byproduct formation

It has been shown in several studies that the pH has a significant effect on the reactivity of compounds, the formation of byproducts, and the overall effectiveness of AOPs (Bojanowska-Czajka et al., 2006; Homlok et al., 2010; Panades et al., 2000). The reactivity of hydrogen atoms at the α position of aliphatic acids, for example, can depend

on whether or not the carboxylic acid group is protonated or dissociated (Hewgill and Proudfoot, 1976). However, the effect of pH on the decomposition of alicyclic carboxylic acids by the UV/H_2O_2 process has not been investigated. Furthermore, decreasing the pH facilitates the removal of the solid particles from the OSPW (Zhu et al., 2011); therefore, a study of the effect of pH on the UV/H_2O_2 treatment is very important.

The pKa of CHA is 4.9 (Serjeant and Dempsey, 1979). The initial pH of the CHA solution in two experiments was adjusted to 3.0 ± 0.1 and 9.0 ± 0.1; however no change in the pH (no more than 0.2) was observed after the treatment. The results showed that at pH 3 (protonated CHA) and pH 9 (dissociated CHA) there was no significant difference in the pseudo-first order rate constant of CHA decomposition (Figure 2-5). Thus, our observation at different pH, suggests that the hydrogen at the α position was not a significant source of overall reactivity.
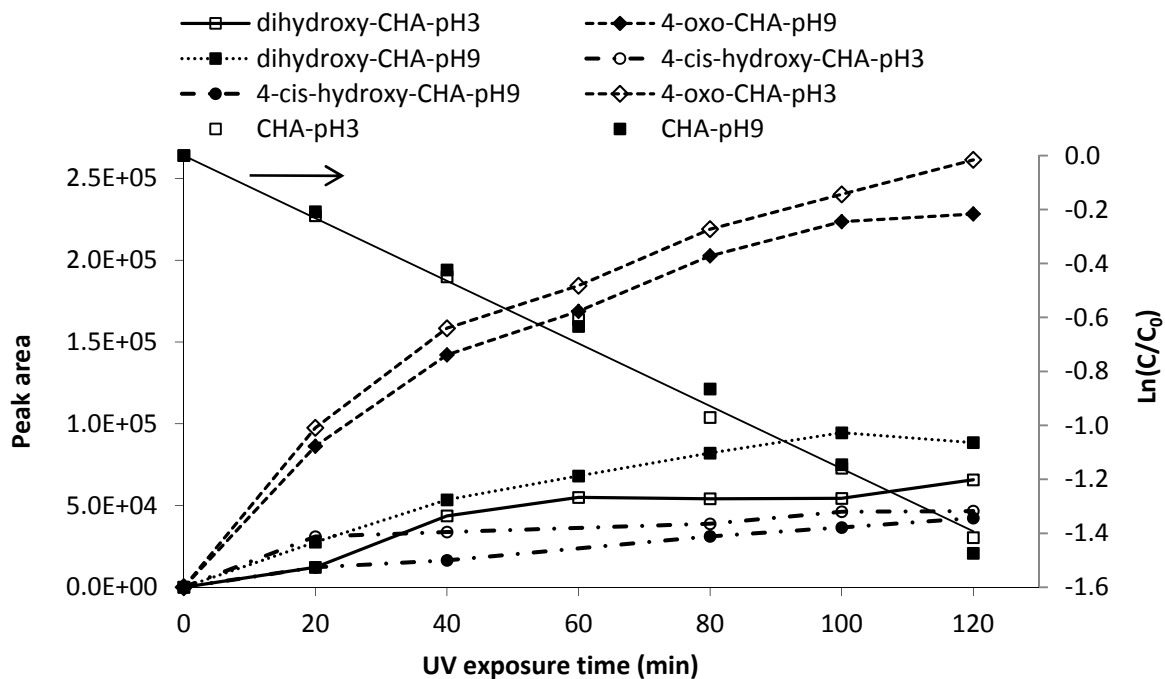
Figure 2-5. Degradation and byproducts formation during UV/H_2O_2 treatment of cyclohexanoic acid at pH 3 and 9 ($[CHA]_0 = 50$ mg/L, 300 mg/L H_2O_2, UV lamp irradiance = 0.11 mW/cm^2); retention times: 4-oxo-CHA 12 min; dihydroxy-CHA 17 min; cis-4-hydroxy-CHA 13 min.

In a previous study at pH 9, the degradation mechanism for CHA was described by reaction of •OH with CHA to produce an organic radical, which then reacted with dissolved molecular oxygen to form a peroxyl radical (Drzewicz et al., 2010). The peroxyl radical was then proposed to undergo a disproportionation reaction yielding oxo-CHA and hydroxy-CHA (reaction 2-3), or a unimolecular decay, catalyzed by hydroxide anion, yielding only oxo-CHA (reaction 2-4).

41

$$\text{(2-3)}$$

$$\text{(2-4)}$$
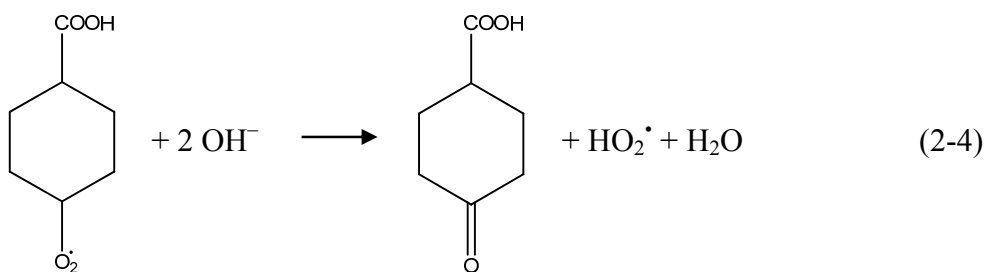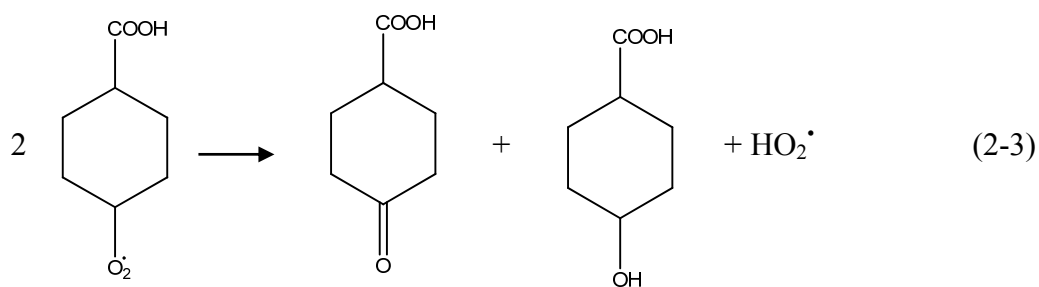
In this study, in order to confirm the proposed mechanism, we conducted the further investigations of byproduct formation under alkaline and acid conditions. If the reaction involving hydroxide ion was a significant process, then at pH 9 a relatively higher formation rate of the oxo-CHA should be observed, and a relatively lower formation rate of hydroxy-CHA should be observed, compared to pH 3. However, no experimental evidence for this was observed. In fact, there was less oxo-CHA at pH 9 than at pH 3 (Figure 2-5). This suggests that the peroxyl-CHA radical is relatively stable and does not undergo rapid unimolecular decay to oxo-CHA. As a result, the pH has no measurable effect on the type and relative yield of byproducts formed during the treatment of CHA in UV/H_2O_2 process in ultrapure water.

2.3.4 Effect of radical scavengers on the CHA treatment

Two of the most dominant anions in OSPW are carbonate and chloride, which are well-known radical scavengers. Carbonate and bicarbonate can react with •OH radicals (reactions 2-5 and 2-6) to form carbonate and bicarbonate radicals ($CO_3^-•$ and $HCO_3•$) (Buxton et al., 1988). However, at pH 7 to 9, the prevalent anion in OSPW is bicarbonate, which is less reactive toward •OH than the carbonate ion.

$$HCO_3^- + •OH \longrightarrow OH^- + HCO_3• \qquad k_{OH} = 8.5 \times 10^6 \ M^{-1} \ s^{-1} \qquad (2\text{-}5)$$

$$CO_3^{2-} + •OH \longrightarrow OH^- + CO_3^-• \qquad k_{OH} = 3.9 \times 10^8 \ M^{-1} \ s^{-1} \qquad (2\text{-}6)$$

The carbonate radical is an electrophilic species that is very reactive toward electron-rich compounds, such as anilines (Larson and Zepp, 1988; Mazellier et al., 2003), phenols (Busset et al., 2007), sulfur containing compounds and carboxylic acids (Neta et al., 1988), albeit less reactive than •OH. Carbonate radicals last longer in solution than •OH and have high oxidation potential (E^0_{red} = 2.1 V). Carbonate may also react with H_2O_2 to form $HO_2•$, which is poorly reactive toward organic compounds (Draganic et al., 1991). Study of the influence of carbonate on the degradation rate of NAs is also important because addition of carbon dioxide may be used for densification of oil sand tailings (Zhu et al., 2011).

The other radical scavenger, chloride, also reacts with •OH with the second-order rate constant of $4.3 \times 10^9 \ M^{-1} \ s^{-1}$ (Buxton et al., 1988), which may have an additional

negative effect on the AOP due to scavenging. Regardless, chlorine radicals (dichloride anion radical and chlorine atom) are formed during the UV/H_2O_2 treatment of solutions containing chloride (Jayson et al., 1973). Chlorine radicals are very reactive species toward organic compounds and are powerful oxidants (Martire et al., 2001). Furthermore, a final product of oxidation of chloride in the UV/H_2O_2 process is chlorine (Yu, 2004). Chlorine forms hypochlorous acid in water which is also a moderate oxidant and can be reactive toward organic compounds (Yu and Barker, 2003). An additional reaction that may occur during UV/H_2O_2 treatment is the reaction of hypochlorite with H_2O_2. Singlet oxygen is one of the products of this reaction which is well-known as an oxidant of organic species (Held et al., 1978).

Investigation of the scavenging effect of chloride and bicarbonate on the decomposition of CHA was performed in two separate solutions: the first contained 50 mg/L CHA and 500 mg/L Cl^-, and the second contained 50 mg/L CHA and 700 mg/L CO_3^{2-} in ultrapure water. These concentrations of CHA, chloride and carbonate were chosen to approximate the average concentrations in the OSPW. The chloride anion rate constant for reaction with •OH is $4.3 \times 10^9 \, M^{-1} \, s^{-1}$ (Buxton et al., 1988), thus in OSPW the chloride anion may compete effectively for •OH with CHA for which the rate constant is only slightly higher, $5.5 \times 10^9 \, M^{-1} \, s^{-1}$ at pH 9 (Anbar et al., 1966). Comparatively, the bicarbonate hydroxyl-radical rate constant is $8.5 \times 10^6 \, M^{-1} \, s^{-1}$; thus bicarbonate can effectively compete with CHA if the concentrations are about 1000 times higher than that of CHA.

Figure 2-6 shows the results of the CHA treatment with UV/H_2O_2 in ultrapure water and in presence of chloride and bicarbonate ions at pH 9. The presence of 500 mg/L Cl⁻ in a 50 mg/L CHA solution decreased the pseudo first-order decomposition rate constant by 23%, whereas the presence of 700 mg/L bicarbonate decreased the rate by 55%.
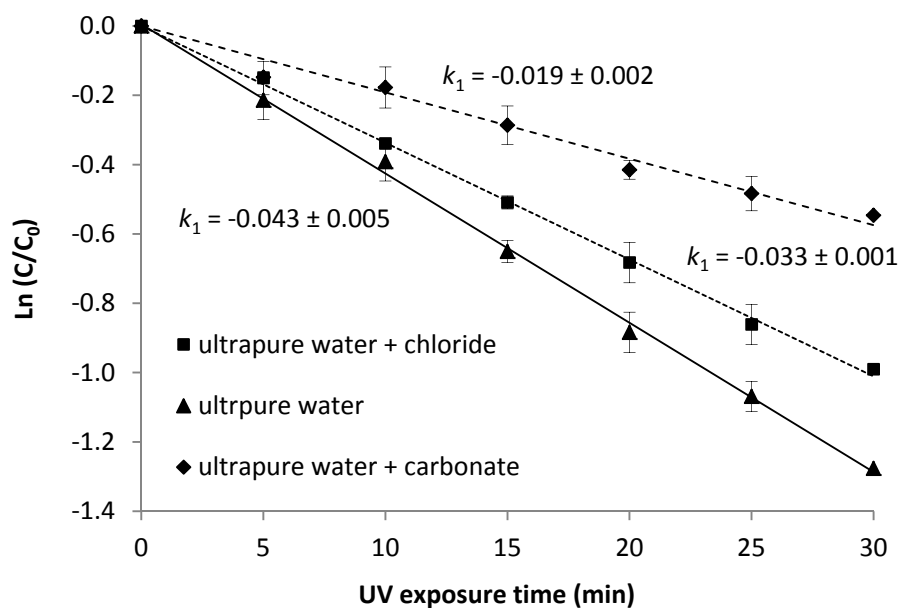
Figure 2-6. Decomposition of CHA in ultrapure water and in presence of separate solutions one containing 500 mg/L chloride (Cl⁻) and the other one containing 700 mg/L carbonate (CO_3^{2-}) ions at pH 9 ([CHA]$_0$ = 50 mg/L, 300 mg/L H_2O_2 in both solutions); k_1: pseudo-first-order rate constant (min⁻¹); UV lamp irradiance = 0.20 mW/cm².

Even though the molar concentration of carbonate and chloride in the experiments were not the same and we cannot compare their scavenging effect to each other, the

results indicated that carbonate at concentrations present in OSPW had a higher scavenging effect on the CHA degradation in UV/H_2O_2 process than did chloride, also at the same concentration as in OSPW.

Decreasing the scavenging effect of carbonate by acidification of the OSPW is not recommended because this would also increase the salinity of OSPW, and this may furthermore not be viable due to the additional treatment costs. Additionally, it has been shown that the •OH scavenging effect of chloride in UV/H_2O_2 systems increases at low pH (Liao et al., 2001).

Consumption of H_2O_2 during the UV/H_2O_2 process was also investigated in the UV/H_2O_2 process of CHA. It was observed that the H_2O_2 consumption increased from 2% in ultrapure water to 5% and 12% in presence of chloride and carbonate, respectively.

Despite the lower reactivity, the presence of chloride ion did not change the type of byproducts formed, nor was there an effect on the relative proportion of byproducts (Figure 2-7). The same behaviour was observed in the presence of carbonate ion (Figure 2-8).
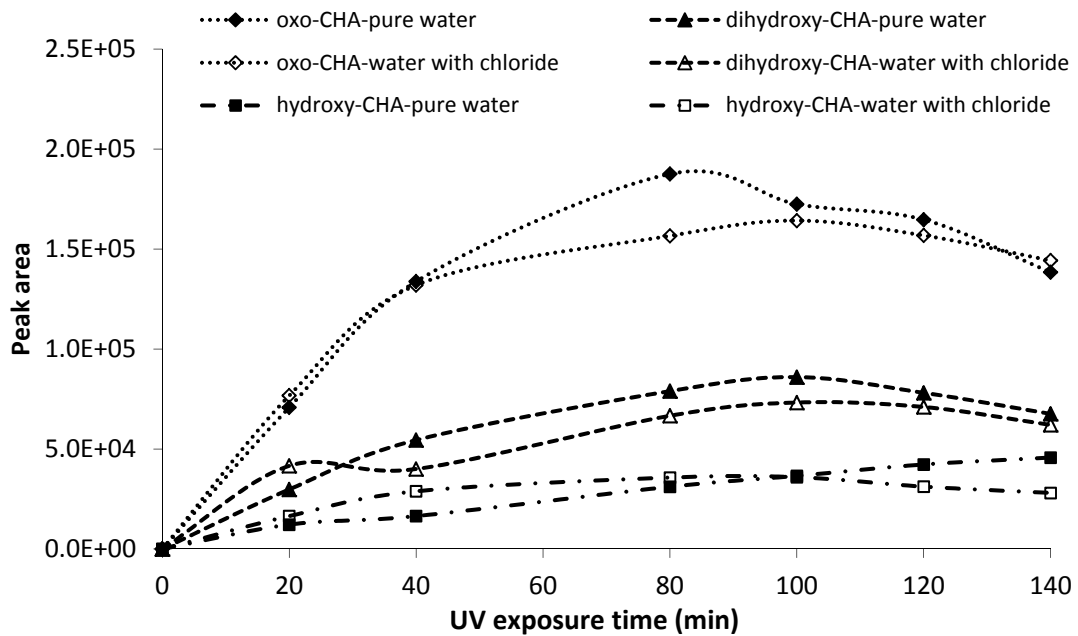
Figure 2-7. Formation of three major byproducts during UV/H_2O_2 degradation of CHA at pH 9 ([CHA]$_0$ = 50 mg/L, 300 mg/L H_2O_2, UV lamp irradiance = 0.11 mW/cm^2) in ultrapure water and in ultrapure water with chloride.
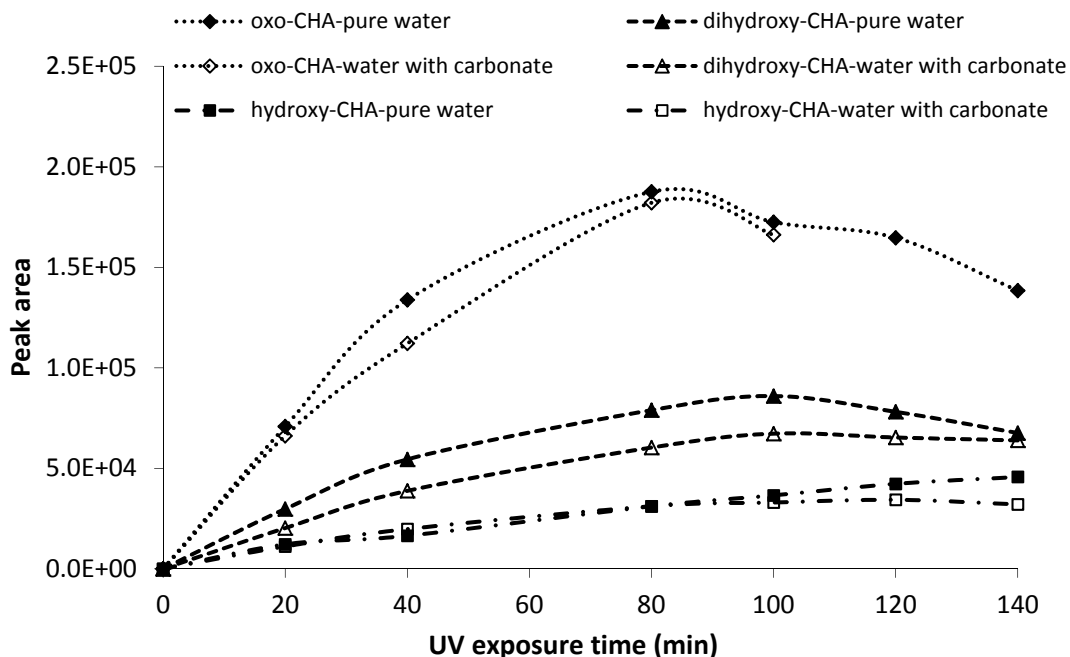
Figure 2-8. Formation of three major byproducts during UV/H_2O_2 degradation of CHA at pH 9 ([CHA]$_0$ = 50 mg/L, 300 mg/L H_2O_2, UV lamp irradiance = 0.11 mW/cm^2) in ultrapure water and in ultrapure water with carbonate; retention times: 4-oxo-CHA 12 min; dihydroxy-CHA 17 min; cis-4-hydroxy-CHA 13 min.

2.3.5 The effect of real OSPW water matrix on decomposition of CHA

It is expected that dissolved organic matter in water can affect the decomposition rate of pollutants by the UV/H_2O_2 process. As with pollutants, organic compounds may react directly with H_2O_2, compete for •OH or absorb UV light. Organic compounds may also react with organic radical intermediates formed during the treatment, thus decreasing the decomposition rate of the target pollutants.

OSPW was treated with PAC in order to remove a portion of dissolved organic matter. After the PAC adsorption, the COD content, as well as the total extractable

organic acid concentration, were decreased significantly, while the alkalinity and Cl⁻ ion concentration remained unchanged (Table 2-3). In real applications of AOPs in oil sand industry, sequential treatments will be applied and it is crucial to know how each step of the OSPW treatment can affect the following step.

Table 2-3. OSPW quality parameters before and after PAC adsorption.

	COD[1] (mg/L)	Extractable Organic Acids[2]	Alkalinity[3] (mg/L)	[Cl⁻][4] (mg/L)	UV absorbance[5]	pH
OSPW	225–258	65–70 mg/L	672–708	400-600	0.605	8.4-8.8
OSPW after PAC adsorption	< 10	< 5 mg/L	660–697	400-600	0.040	8.6-8.9

[1]Chemical Oxygen demand (as mg O_2/L), measured according to Standard Method 5220 D; [2] measured using FT-IR; [3]measured based on Standard Method 2320 (mg/L as $CaCO_3$); [4]measured by Dionex-ICS-2500 ion chromatography; [5]the average UV absorbance at 253.7 nm

As expected, the highest CHA degradation rate occurred in ultrapure water, followed by the OSPW after PAC adsorption, followed by the slowest rate in raw OSPW (Figure 2-9). The pseudo-first order rate constant for CHA degradation in raw OSPW was 81% lower than that in ultrapure water. This may be explained by the fact that in the presence of COD, bicarbonate, NAs and organic compounds in the OSPW reduce the •OH concentration that is available to react with CHA, due to their combined scavenging effect (Afzal et al., 2010; Chelme-Ayala et al., 2010). Furthermore, some of the

substances present in the OSPW absorb UV at 253.7 nm (the absorbance of OSPW at 253.7 nm is presented-Table 2-3); hence they may compete for photons, thus reducing the formation of •OH radicals and the subsequent degradation rate of CHA.

Compared with raw OSPW, the CHA degradation rate increased after PAC adsorption, but still remained significantly lower (62%) than its rate in ultrapure water. There are unknown constituents such as organic matter which are likely radical scavengers. The formation of byproducts during decomposition of CHA in OSPW was not investigated because of high interferences in chromatographic determination from water matrix.
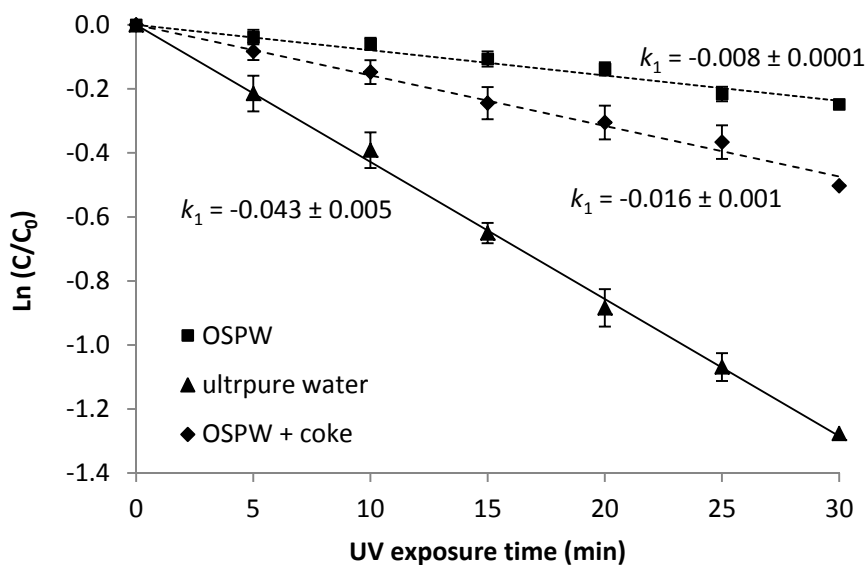
Figure 2-9. Decomposition of CHA in raw OSPW and OSPW after PAC adsorption (both filtered through 0.45 μm) ([CHA]$_0$ = 50 mg/L, 300 mg/L H_2O_2); k_1: pseudo-first-order rate constant (min^{-1}); UV lamp irradiance = 0.20 mW/cm^2.

50

2.4 Environmental significance and future work

This study demonstrates that UV/H$_2$O$_2$ is a promising process for the removal of CHA as a model NA compound in ultrapure water. This process can be applied to other NAs due to the similarity of the basic structure. However, the presence of radical scavengers needs to be carefully considered during the NA remediation in OSPW, because they may impose the adverse effect on the process efficiency. To compare different processes for management purposes, the treatment of model NA compounds using ozonation and the O$_3$/H$_2$O$_2$ process will be studied. Advanced oxidation technologies can be considered as great potential for OSPW remediation, especially if these processes are applied in combination with microbial degradations.

2.5 Conclusions

The hydroxyl radical initiated degradation of a model OSPW alicyclic carboxylic acid, cyclohexanoic acid, in presence of carbonate and chloride ion, at two different pHs, and in OSPW matrix revealed new information about the feasibility of application of UV/H$_2$O$_2$ process for the removal of NAs from OSPW as follows.

- Increasing the concentration of H$_2$O$_2$ increased the CHA degradation rate up to the optimal molar concentration ratio of 23.
- Changing the pH in ultrapure water had no significant effect on the CHA degradation rate and the formed byproducts.

- Carbonate and chloride ions, at concentrations similar to those in the OSPW, decreased the CHA degradation rate by 55% and 23%, respectively.

- The presence of the scavengers decreased the formation and further degradation of byproducts.

- Besides carbonate and chloride, other organic and inorganic compounds present in OSPW competed with CHA for reaction with •OH.

- PAC adsorption of OSPW may increase the efficiency of the UV/H_2O_2 process because of the removal of the some organic compounds.

As an overall conclusion, it was demonstrated that UV/H_2O_2 is an applicable method for CHA removal as a model NA in ultrapure water. However, the effect of radical scavengers on treatment efficiency should be considered in the real OSPW NA remediation.

2.6 Recommendation

Acidification of OSPW, in order to decrease the concentration of the carbonate may improve the UV/H_2O_2 process efficiency. However, the higher scavenging effect of chloride at lower pH and increasing the ionic strength of the water because of the acidification may reduce the benefit of carbonate removal.

2.7   References

Acero JL, von Gunten U. Influence of carbonate on the ozone/hydrogen peroxide based advanced oxidation process for drinking water treatment. Ozone-Sci Eng 2000;22: 305-28.

Afzal A, Oppenlander T, Bolton JR, Gamal El-Din M. Anatoxin-a degradation by advanced oxidation processes: vacuum-UV at 172 nm, photolysis using medium pressure UV and UV/H_2O_2. Water Res 2010;44: 278-86.

Allen EW. Process water treatment in Canada's oil sands industry: I. Target pollutants and treatment objectives. J Environ Eng Sci 2008a;7:123-38.

Allen EW. Process water treatment in Canada's oil sands industry: II. A review of emerging technologies. J Environ Eng Sci 2008b;7:499-524.

Anbar M, Meyerste D, Neta P. Reactivity of aliphatic compounds towards hydroxyl radicals. J Chem Soc B 1966;8:742-47.

Bielski BHJ, Cabelli DE, Arudi RL, Ross AB. Reactivity of HO_2/O^{2-} radicals in aqueous-solution. J Phys Chem Ref Data 1985;14:1041-100.

Bojanowska-Czajka A, Drzewicz P, Kozyra C, Nalecz-Jawecki G, Sawicki J, Szostek B, Trojanowicz M. Radiolytic degradation of herbicide 4-chloro-2-methyl phenoxyacetic acid (MCPA) by gamma-radiation for environmental protection. Ecotoxicol Environ Saf 2006;65:265-77.

Busset C, Mazellier P, Sarakha M, De Laat J. Photochemical generation of carbonate radicals and their reactivity with phenol. J Photoch Photobio A 2007;185:127-32.

Buxton GV, Greenstock CL, Helman WP, Ross AB. Critical-review of rate constants for reactions of hydrated electrons, hydrogen-atoms and hydroxyl radicals ($\bullet$OH/$\bullet$O$^-$) in aqueous-solution. J Phys Chem Ref Data 1988;17:513-886.

Chelme-Ayala P, Gamal El-Din M, Smith DW. Degradation of bromoxynil and trifluralin in natural water by direct photolysis and UV plus H_2O_2 advanced oxidation process. Water Res 2010;44:2221-8.

Clesceri L S, Greenberg AE, Eaton AD. Standard methods for the examination of water and wastewater, AWWA, 2005.

Draganic ZD, Negron-Mendoza A, Sehested K, Vujosevic SI, Navarro-Gonzales R, Albarran-Sanchez MG, Draganic IG. Radiolysis of aqueous solutions of ammonium bicarbonate over a large dose range. Radiat Phys Chem 1991;38:317-21.

Drzewicz P, Afzal A, Gamal El-Din M, Martin JW. Degradation of a model naphthenic Acid, cyclohexanoic acid, by vacuum UV (172 nm) and UV (254 nm)/H_2O_2. J Phys Chem A 2010;114:12067-74.

Gamal El-Din M, Fu HJ, Wang N, Chelme-Ayala P, Perez-Estrada L, Drzewicz P, Martin JW, Zubot W, Smith DW. Naphthenic acids speciation and removal during

petroleum-coke adsorption and ozonation of oil sands process-affected water. Sci Total Environ 2011;40:5119-25.

Headley JV, Du JL, Peru KM, McMartin DW. Electrospray ionization mass spectrometry of the photodegradation of naphthenic acids mixtures irradiated with titanium dioxide. J Environ Sci Heal A 2009;44:591-7.

Headley JV, McMartin DW. A review of the occurrence and fate of naphthenic acids in aquatic environments. J Environ Sci Heal A 2004;39:1989-2010.

Held AM, Halko DJ, Hurst JK. Mechanisms of chlorine oxidation of hydrogen-peroxide. J Am Chem Soc 1978;100:5732-40.

Hewgill FR, Proudfoot GM. Regioselective oxidation of aliphatic-acids by complexed hydroxyl radicals. Aust J Chem 1976;29:637-47.

Holowenko FM, MacKinnon MD, Fedorak PM. Characterization of naphthenic acids in oil sands wastewaters by gas chromatography-mass spectrometry. Water Res 2002;36:2843-55.

Homlok R, Takacs E, Wojnarovits L. Radiolytic degradation of 2,4-dichlorophenoxyacetic acid in dilute aqueous solution: pH dependence. J Radioanal Nucl Chem 2010;284:415-9.

Jayson GG, Parsons BJ, Swallow AJ. Some simple, highly reactive, inorganic chlorine derivatives in aqueous-solution - their formation using pulses of radiation and

their role in mechanism of Fricke Dosimeter. J Chem Soc Faraday 1973;1597-607.

Klassen NV, Marchington D, McGowan HCE. H_2O_2 Determination by the I_3^- method and by $KMnO_4$ titration. Anal Chem 1994;66:2921-5.

Larson RA, Zepp RG. Reactivity of the carbonate radical with aniline derivatives. Environ Toxicol Chem 1988;7:265-74.

Liao CH, Kang SF, Wu FA. Hydroxyl radical scavenging role of chloride and bicarbonate ions in the H_2O_2/UV process. Chemosphere 2001;44:1193-200.

Lo CC, Brownlee BG, Bunce NJ. Mass spectrometric and toxicological assays of Athabasca oil sands naphthenic acids. Water Res 2006;40:655-64.

Martin JW, Barri T, Han XM, Fedorak PM, Gamal El-Din M, Perez L, Scott AC, Jiang JT. Ozonation of oil sands process-affected water accelerates microbial bioremediation. Environ Sci Technol 2010;44:8350-6.

Martin JW, Han XM, Peru KM, Headley JV. Comparison of high- and low-resolution electrospray ionization mass spectrometry for the analysis of naphthenic acid mixtures in oil sands process water. Rapid Commun Mass Spectrom 2008;22:1919-24.

Martire DO, Rosso JA, Bertolotti S, Le Roux GC, Braun AM, Gonzalez MC. Kinetic study of the reactions of chlorine atoms and $Cl_2^{\bullet-}$ radical anions in aqueous

solutions. II. Toluene, benzoic acid, and chlorobenzene. J Phys Chem A. 2001;105:5385-92.

Masliyah J, Zhou Z, Xu Z, Czarnecki J, Hamza H. Understanding water-based bitumen extraction from Athabasca oil sands. Can J Chem Eng. 2004; 82: 628–54.

Mazellier P, Leroy E, De Laat J, Legube B. Degradation of carbendazim by UV/H_2O_2 investigated by kinetic modelling. Environ Chem Lett 2003;1:68-72.

McMartin DW, Headley JV, Friesen DA, Peru KM, Gillies JA. Photolysis of naphthenic acids in natural surface water. J Environ Sci Heal A 2004;39:1361-83.

Neta P, Huie RE, Ross AB. Rate constants for reactions of inorganic radicals in aqueous-solution. J Phys Chem Ref Data 1988;17:1027-284.

Panades P, Ibarz A, Esplugas S. Photodecomposition of carbendazim in aqueous solutions. Water Res 2000;34:2951-4.

Parsons S. Advanced oxidation processes for water and wastewater treatment. IWA, London; 2004.

Prousek J. Advanced oxidation processes for water treatment: Photochemical processes. Chem Listy 1996;90:307-15.

Schramm LL, Stasiuk EN, MacKinnon M. Surfactants in Athabasca oil sands slurry conditioning, flotation recovery, and tailings process. In Surfactants, fundamentals and applications in the petroleum industry; Schramm, LL, Cambridge University Press; Cambridge, 2000.

57

Scott AC, MacKinnon MD, Fedorak PM. Naphthenic acids in athabasca oil sands tailings waters are less biodegradable than commercial naphthenic acids. Environ Sci Technol 2005;39:8388-94.

Scott AC, Young RF, Fedorak PM. Comparison of GC-MS and FT-IR methods for quantifying naphthenic acids in water samples. Chemosphere 2008a;73:1258-64.

Scott AC, Zubot W, MacKinnon MD, Smith DW, Fedorak PM. Ozonation of oil sands process water removes naphthenic acids and toxicity. Chemosphere 2008b;71:156-60.

Serjeant EP and Dempsey B. Ionization constants of organic acids in aqueous solution. Elsevier Sci & Technol Books; 1979.

Stenman D, Carlsson M, Jonsson M, Reitberger T. Reactivity of the carbonate radical anion towards carbohydrate and lignin model compounds. J Wood Chem Technol 2003;23:47-69.

Wu CL, Linden KG. Degradation and byproduct formation of parathion in aqueous solutions by UV and UV/H_2O_2 treatment. Water Res 2008;42:4780-90.

Yu XY. Critical evaluation of rate constants and equilibrium constants of hydrogen peroxide photolysis in acidic aqueous solutions containing chloride ions. J Phys Chem Ref Data 2004;33:747-63.

Yu XY, Barker JR. Hydrogen peroxide photolysis in acidic aqueous solutions containing chloride ions. II. Quantum yield of •OH radicals. J Phys Chem A 2003;107:1325-32.

Zhu R, Liu QX, Xu ZH, Masliyah JH, Khan A. Role of dissolving carbon dioxide in densification of oil sands tailings. Energ Fuel 2011;25:2049-57.

3 EFFECT OF MOLECULAR STRUCTURE ON THE RELATIVE REACTIVITY OF NAPHTHENIC ACIDS IN THE UV/H₂O₂ ADVANCED OXIDATION PROCESS[*]

3.1 Introduction

In Northern Alberta, bitumen is extracted from the oil sands using hot caustic water. The resulting large volumes of oil sands process-affected water (OSPW) must be stored in large tailings ponds because of a zero discharge policy (Masliyah et al., 2004). The acute and chronic toxicity of fresh OSPW to aquatic organisms are commonly attributed to a complex mixture of organic acids that include naphthenic acids (NAs) (Clemente and Fedorak, 2005). The concentration of NAs in tailing ponds range from 40 to 70 mg/L and can reach as high as 125 mg/L in fresh OSPW, as measured by Fourier transform infrared spectroscopy (FT-IR) (Allen, 2008). Reports by Garcia-Garcia et al. (2011) showed that commercial NAs, as well as the organic fraction of OSPW have immunotoxic properties by affecting immune gene expression in different mammalian organs. Increased mortality was also observed in fish after exposure to commercial NAs and extractable organic acids concentration of OSPW (Dokholyan and Magomedov, 1983).

NAs refer to a wide group of aliphatic and alicyclic carboxylic acids with the general formula: $C_nH_{2n+Z}O_2$, whereby n is the number of carbons and Z is zero or an even negative number referring to the number of saturated rings ($Z = 0$, no ring; $Z = -2$, one ring; $Z = -4$, two rings, etc.; however Z may also be confounded by the presence of double bonds) (Rogers et al., 2002). The physical, chemical, and toxicological properties of NAs depend on their molecular structure (Qu et al., 2007; Han et al., 2008; Martin et al., 2008; Frank et al., 2009; Jones et al., 2011). Naphthenic acids are amphipathic compounds with surfactant-like properties that can accumulate at aqueous/non-aqueous interfaces such as between water and particles (Rogers et al., 2002). Individual NAs were shown to have different toxicities to *Vibrio fischeri* because of differences in hydrophobicity and aqueous solubility (Jones et al., 2011). It has been reported that NAs with lower molecular weights (more hydrophilic) are more toxic than those ones with the higher molecular weights (more hydrophobic and less water soluble) (Jones et al., 2011). Studies on the microbial degradation of OSPW NAs, or of model NA compounds showed a relationship between biodegradability and molecular structure. Smith et al. (2008) also showed that biotransformation decreased as the NA side chain branching increased. Additionally, the intramolecular hydrogen bonding of geometric isomers of model NAs was reported to make slow microbial biodegradation (Headley et al., 2002). The above literatures demonstrate that biodegradation of NAs is strongly correlated with structure, and thus it is wise to understand the structure-reactivity of any treatment proposed for OSPW.

The degradation of NAs using photolysis and advanced oxidation processes (AOPs) has been investigated (McMartin et al., 2004; Scott et al., 2008; Headley et al., 2009; Drzewicz et al., 2010; Martin et al., 2010; Perez-Estrada et al., 2011). NAs do not absorb light in the solar wavelength region; therefore, direct photolysis using both natural and artificial sunlight is not an effective process for the degradation of NAs. The estimated half-life of *cis-* and *trans-* isomers of NAs exposed to solar and ultraviolet (UV) light at 253.7 (~254) nm was in the range of thousands of hours, to tens of hours, respectively, in experiments using natural water (McMartin et al., 2004). The presence of inorganic and organic constituents in natural water leads the degradation mechanism to indirect photolysis due to the possible formation of radicals. Previously, it was shown that UV/hydrogen peroxide (H_2O_2) is an effective AOP for the degradation of a model NA compound, cyclohexanoic acid (Afzal et al., 2012). During the ozonation process at alkaline pH (pH = 8), in which both ozone and hydroxyl radicals (•OH) are involved, model NA compounds and OSPW NAs with more rings and more carbons underwent faster degradation (Perez-Estrada et al., 2011). Whether or not the same structure-reactivity can be achieved in other AOPs, where only •OH is present, remains to be tested.

The main objective of this study was to investigate the relative structure-reactivity of pure model NAs and complex mixture of real OSPW NAs toward •OH in the UV/H_2O_2 AOP. Based on a previous study of ozonation of NAs, here it was hypothesized that an increase in the numbers of carbon atoms and rings, as well as increasing alkyl

branching in the NA molecule structure would lead to higher levels of oxidation (i.e., more reactivity) towards •OH. A relative kinetics method, using selected model NA compounds, was used to evaluate the effect of NA structure on reactivity towards •OH. The structure-reactivity of the complex and undefined mixture of NAs in OSPW was also evaluated by the UV/H_2O_2 AOP.

3.2 Material and methods

3.2.1 Chemicals and reagents
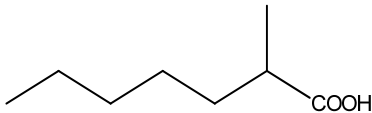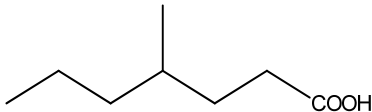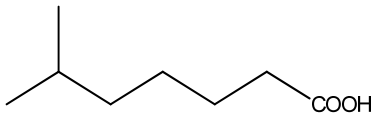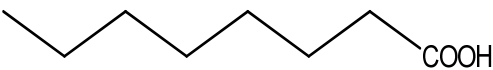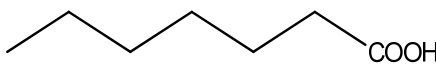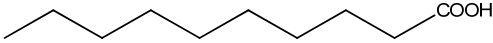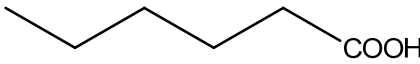
The following model NA compounds were purchased from TCI America Organic Chemicals (Oregon, US): OA (octanoic acid, $C_8H_{16}O_2$, Z = 0), 2meHPA (2-methylheptanoic acid, $C_8H_{16}O_2$, Z = 0), 4prCHA (4-propylcyclohexanecarboxylic acid, $C_{10}H_{18}O_2$, Z = –2), 4buCHA (4-butylcyclohexanecarboxylic acid, $C_{11}H_{20}O_2$, Z = –2), 4tbuCHA (4-*tert*-butylcyclohexanecarboxylic acid, $C_{11}H_{20}O_2$, Z = –2), 4meCHA (4-methylcyclohexanecarboxylic acid, $C_8H_{14}O_2$, Z = –2), HPA (heptanoic acid, $C_7H_{14}O_2$, Z = 0), and compound HXA (hexanoic acid, $C_6H_{12}O_2$, Z = 0).
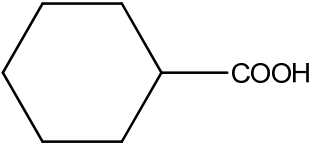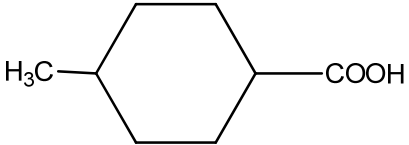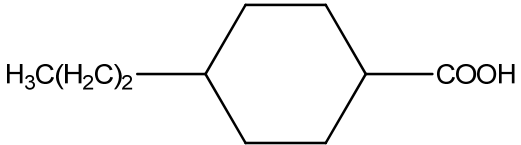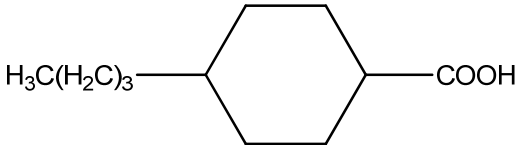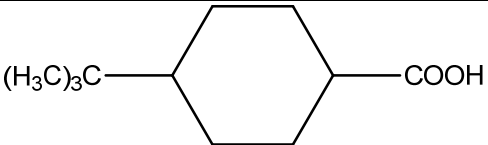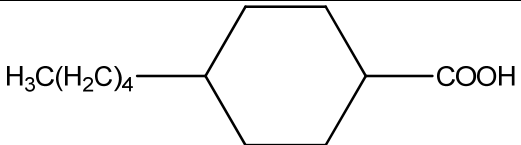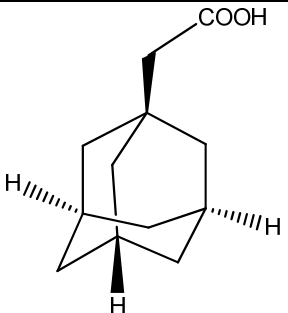
Model NA compounds 4meHPA (4-methylheptanoic acid, $C_8H_{16}O_2$, Z = 0) and 6meHPA (6-methylheptanoic acid, $C_8H_{16}O_2$, Z = 0) were purchased from Narchem Corporation (Chicago, US).

Model NA compounds 4pnCHA (4-pentylcyclohexanecarboxylic acid, $C_{12}H_{22}O_2$, Z = –2), AA (1-adamantaneacetic acid, $C_{12}H_{18}O_2$, Z = -6), CHA (cyclohexanecarboxylic acid, $C_7H_{12}O_2$, Z = –2), DA (decanoic acid, $C_{10}H_{20}O_2$, Z = 0), and also the internal

standard (tetradecanoic acid-1-^{13}C, $C_{14}H_{28}O_2$, Z = 0) were obtained from Sigma-Aldrich

Canada (Oakville, ON, Canada). Chemical structures of all the model NA compounds are

presented in Table 3-1.

Table 3-1. Chemical structure of the model NA compounds.

Compound	Formula	Structure
2-methylheptanoic acid	$C_8H_{16}O_2$	
4-methylheptanoic acid	$C_8H_{16}O_2$	
6-methylheptanoic acid	$C_8H_{16}O_2$	
octanoic acid	$C_8H_{16}O_2$	
heptanoic acid	$C_7H_{14}O_2$	
decanoic acid	$C_{10}H_{20}O_2$	
hexanoic acid	$C_6H_{12}O_2$	

Compound	Formula	Structure
cyclohexanecarboxylic acid	$C_7H_{12}O_2$	
4-methylcyclohexanecarboxylic acid	$C_8H_{14}O_2$	H_3C—⬡—COOH
4-propylcyclohexanecarboxylic acid	$C_{10}H_{18}O_2$	$H_3C(H_2C)_2$—⬡—COOH
4-butylcyclohexanecarboxylic acid	$C_{11}H_{20}O_2$	$H_3C(H_2C)_3$—⬡—COOH
4-*tert*-butylcyclohexanecarboxylic acid	$C_{11}H_{20}O_2$	$(H_3C)_3C$—⬡—COOH
4-pentylcyclohexanecarboxylic acid	$C_{12}H_{22}O_2$	$H_3C(H_2C)_4$—⬡—COOH
1-adamantaneacetic acid	$C_{12}H_{18}O_2$	

Catalase from bovine liver (2950 units/mg solid) was purchased from Sigma-Aldrich. Other chemicals and reagents including 50% sodium hydroxide, 80% perchloric acid, 30% H_2O_2, ammonium acetate, acetic acid, and methanol were purchased from Fisher Scientific Co. Canada (Edmonton, AB, Canada).

Ultrapure water was obtained from a Millipore and Elga system equipped with an Elix UV lamp (Manufacturer). OSPW was supplied by Syncrude Canada Ltd. (Fort McMurray, AB, Canada). Table 3-2 shows the main characteristics of OSPW.

Table 3-2. Characteristics of OSPW.

Parameter	Average value
pH	8.77 ± 0.03
Turbidity (NTU)	186 ± 16
Total organic carbon (mg/L)	72 ± 2
Chemical oxygen demand (mg/L)	317 ± 17
Biochemical oxygen demand (mg/L)	5.58 ± 0.06
Carbonate (mg/L)	26 ± 3
Bicarbonate (mg/L)	587 ± 4
Sodium (mg/L)	857 ± 15
Chloride (mg/L)	579 ± 20
Sulfate (mg/L)	160 ± 5
Nitrate (mg/L)	8.60 ± 0.03

3.2.2 UV/H₂O₂ experiments using model NA compounds

All the UV/H$_2$O$_2$ experiments were performed using a UV collimated beam apparatus (Calgon Carbon Corporation, Pittsburg, PA, USA) equipped with a 10 W low-pressure (LP) UV lamp with a monochromatic emission predominantly at 253.7 nm, and with irradiance at the sample position of 0.30 mW/cm^2.

Stock solution (100 mg/L - except for the compounds with lower water solubility) of each model compound was prepared in a 0.1 N solution of NaOH. The UV/H$_2$O$_2$ experiments were performed using the same molar concentration of a pair of compounds to evaluate their relative kinetics for specific reason (the number of carbons, alkyl branching, and cyclicity). For this, the solution of 0.04 mM of binary mixtures of compounds being compared was prepared and the pH of the solution was adjusted to 8 (the usual pH of OSPW). Then, 15 mL of the mixture of two compounds were taken and H$_2$O$_2$ with the ratio of 1:23 (Drzewicz et al., 2010) was added right prior the UV exposure. The solution was irradiated to the LP UV lamp with a 17 cm distance from the top of the solution. The samples were taken for the NA analysis at 2, 5, 7, 10, and 15 min. Catalase was used to quench any H$_2$O$_2$ residuals in the sample vials as needed.

The reactor was a glass Petri dish (60 mm diameter) and it was used under a completely mixed condition without turbulence (using a small magnetic stir bar). The experiments were carried out at room temperature (21 ± 2) °C. All the experiments were performed three times and combined for analysis. Regression analysis was performed and

95% confidence intervals were calculated for the slopes of the lines in the studies of relative kinetics.

3.2.3   UV/H_2O_2 experiments using OSPW

The OSPW was filtered through a 0.45 μm polyvinylidene fluoride (PVDF) membrane filter to remove particles and suspended organics for better UV performance by increasing the water transmittance. Because of the hydrophobic-hydrophobic interaction between NAs (due to their surfactant-like properties) and the membrane surface of the PVDF filter (Horowitz et al., 1996; Morrison and Benoit, 2001; Hedberg et al., 2011; Guo et al., 2012) as well as the possible attachment of the NAs to suspended particles, approximately 15% of NAs were removed by filtration. The initial concentration of NAs (after filtration) was approximately 40 mg/L (using UPLC - high resolution mass spectrometry). The ratio of H_2O_2 to NA concentration (23) was established previously for cyclohexanoic acid as a model NA compound (Drzewicz et al., 2010) and was adopted in this study. However, more H_2O_2 had to be added to the OSPW because of the presence of •OH scavengers, including high concentrations of chloride and bicarbonate (579 ± 20 mg/L chloride and 587 ± 4 mg/L bicarbonate) (Pourrezaei et al., 2011). Therefore, H_2O_2 was added to 50 mL of OSPW to achieve an H_2O_2 concentration of 250 mg/L and exposed to the UV beam in an 80 mL beaker for 90 min. Samples were taken at 5, 10, 20, 30, 40, 60, 80, and 90 min of the treatment and analyzed for NAs.

3.2.4 Analysis of model NA compounds

All the model NA compounds were analyzed using a high performance liquid chromatograph (HPLC) coupled to an ion trap mass spectrometer (Varian 500-MS). A Phenomenex, C8, 5 μm, 150 mm × 3 mm column was used for separations of two compounds each time. The chromatographic conditions were slightly different for one pair of compounds to the other; however the most dominant separating method was as follows: A, 100% methanol, and B, 4 mM ammonium acetate (aqueous) with 0.1 % acetic acid, gradient elution from 55% to 85% A over 20 min and returned to 55% A for 10 min for re-equilibration. The flow was 200 μL/min with the 20 μL injection volume, and column temperature was 40 °C.

3.2.5 Analysis of OSPW NAs

For analysis of OSPW NAs, samples (5 mL) were centrifuged for 10 min at 10,000 RPM and 500 μL of the supernatant was placed in a 2 mL glass vial with 450 μL of methanol and 50 μL of an internal standard solution (tetradecanoic acid-1-^{13}C); final concentration of internal standard was 200 ng/mL. A Waters Acquity UPLC® System (Milford, MA, USA) was employed for efficient and rapid chromatographic separation of the NAs and oxidized products. Chromatographic separations were run on a Waters UPLC Phenyl BEH column (1.7 μm, 150 mm × 1 mm,) using a mobile phase of: A, 10 mM ammonium acetate solution prepared in Optima-grade water, and B, 10 mM ammonium acetate in 50% methanol 50% acetonitrile, both Optima-grade. Gradient

elution was as follows: 1% B for the first 2 min, then ramped to 60% B by 3 min, to 70% B by 7 min, to 95% B by 13 min, followed by a hold until 14 min and finally returned to 1% B, followed by a further 5.8 min re-equilibration time. The flow was constant at 100 μL/min and column temperature was kept at 50 °C, while samples were maintained at 4 °C. Detection was performed with a high resolution Synapt G2 HDMS mass spectrometer equipped with an electrospray ionization source operating in negative ion mode. The system was controlled using MassLynx® ver. 4.1. Tuning and calibration were performed using standard solutions of lucine enkaphenlin and sodium formate, respectively, provided by Waters Corporation (Milford, MA, USA). TargetLynx® ver. 4.1 was used for data analysis of the target compounds, and the relative ratio of the chromatographic peak area of each analyte to that of the internal standard was calculated for subsequent analysis.

3.2.6   Oxidation kinetics

A relative-kinetics method was used to determine the relative reactivity of a pair of model NA compound mixtures (Atkinson et al., 1983). In this method, the same molar concentrations of two compounds ($[A_0]$ and $[B_0]$ at time 0) were exposed to •OH for 30 min. The instantaneous concentration of A and B at each time point was [A] and [B]. A plot of $\ln([A_0]/[A])$ versus $\ln([B_0]/[B])$ was drawn which was linear (equation 3-1) with a slope of the ratio of the rate constants (k_A/k_B). A slope significantly greater than 1 indicates that A is more reactive than B. Similarly, a slope significantly less than 1

70

indicates that B is more reactive than A. Microsoft Excel® software was used to perform the regression analysis; if the 95% confidence interval for the slope did not include 1, the degradation (cause by •OH oxidation) kinetics of the two compounds was deemed to be significantly different.

$$\ln\left(\frac{[A_0]}{[A]}\right) = \frac{k_A}{k_B} \ln\left(\frac{[B_0]}{[B]}\right)$$
$$(3-1)$$

3.3   Results and discussion

3.3.1   Effect of a tertiary carbon on the relative reactivity of acyclic model NA compounds

The reactivity of carboxylic acids with •OH depends, in part, on the stability of the intermediate radicals due to hydrogen (H) atom abstractions, mainly at the α position (Hewgill and Proudfoot, 1976; Hewgill and Proudfoot, 1977). The stability of the radicals formed at the α position depends on the mesomeric effect of the dissociated carboxylic acid group. It is known that the presence of halogen atoms at the α position increases the mesomeric effect because of the increase in acid strength, whereas the presence of one or more methyl groups decreases the acid strength and hence the mesomeric effect in the molecule (Hewgill and Proudfoot, 1976). It has also been found that the deactivating effect of a methyl group arising from the mesomeric effect decreases with an increase in

71

the distance from the carboxylic acid group (Hewgill and Proudfoot, 1976). Minakata et al. (2009) showed that the electron-donating/withdrawing ability of a functional group affects the reactivity of the compounds towards •OH. It was shown that an electron-donating functional group, such as alkyl, increases the overall reaction rate because of a decrease in the activation energy (Minakata et al., 2009).

In this work, the effect of a tertiary carbon, and its position relative to the carboxylate group was studied using a set of four compounds. Linear octanoic acid (OA-$C_8H_{16}O_2$) was compared with three methyl substituted heptanoic acids with the same molecular formula (2meHPA, 4meHPA, and 6meHPA - $C_8H_{16}O_2$). It was shown that 2meHPA, with methyl substitution at the α position was significantly less reactive than the linear OA (based on the regression analysis with 95% confidence interval) (Figure 3-1) with the $k_{2meHPA}/k_{OA} = 0.93$ (0.89-0.97). On the other hand, 4meHPA was slightly more reactive than OA; (Figure 3-2) with the $k_{4meHPA}/k_{OA} = 1.04$ (1.01-1.07). Finally, the rate of 6meHPA was not significantly different from that of OA (Figure 3-3) with the $k_{6meHPA}/k_{OA} = 0.99$ (0.96-1.02). By adding an alkyl branching-point to the molecular structure, a tertiary carbon is introduced, and due to the higher stability of tertiary carbon-centered radicals, compared to primary and secondary radicals, it was expected that the rate would increase. However, the distance of the tertiary carbon from the COOH group may change the stability of the carbon-centered radicals (Anbar et al., 1966), and a one-directional trend was expected as the distance of the methyl group increased from the COOH group. Nonetheless, this behaviour was not observed and consequently, the effect

of a tertiary carbon on acyclic model NA compounds may have different effects on NA

degradation rates, depending on the position of the branching relative to the carboxylate

group.

Figure 3-1. Relative kinetics for binary mixture of model NA compounds using the UV/H_2O_2
process to study the effect of position of alkyl branching on the reactivity; OA and 2meHPA:
[NAs]: 0.04 mM; [H_2O_2]: 1.8 mM; UV exposure time: 15 min.

Figure 3-2. Relative kinetics for binary mixture of model NA compounds using the UV/H_2O_2 process to study the effect of position of alkyl branching on the reactivity, OA and 2meHPA: [NAs]: 0.04 mM; [H_2O_2]: 1.8 mM; UV exposure time: 15 min.

Figure 3-3. Relative kinetics for binary mixture of model NA compounds using the UV/H_2O_2 process to study the effect of position of alkyl branching on the reactivity; OA and 2meHPA: [NAs]: 0.04 mM; [H_2O_2]: 1.8 mM; UV exposure time: 15 min. Data points are from three experimental replicates combined for analysis.

In the study by Perez-Estrada et al. (2011), similar effect of a tertiary carbon on the structure-reactivity of OA, 2meHPA, 4meHPA, and 6meHPA was observed during ozonation (see Table 3-3). The slight discrepancy in the results with the present study may be due to the effect of molecular ozone during the ozonation process applied at alkaline pH (pH = 8). At this pH, the effects of both molecular ozone and •OH can be significant (Hoigné and Bader, 1976; Gottschalk, 2000). Molecular ozone may indeed not react directly with the NAs; however, it participates in secondary reactions with radicals, thereby affecting the reactivity.

In order to have better understanding of the structure-reactivity of linear NA compounds with different positions of branching, rate constants of the NAs used in this study were estimated using two models. The rates were calculated by the summation of the partial specific reactivities of H atoms at different positions in the molecule. Anbar et al. (1966) showed that hydrogen atoms in the α position to the carboxylate group react at 0.14, 1.75, and 5.3×10^8 $M^{-1} s^{-1}$ per H atom on a primary ($CH_3CO_2^-$), secondary ($RCH_2CO_2^-$), and tertiary ($R_2CHCO_2^-$) carbons, respectively. Hydrogen atoms in other positions react at 0.36, 3.0 and 8.4×10^8 $M^{-1} s^{-1}$ per H atom on a primary, secondary and tertiary carbon, respectively (Anbar et al., 1966). Using this model, relative reaction rates were estimated for OA, 2meHPA, 4meHPA, and 6meHPA (Anbar et al., 1966) (see Table 3-3).

Table 3-3. Estimated and measured relative rate of the reaction between model NA compounds OA, 2meHPA, 4meHPA, and 6meHPA with •OH.

Relative rates	Estimated[31] (Anbar et al. model)	Estimated (Minakata et al. model)	Experimental Ozonation (perez et al. 2011)	Experimental UV/H_2O_2 (this study)
2meHPA/OA	0.91	0.87	0.92	0.93 ± 0.04
4meHPA/OA	0.93	1.09	1.22	1.04 ± 0.03
6meHPA/OA	0.93	1.08	0.95	0.99 ± 0.03

Using the group contribution method (GCM) of Minakata et al. (2009), overall reaction rate constants, and relative rates, were calculated assuming an H-atom abstraction mechanism (Table 3-3). In this method, the reactivity of each individual C-H bond depends on the functional groups around it. For instance, the presence of an electron-withdrawing group such as a carboxylic acid (COOH) decreases the rate of abstraction at the C-H bond α to the COOH group by a factor of 0.043 (See Appendix B for detailed and example theoretical rate calculations). The experimental rate constants here were in good agreement with the Minakata et al. (2009) model, except for the ratio of 6meHPA/OA, but not in good agreement with Anbar et al. (1966). This discrepancy might arise from the difference in the experimental protocols, including the source of the •OH generated in the studies. Here, the experiments were performed in the presence of H_2O_2 and UV, and H_2O_2 may have an effect on the overall reactivity of the NAs due to

the possible reaction with intermediate radicals. Anbar et al. (1966) used the γ-ray radiolysis method, in which, pure •OH is generated. In a previous ozonation study (Perez-Estrada et al., 2011) there was also poor agreement with Anbar et al. (1966), possibly because molecular ozone may have an effect on the reactivity with NAs. Additionally, Anbar et al. (1966) developed the partial reactivities of H atoms using the isomers of pentanoic and hexanoic acid. We extrapolated their data for our compounds (i.e. octanoic acid and heptanoic substitutes), which may be a source of discrepancy due to the surfactant-like properties (Gottschalk et al., 2000; Koleva, 2012) of NAs with higher number of carbons; albeit the method of Minakata et al. (2009) also does not account for this. On the other hand, Minakata et al. (2009) accounted for all possible functional groups attached to each C for their rate calculation which makes their method more valid.

3.3.2 Effect of a quaternary carbon on the reactivity of alkyl substituted cyclic model NA compounds

For the investigation of the effect of alkyl branching on the reactivity of cyclic NA compounds in the UV/H_2O_2 process, two model compounds; 4buCHA and 4tbuCHA with the same number of carbons, hydrogens, and saturated rings ($C_{11}H_{20}O_2$, Z = -2) were selected. The results demonstrated that the presence of a *tert*-butyl substitution (i.e., a quaternary carbon) at position 4 of the saturated ring significantly decreased the reactivity compared with a linear butyl substitution (Figure 3-4) with the $k_{4tbuCHA}/k_{4buCHA} = 0.74$ (0.71-0.76). This was expected because quaternary carbon has no H available for

abstraction. The other available H atoms in 4tbuCHA molecule are attached to the three primary carbons ($3 \times RCH_3$) on *tert*-butyl group, and these have little reactivity because they form the least stable carbon-centred radicals during H abstraction. Comparable results were observed by Pérez-Estrada et al. (2011) during the ozonation of these model NA compounds. The estimated relative reactivity according to the model of Minakata et al. (2009) was 0.75, very similar to the experimental value.
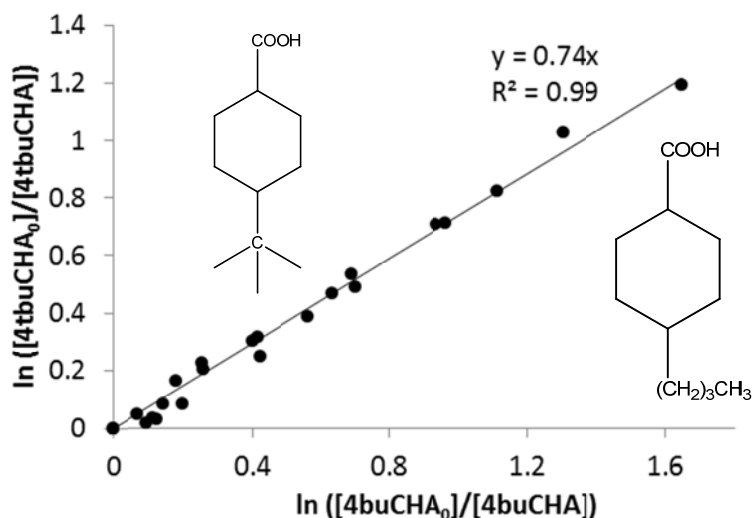
Figure 3-4. Relative kinetics for binary mixture of model NA compounds using the UV/H_2O_2 process to study the effect of quaternary carbon on the reactivity: [NAs]: 0.04 mM; [H_2O_2]: 1.8 mM; UV exposure time: 15 min. Data points are from three experimental replicates combined for analysis.

3.3.3   Effect of the carbon number on the reactivity of model NA compounds

The effect of the number of carbons on the reactivity of NAs in the UV/H_2O_2 process was investigated using a series of linear and cyclic model NA compounds. Among the linear model NAs, hexanoic acid (HXA- $C_6H_{12}O_2$) was selected as a reference

compound (rate constant with $\cdot OH = 3.3 \times 10^9$ M^{-1} s^{-1}) (Meylan and Howard, 1993) to establish the rate constants of octanoic acid (OA-$C_8H_{16}O_2$), and heptanoic acid (HPA-$C_7H_{14}O_2$). It was shown that heptanoic acid (7 carbons) was significantly less reactive than octanoic acid (8 carbons) (Figure 3-5); k_{HPA}/k_{OA} = 0.94 (0.87-0.96). The same behaviour was observed (Figure 3-6) for the compounds OA and HXA (6 carbons); k_{HXA}/k_{OA} = 0.94 (0.89-0.99).
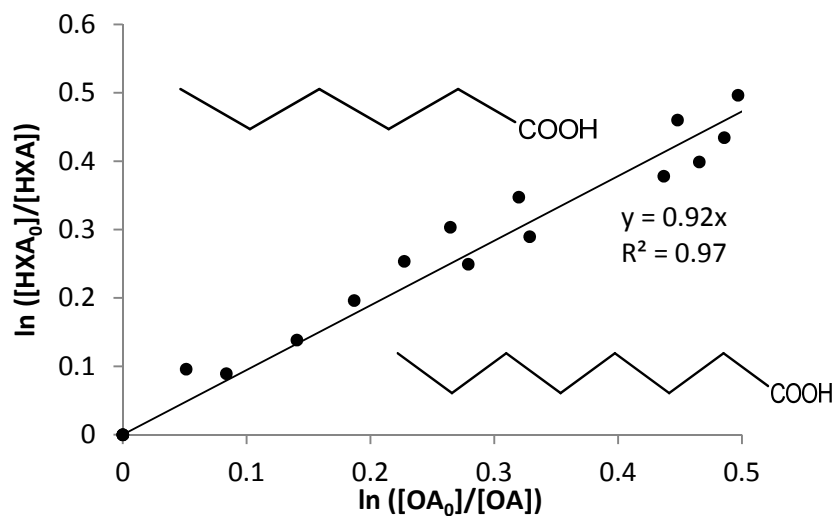
Figure 3-5. Relative kinetics for binary mixture of model NA compounds using the UV/H_2O_2 process to study the effect of number of carbons on the reactivity of linear compounds; OA and HXA: [NAs]: 0.04 mM; [H_2O_2]: 1.8 mM; UV exposure time: 15 min.
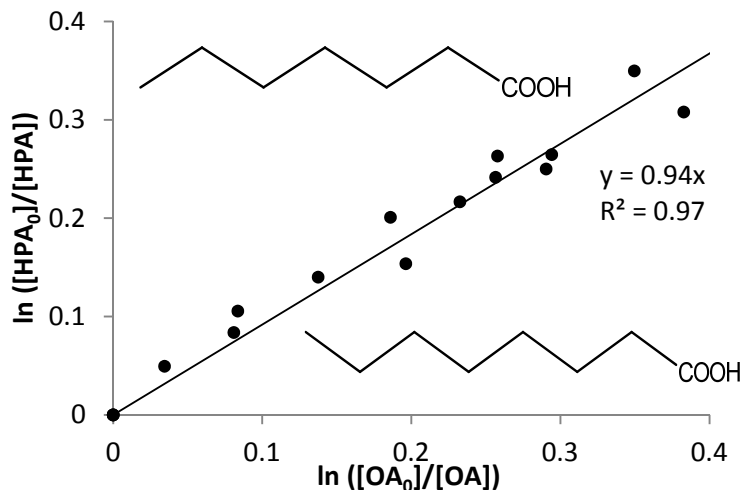
Figure 3-6. Relative kinetics for binary mixture of model NA compounds using the UV/H_2O_2 process to study the effect of number of carbons on the reactivity of linear compounds; OA and HPA: [NAs]: 0.04 mM; [H_2O_2]: 1.8 mM; UV exposure time: 15 min.

The rate constants increased from hexanoic acid to octanoic acid with increasing number of carbons (Figure 3-7). Interestingly, the rate constant for DA was two times higher than for octanoic acid, whereas comparing the rate constants of OA to HXA, the increase was only 20%. As shown in Figure 3-7, an increment of the degradation rate constant with increasing number of carbons was observed in linear compounds. The main reason for this increase may be explained by the increment of hydrogen atoms available for abstraction when one carbon is added to a compound, leading to higher reactivity. Moreover, in aqueous phase, the abstraction of H atom from C-H bond happens before an O-H bond because of the smaller bond dissociation energy of C-H bond (Luo, 2002). On the other hand, the alkyl groups weaken the C-H bond by releasing of steric compression

as these groups move apart to form a planar radical, increasing the •OH reactivity (Minakata et al., 2009).
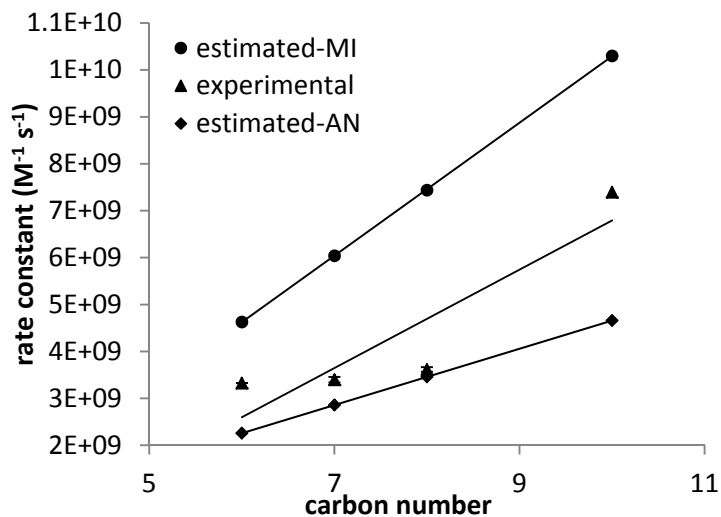
Figure 3-7. Effect of the carbon number on the rate constants of linear NAs; comparison between experimental data and theoretical data from Anbar et al. (AN) (1966) and Minakata et al. (2009) (MI) models.

In the case of the cyclic compounds, CHA was selected as a reference compound (rate constant = $5.5 \times 10^9 \, M^{-1} \, s^{-1}$) (Anbar et al,. 1966) for establishing the rate constants of 4meCHA, 4prCHA, and 4pnCHA. It was shown that 4-methyl cyclohexanoic acid (8 carbons) was significantly more reactive (Figure 3-8) than cyclohexanoic acid (7 carbons) with the $k_{4meCHA}/k_{CHA} = 1.16$ (1.11-1.21). The same behaviour was observed (Figure 3-9) for the compounds 4prCHA (10 carbons) and 4pnCHA (12 carbons) with the

k_{4pnCHA}/k_{4prCHA} = 1.15 (1.11-1.20), and also for the compounds CHA and 4prCHA with the k_{4prCHA}/k_{CHA} = 1.6 (1.59-1.78) (Figure 3-10).
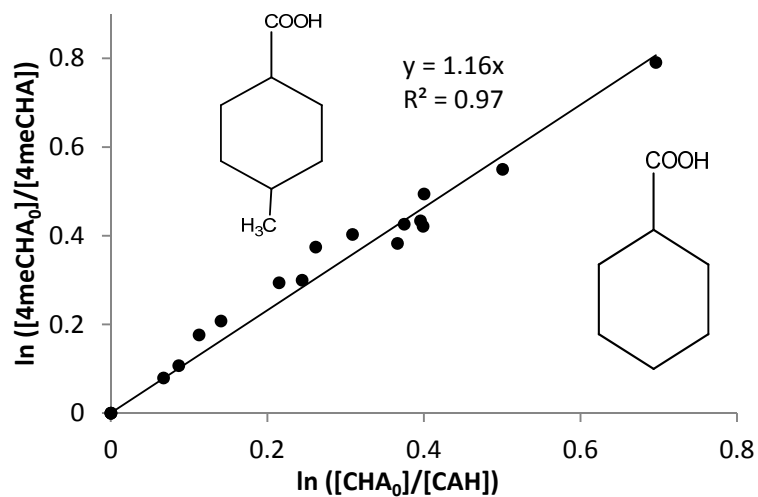
Figure 3-8. Relative kinetics for binary mixture of model NA compounds using the UV/H_2O_2 process to study the effect of number of carbons on the reactivity of cyclic compounds; CHA and 4meCHA: [NAs]: 0.04 mM; [H_2O_2]: 1.8 mM; UV exposure time: 15 min.
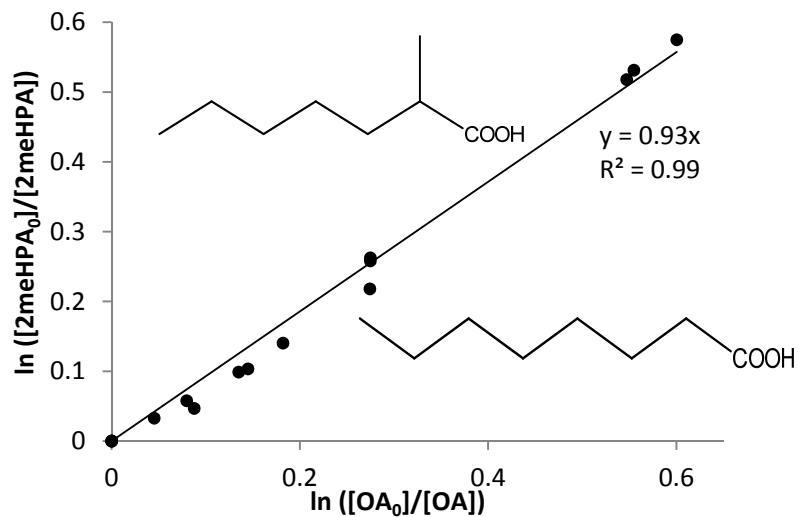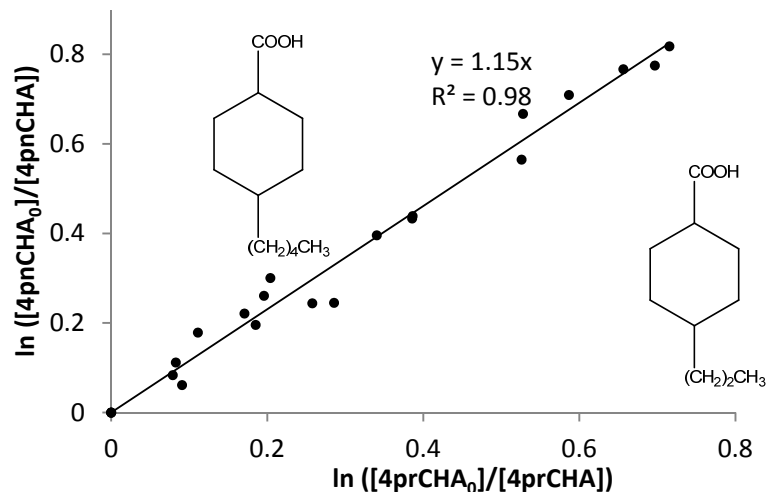
Figure 3-9. Relative kinetics for binary mixture of model NA compounds using the UV/H_2O_2 process to study the effect of number of carbons on the reactivity of cyclic compounds; 4prCHA and 4pnCHA: [NAs]: 0.04 mM; [H_2O_2]: 1.8 mM; UV exposure time: 15 min.
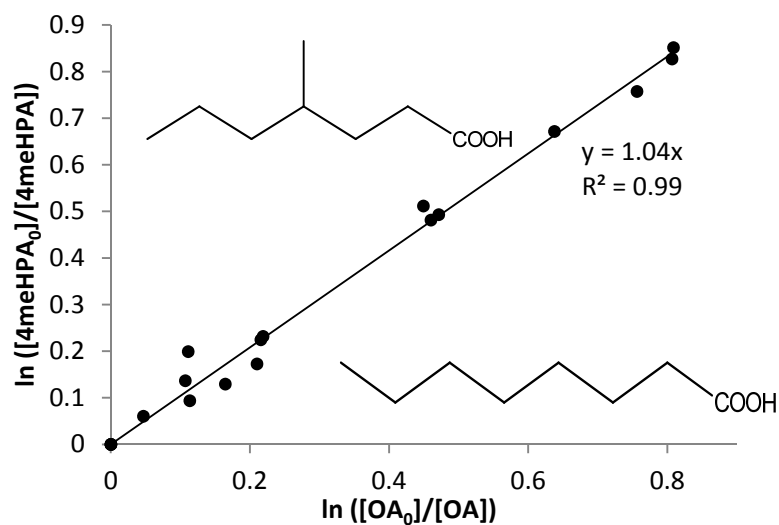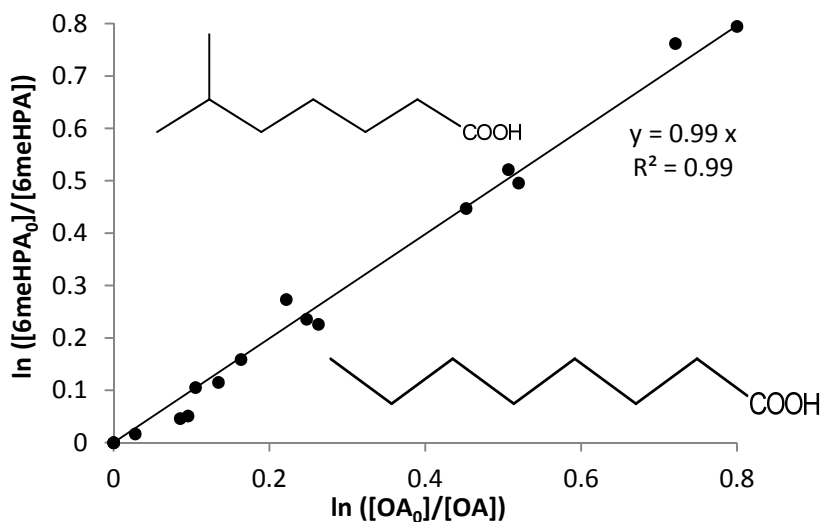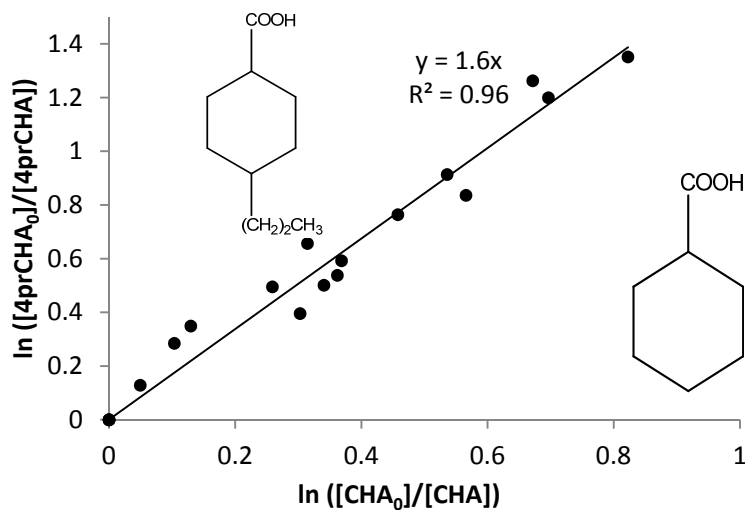

Figure 3-10. Relative kinetics for binary mixture of model NA compounds using the UV/H_2O_2 process to study the effect of number of carbons on the reactivity of cyclic compounds; CHA and 4prCHA: [NAs]: 0.04 mM; [H_2O_2]: 1.8 mM; UV exposure time: 15 min.

It was found that the rate constants increased linearly from CHA to 4pnCHA with increasing the number of substituent carbons (Figure 3-11). Theoretical rate constants calculated based on the two previously explained methods (Anbar et al., 1966; Minakata et al., 2009) are also presented (Figures 3-7 and 3-11), supporting the notion that increasing the reactivity is anticipated with more carbon (and hydrogen) atoms in the molecule.
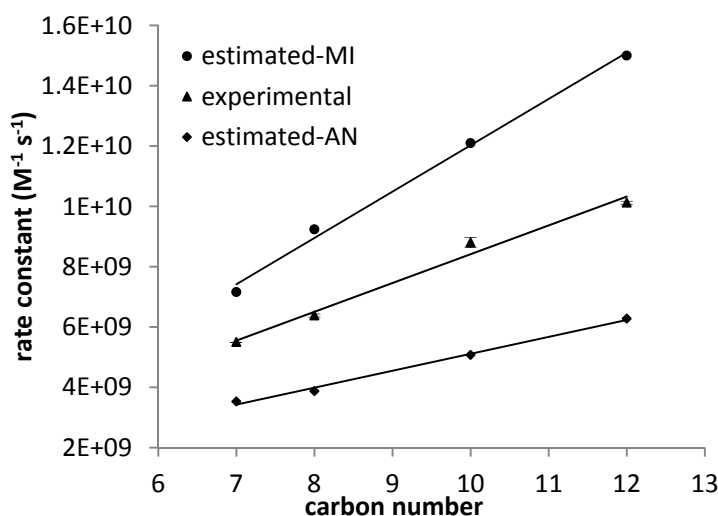
Figure 3-11. Effect of the carbon number on the rate constants of cyclic NAs; comparison between experimental data and theoretical data from Anbar et al. (AN) (1966) and Minakata et al. (2009) (MI) models.

3.3.4 Effect of cyclicity on the reactivity of model NA compounds

The effect of the saturated rings on the reactivity of NAs with •OH was studied using four model compounds. Linear decanoic acid (DA-$C_{10}H_{20}O_2$) was compared with

mono-cyclic 4-propylcyclohexanoic acid (4prCHA, $C_{10}H_{18}O_2$, Z = –2), and the mono-cyclic compound 4-pentylcyclohexanoic acid (4pnCHA, $C_{12}H_{22}O_2$, Z = –2) was compared with the tricyclic compound 1-adamantaneacetic acid (AA, $C_{12}H_{18}O_2$, Z = –6).

It was demonstrated (Figure 3-12) that cyclic 4prCHA was significantly more reactive than linear DA with the k_{4prCHA}/k_{DA} = 1.19 (1.13-1.25). A likely explanation is that the mono-cyclic compound (4prCHA) has two tertiary carbons, and the reactivity of H atoms on these tertiary carbons is higher compared with the reactivity of H atoms on primary and secondary carbons in linear compound (DA). The result is furthermore impressive in that the 4prCHA has two fewer hydrogen atoms than DA available for abstraction, yet 4prCHA was still more reactive. The ratio of rate constants of 4prCHA and DA, estimated using Anbar et al. (1966) was 1.10, and using Minakata et al. (2009) was 1.17, both in the range of the experimental data (1.13-1.25) in this study.

Contrary to the comparison of a linear and monocyclic NA compound, it was demonstrated (Figure 3-13) that 4pnCHA, a mono-cyclic NA, was more reactive than AA, which is effectively a three ringed structure; k_{4pnCHA}/k_{AA} = 1.14 (1.09-1.19). The number of carbons of the two compounds is the same; however, AA has 4 fewer H atoms compared with 4pnCHA. On the other hand, AA has 3 tertiary carbons in comparison with 4pnCHA that has only two tertiary carbons. Nonetheless, it is important to note that the energies of adamantyl tertiary C-H bonds (as in AA) are similar to the energy of a secondary C-H bond in an unstrained molecule (Kruppa and Beauchamp, 1986). With this in mind, and the fact that 4pnCHA has more hydrogen, this may explain why the

85

reactivity of tricyclic AA was lower than monocyclic 4pnCHA, even though AA has an extra tertiary carbon.
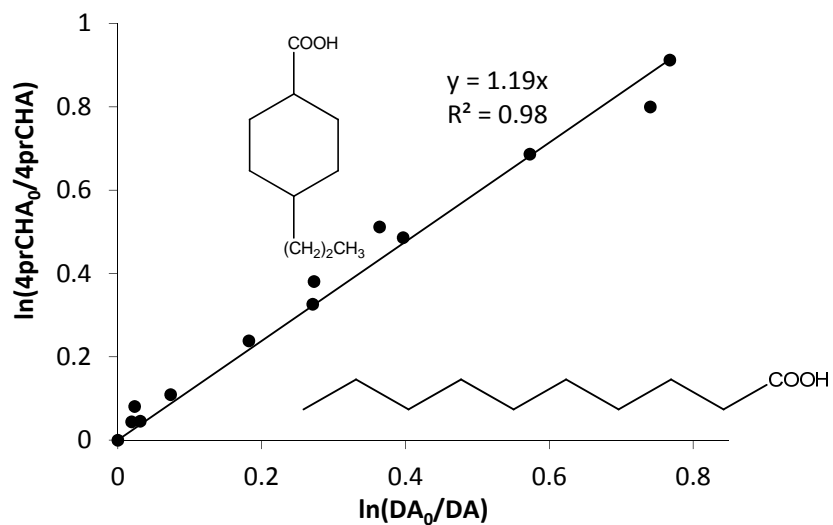
Figure 3-12. Relative kinetics for binary mixture of model NA compounds using the UV/H_2O_2 process to study the effect of cyclicity on the rates; linear and monocyclic.
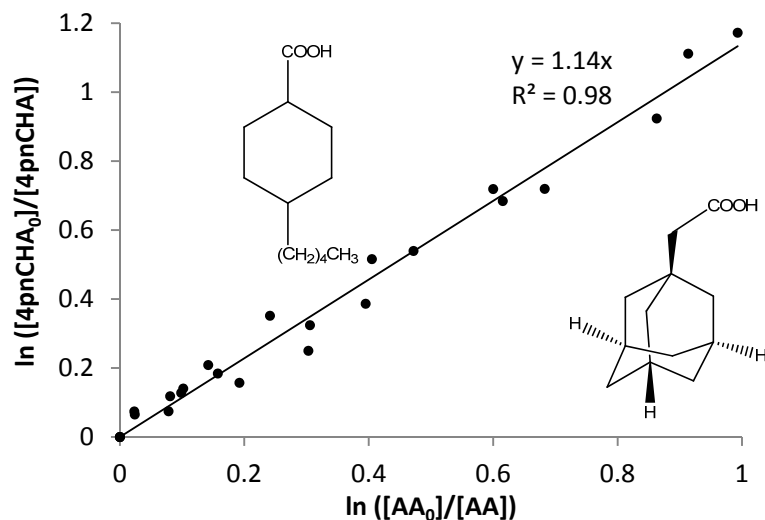
Figure 3-13. Relative kinetics for binary mixture of model NA compounds using the UV/H$_2$O$_2$ process to study the effect of cyclicity on the rates; monocyclic and tricyclic.

The stability of the formed radicals can also be an important consideration. The radical formed by H abstraction in AA at any of the saturated rings is expected to have sp^2 planar hybridization (Anbar et al., 1966). Such a radical would normally tend to have approximately a 120° angle between the bonds, but the cage structure of AA may make the attainment of such angles impossible due to the strain of the molecule (Schleyer et al., 1970). Interestingly, the results of an ozonation study (Perez-Estrada et al. 2011) showed contrary results for the same two model NA compounds. Pérez-Estrada et al. (2011) found that AA had higher reactivity than 4 pnCHA as a result of its 3 tertiary C-H bonds compared to the 2 tertiary C-H bonds in 4 pnCHA, confirming the higher overall reactivity of NAs with greater number of rings during ozonation process.

3.3.5 Application of the UV/H$_2$O$_2$ process for the degradation of OSPW NAs

The oxidation leading to the degradation of OSPW NAs was investigated in the presence of 250 mg/L H$_2$O$_2$ in OSPW over 90 min under UV irradiance. OSPW was filtered before the treatment in order to remove the suspended particles that may affect the efficiency of the process. Application of UV/H$_2$O$_2$ as an advanced oxidation process in water and/or wastewater treatment is not a primary or secondary step (Legrini et al., 1993). In most cases, these processes are applied as polishing steps after coagulation/flocculation followed by sedimentation and/or filtration, but before biological treatment to achieve the maximum efficiency of the UV/H$_2$O$_2$ process. In a control experiment, after 90 min in the dark, the concentration of NAs in the OSPW decreased by 13% in presence of 250 mg/L H$_2$O$_2$. There are numerous transition metal species in OSPW such as iron, vanadium, copper, manganese, etc., that may act as Fenton reagents with H$_2$O$_2$ in the dark (Goldstein et al., 1993; Watts et al., 2005) to form hydroxyl radicals (Allen, 2008; Gagné et al., 2011; Pourrezaei et al., 2011). In an additional control experiment, in the absence of H$_2$O$_2$, a slight degradation (~5%) in OSPW NAs was observed after 90 min of irradiation. The combined application of UV and H$_2$O$_2$ significantly increased OSPW NA removal efficiency. After 60 min of the process, 92% of NAs were removed. The NA removal further increased to 97% after 80 min and reached 99% after 90 min. The observed overall pseudo first-order degradation rate of the total OSPW NAs in UV/H$_2$O$_2$ process was 0.050 min^{-1} which is equivalent to the fluence

based rate of 0.01 cm^2/mJ (Figure 3-14). Detailed calculations of UV dose are presented in Appendix.

k' = -0.01
R^2 = 0.97
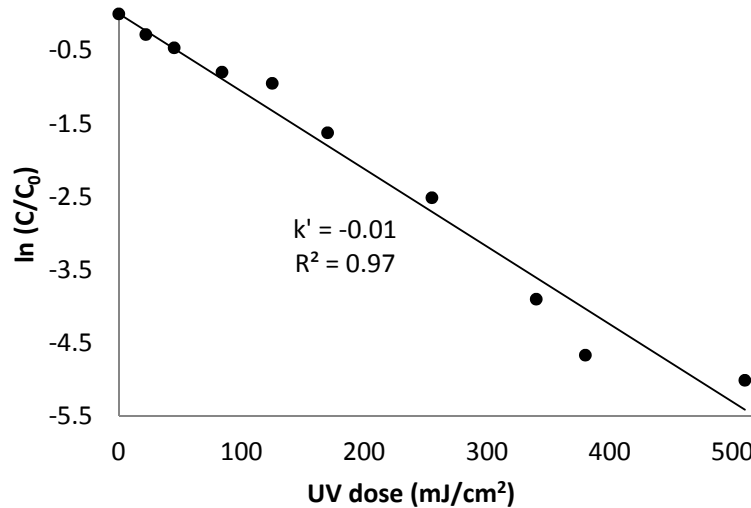
Figure 3-14. Degradation of OSPW NAs using UV/H$_2$O$_2$. Fluence based rate constant is in cm^2/mJ.

Because the oxidation of organic compounds may lead to the formation of byproducts, in some cases more toxic than their precursors, the acute toxicity of untreated and treated OSPW samples was measured using the Microtox bioassay (Figure 3-15). The results indicated that the toxic effects of the OSPW samples on the *Vibrio fischeri* decreased after UV exposure. The volume percent of sample that caused a 20% decrease in luminescence (IC$_{20}$) increased (i.e. reduction of toxicity) from 36.5 ± 0.3% in untreated OSPW to 47.3 ± 2.8% in treated OSPW after 90 min of UV exposure. These results indicate that UV/H$_2$O$_2$ has a promising potential to be used as a treatment alternative for the detoxification of OSPW. However, further research is warranted to investigate the

effect of the OSPW matrix on the treatment efficiency and to optimize the treatment performance.
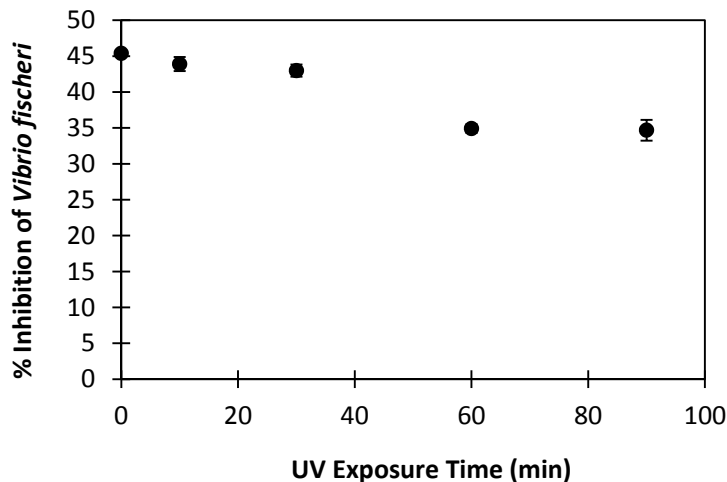
Figure 3-15. Toxic effects of treated OSPW samples on *Vibrio fischeri* using 81.9% screening test Microtox protocol.

3.3.6 Structure reactivity of OSPW NAs in the UV/H$_2$O$_2$ process

The structure dependence of the observed overall pseudo-first order kinetics of OSPW NAs in UV/H$_2$O$_2$ process after 40 min of UV exposure is shown in Figure 3-16. In general, within each Z group of NAs, by increasing the number of carbons, the pseudo-first order rate constant also increased. For instance, for Z = –4 NAs (i.e. NAs with 2 saturated rings) the pseudo-first order degradation rate constants for NAs with n = 13 to n = 17 were as follows: 0.0295 ± 0.013, 0.0324 ± 0.012, 0.0347± 0.013, 0.0390 ± 0.018, and 0.0430 ± 0.008 min^{-1}, respectively. This trend with number of carbon was expected,

and was observed with the model compounds (See Appendix C for NA speciation Figures and Tables).
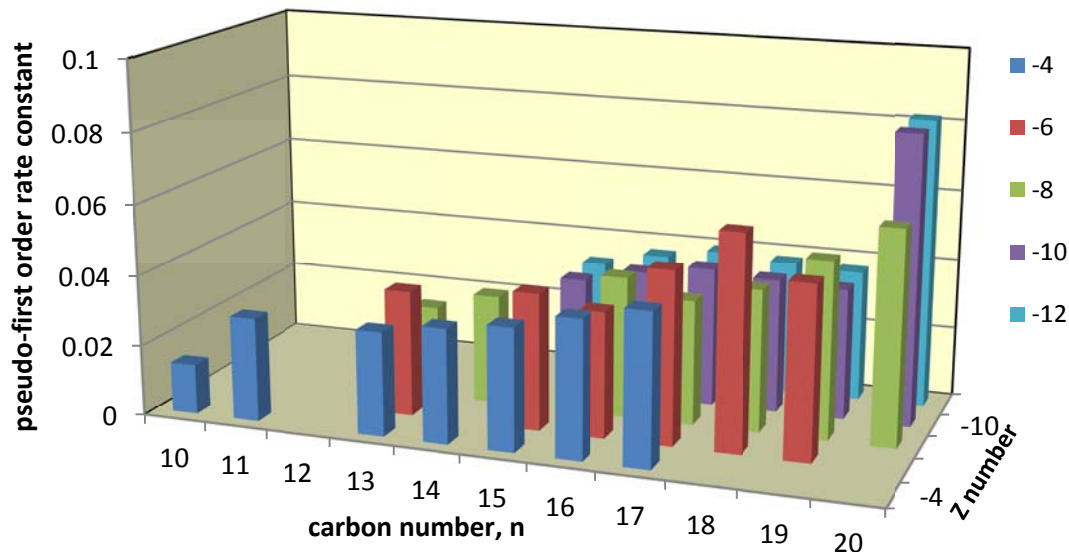
Figure 3-16. Structure dependence of pseudo-first order kinetics of OSPW NAs (250 mg/L H_2O_2 and 40 min UV exposure).

Among NAs with the same number of carbons, no consistent specific trend, in the degradation rates, was observed with respect to Z. For instance, in the group of n = 17, the degradation rates from Z = –4 to Z = –12 were as follows: 0.0430 ± 0.008, 0.0489 ± 0.006, 0.0354 ± 0.016, 0.0395 ± 0.007, and 0.0395 ± 0.007 min^{-1}, respectively. It is not clear why for the higher Z numbers, the rates start decreasing in some cases; however, this behaviour was similar to that of model NA compounds. The possible reason of this behaviour might arise from the energy bond of tertiary carbon in compounds with higher numbers of the rings. Interestingly, the structure reactivity of OSPW NAs in the

91

ozonation process was the opposite, with compounds with more rings undergoing faster degradation.

It should be noted that the Z number in the NA formula may be equivalent to the presence of a carbon double bond and/or aromatic rings in the molecule (Mohamed et al., 2008). It is well-known that ozone is highly reactive with aromatic compounds and carbon double bonds (Dore et al., 1980; Hoigne and Bader, 1983; Hoigne and Bader, 1983); therefore, the behaviour of OSPW NAs during the ozonation process is expected due to the presence of molecular ozone.

3.4 Environmental significance

Previous studies showed that the ozonation of OSPW can degrade NAs, but some un-oxidized fractions, that are easily biodegradable, remain in the solution (Martin et al., 2010). Here we examined if the same behaviour might be expected in the UV/H_2O_2 process due to similar structure reactivity. However, we have shown that the structure-reactivity of cyclic compounds is different, suggesting that •OH or molecular ozone may be important determinants of the overall reactivity of NA compounds. The findings of the current study showed that NAs with higher number of carbons are preferentially degraded in the UV/H_2O_2 process. The relationship between the degradation rate and the number of rings showed no specific trend among NAs with one or more rings. The application of UV/H_2O_2 AOP is currently being studied to determine its potential as a viable alternative to accelerate the degradation persistent organic compounds in OSPW. Further studies

investigating the effect of UV/H_2O_2 on subsequent microbial biodegradation are underway.

3.5 Conclusions

Highly cyclic or branched NAs are highly biopersistent in tailings ponds, thus understanding structure-reactivity relationship for NAs is very important for OSPW reclamation. In this study, it was hypothesized that large, branched and cyclic NAs may be better oxidized in the UV/H_2O_2 process than small, linear and acyclic NAs. The main conclusions of this study are as follows.

- Relative rate measurements using binary mixtures of model NA compounds confirmed that reactivity favoured compounds with more carbons.

- Relative rate measurements also confirmed that reactivity favoured NAs with one saturated ring, relative to the corresponding linear NAs.

- For model compound with three rings, no increased reactivity was observed relative to mono-cyclic NA.

- UV/H_2O_2 treatment of OSPW confirmed our findings with model compounds, indicating that the compounds with more carbons are favoured for degradation.

- Increasing the number of rings (or double bond equivalents) in OSPW NAs did not show any clear structure-reactivity.

3.6 Recommendation

Microbial degradation studies of the UV/H$_2$O$_2$ treated OSPW should be conducted to examine the overall benefit of this treatment for the real applications.

3.7 References

Afzal A, Drzewicz P, Martin JW, Gamal El-Din M. Decomposition of cyclohexanoic acid by the UV/H$_2$O$_2$ process under various conditions. Sci Total Environ 2012; 426:387-392.

Allen EW. Process water treatment in canada's oil sands industry: I. Target pollutants and treatment objectives. J Environ Eng Sci 2008;7:123-138.

Anbar M, Meyerste D, Neta P. Reactivity of aliphatic compounds towards hydroxyl radicals. J Chem Soc B 1966;8:742-747.

Atkinson R, Aschmann SM, Carter WPL. Rate constants for the gas-phase reactions of OH radicals with a series of bicycloalkanes and tricycloalkanes at 299 $\pm$ 2 k - effects of ring strain. Int J Chem Kinet 1983;15:37-50.

Clemente JS, Fedorak PM. A review of the occurrence, analyses, toxicity, and biodegradation of naphthenic acids. Chemosphere 2005;60:585-600.

Dokholyan BK, Magomedov AK. Effect of sodium naphthenate on survival and some physiological–biochemical parameters of some fishes. J Ichthyology 1983;23:125-132.

Dore M, Langlais B, Legube B. Mechanism of the reaction of ozone with soluble aromatic pollutants. Ozone-Sci Eng 1980; 2:39-54.

Drzewicz P, Afzal A, Gamal El-Din M, Martin JW. Degradation of a model naphthenic acid, cyclohexanoic acid, by vacuum UV (172 nm) and UV (254 nm) / H_2O_2. J Phys Chem A 2010;114:12067-12074.

Frank RA, Fischer K, Kavanagh R, Burnison BK, Arsenault G, Headley JV, Peru KM, Van der Kraak G, Solomon KR. Effect of carboxylic acid content on the acute toxicity of oil sands naphthenic acids. Environ Sci Technol 2009;43:266-271.

Gagné C, André C, Douville M, Talbot A, Parrott J, McMaster M, Hewitt M. An examination of the toxic properties of water extracts in the vicinity of an oil sand extraction site. J Environ Monit 2011;13:11.

Garcia-Garcia E, Pun J, Pérez-Estrada LA, Gamal El-Din M, Smith DW, Martin JW, Belosevic M. Commercial naphthenic acids and the organic fraction of oil sands process water downregulate pro-inflammatory gene expression and macrophage antimicrobial responses. Toxicol Lett 2011;203:62-73.

Goldstein S, Meyerstein D, Czapski G. The fenton reagents. Free Radical Bio Med 1993;15:435-445.

Gottschalk C, Libra JA, Saupe A. Ozonation of Drinking Water and of Wastewater; Wiley-Vch: Weinheim, Federal Republic of Germany, 2000.

95

Guo XY, Wang XL, Zhou XZ, Kong XZ, Tao S, Xing BS. Sorption of four hydrophobic organic compounds by three chemically distinct polymers: Role of chemical and physical composition. Environ Sci Technol 2012;46:7252-7259.

Han XM, Scott AC, Fedorak PM, Bataineh M, Martin JW. Influence of molecular structure on the biodegradability of naphthenic acids. Environ Sci Technol 2008;42;1290-1295.

Headley JV, Du JL, Peru KM, McMartin DW. Electrospray ionization mass spectrometry of the photodegradation of naphthenic acids mixtures irradiated with titanium dioxide. J Environ Sci Heal A 2009:44:591-597.

Headley JV, Peru KM, Tanapat S, Putz G. Biodegradation kinetics of geometric isomers of model naphthenic acids in athabasca river water. Can Water Resour J 2002;27:25-42.

Hedberg Y, Herting G, Wallinder IO. Risks of using membrane filtration for trace metal analysis and assessing the dissolved metal fraction of aqueous media - A study on zinc, copper and nickel. Environ Pollut 2011;159;1144-1150.

Hewgill FR, Proudfoot GM. Regioselective oxidation of aliphatic-acids by complexed hydroxyl radicals. Aust J Chem 1976;29:637-647.

Hewgill FR, Proudfoot GM. An E.S.R. study of oxidation of sodium alkyl sulfates by hydroxyl radicals. Aust J Chem 1977;30:695-697.

96

Hoigné J, Bader H. The role of hydroxyl radical reactions in ozonation processes in aqueous solutions. Water Res 1976;10:377-386.

Hoigné J, Bader H. Rate constants of reactions of ozone with organic and inorganic-compounds in water 1. Non-dissociating organic-compounds. Water Res 1983;17:173-183.

Hoigné J, Bader H. Rate constants of reactions of ozone with organic and inorganic-compounds in water 2. Dissociating organic-compounds. Water Res 1983;17:185-194.

Horowitz AJ, Lum KR, Garbarino JR, Hall GEM, Lemieux C, Demas CR. Problems associated with using filtration to define dissolved trace element concentrations in natural water samples. Environ Sci Technol 1996;30:954-963.

Jones D, Scarlett AG, West CE, Rowland SJ. Toxicity of individual naphthenic acids to vibrio fischeri. Environ Sci Technol 2011;45:9776-9782.

Koleva Y. Application of quantitative structure-activity relationship models to predict the risk assessment of selected naphthenic acids in the environment. C R Acad Bulg Sci 2012;65:365-372.

Kruppa GH, Beauchamp JL. Energetics and structure of the 1-adamantyl and 2-adamantyl radicals and their corresponding carbonium-ions by photoelectron-spectroscopy. J Am Chem Soc 1986;108:2162-2169.

Legrini O, Oliveros E, Braun AM. Photochemical processes for water-treatment. Chem Rev 1993;93:671-698.

Luo Y. Handbook of bond dissociation energies in organic compounds. Boca Raton, Fl, 2002.

Martin JW, Barri T, Han XM, Fedorak PM, Gamal El-Din M, Pérez-Estrada L, Scott AC, Jiang JT. Ozonation of oil sands process-affected water accelerates microbial bioremediation. Environ Sci Technol 2010;44:8350-8356.

Martin JW, Han XM, Peru KM, Headley JV. Comparison of high- and low-resolution electrospray ionization mass spectrometry for the analysis of naphthenic acid mixtures in oil sands process water. Rapid Commun. Mass Sp 2008;22:1919-1924.

Masliyah J, Zhou ZJ, Xu ZH, Czarnecki J, Hamza H. Understanding water-based bitumen extraction from athabasca oil sands. Can J Chem Eng 2004;82:628-654.

McMartin DW, Headley JV, Friesen DA, Peru KM, Gillies JA. Photolysis of naphthenic acids in natural surface water. J Environ Sci Heal A 2004;39:1361-1383.

Meylan WM, Howard PH. Computer estimation of the atmospheric gas-phase reaction-rate of organic-compounds with hydroxyl radicals and ozone. Chemosphere 1993;26;2293-2299.

98

Minakata D, Li K, Westerhoff P, Crittenden J. Development of a group contribution method to predict aqueous phase hydroxyl radical (•OH) reaction rate constants. Environ Sci Technol 2009;43:6220-6227.

Mohamed MH, Wilson LD, Headley JV, Peru KM. Screening of oil sands naphthenic acids by UV-vis absorption and fluorescence emission spectrophotometry. J Environ Sci Heal A 2008;43:1700-1705.

Morrison MA, Benoit G. Filtration artifacts caused by overloading membrane filters. Environ Sci Technol 2001;35:3774-3779.

Pérez-Estrada LA, Han XM, Drzewicz P, Gamal El-Din M, Fedorak PM, Martin JW. Structure-reactivity of naphthenic acids in the ozonation process. Environ Sci Technol 2011;45:7431-7437.

Pourrezaei P, Drzewicz P, Wang YN, Gamal El-Din M, Pérez-Estrada LA, Martin JW, Anderson J, Wiseman S, Liber K, Giesy JP. The impact of metallic coagulants on the removal of organic compounds from oil sands process-affected water. Environ Sci Technol 2011;45:8452-8459.

Qu DR, Zheng YG, Jiang X, Ke W. Correlation between the corrosivity of naphthenic acids and their chemical structures. Anti-Corros Method M 2007;54:211-218.

Rogers VV, Liber K, MacKinnon MD. Isolation and characterization of naphthenic acids from athabasca oil sands tailings pond water. Chemosphere 2002;48:519-527.

Rogers VV, Wickstrom M, Liber K, MacKinnon MD. Acute and subchronic mammalian toxicity of naphthenic acids from oil sands tailings. Toxicol Sci 2002;66:347-355.

Schleyer, P. V.; Williams, J. E.; Blanchard, K. R. Evaluation of strain in hydrocarbons strain in adamantane and its origin. J. Am. Chem. Soc. 1970, 92 (8), 2377-2386.

Scott AC, Zubot W, MacKinnon MD, Smith DW, Fedorak PM. Ozonation of oil sands process water removes naphthenic acids and toxicity. Chemosphere 2008;71:156-160.

Smith BE, Lewis CA, Belt ST, Whitby C, Rowland SJ. Effects of alkyl chain branching on the biotransformation of naphthenic acids. Environ Sci Technol 2008;42:9323-9328.

Watts RJ, Sarasa J, Loge FJ, Teel AL. Oxidative and reductive pathways in manganese-catalyzed fenton's reactions. J Environ Eng-Asce 2005;131:158-164.

4 DEGRADATION MECHANISMS DURING OZONATION OF A MODEL NAPHTHENIC ACID COMPOUND, CYCLOHEXANOIC ACID[*]

4.1 Introduction

In Northern Alberta, Canada, bitumen is extracted from the oil sands using hot water. The resulting large volumes of toxic oil sands process-affected water (OSPW) must be stored in tailings ponds because of a zero discharge policy (Masliyah et al., 2004). The acute and chronic toxicity of OSPW to aquatic organisms are commonly attributed to a complex mixture of organic compounds that include naphthenic acids (NAs) (Headley and McMartin, 2004; Scott et al., 2008; Garcia-Garcia et al., 2011; Hagen et al., 2012). The current approach to remediate OSPW has relied on natural *in situ* microbial degradation in tailing ponds, but this process has proven to be slow (Han et al., 2009) and is unlikely to keep up with the fast expansion of the industry. Therefore, the reclamation of OSPW is a major challenge facing the oil sands industry (Allen, 2008).

Ozonation of OSPW has been investigated through a number of studies at the bench-scale level. It has been shown that ozonation is a promising water reclamation strategy for OSPW (Scott et al., 2008; Martin et al., 2010; El-Din et al., 2011; Perez-

---

[*] A version of this chapter has been submitted to the Journal of Physical Chemistry. Afzal, A., Drzewicz, P., Chelme-Ayala, P., Khosravi, K., Martin, J.W., Gamal El-Din, M.

Estrada et al., 2011). Gamal El-Din et al.(2011) showed that more than 76% of the extractable organic acids (EOA) in OSPW, which includes NAs, were removed using a semi-batch ozonation system at a utilized ozone (O_3) dose of 150 mg/L. It was also shown that ozone preferentially reacted with NAs with more rings (or double bond equivalents) and with more carbon (Gamal El-Din et al., 2011; Perez-Estrada et al., 2011). It was shown by Scott et al. (2008) that OSPW NAs could be removed by ozone, but a fraction of NAs remained after treatment. Despite these findings, the mechanism of degradation of saturated alicyclic carboxylic acids (i.e., NAs) during ozonation has not been investigated to this date.

The general ozone decomposition mechanism in aqueous solution is shown in reactions 4-1 to 4-5 (Tomiyasu et al., 1985; Chelkowska et al., 1992). The transformation of ozone into secondary oxidants (i.e., radical intermediates) in aqueous media is initiated by its reaction with hydroxide ion (OH^-). The ozone decomposition mechanism involves the formation of superoxide radical ($O_2\bullet^-$) and hydroperoxyl radical ($HO_2\bullet$) acting as chain carriers which ultimately results in the formations of $\bullet OH$ and H_2O_2 oxidants, as shown in reactions 4-5 and 4-6) (Staehelin and Hoigne, 1982).

$$O_3 + OH^- \longrightarrow O_2\bullet^- + HO_2\bullet \qquad k = 40\text{-}70 \text{ M}^{-1}\text{ s}^{-1} \qquad (4\text{-}1)$$

$$HO_2\bullet \longleftrightarrow H^+ + O_2\bullet^- \qquad pK_a = 4.8 \qquad (4\text{-}2)$$

$$O_3 + O_2\bullet^- \longrightarrow O_3\bullet^- + O_2 \qquad k = 1.6 \times 10^9 \text{ M}^{-1}\text{ s}^{-1} \qquad (4\text{-}3)$$

$$O_3\bullet^- + H^+ \longleftrightarrow HO_3\bullet \qquad k = 5.0 \times 10^{10} \text{ M}^{-1}\text{ s}^{-1} \qquad (4\text{-}4)$$

$$HO_3\bullet \quad \longleftrightarrow \quad \bullet OH + O_2 \qquad\qquad k = 1.1 \times 10^5 \text{ M}^{-1} \text{ s}^{-1} \qquad\qquad (4\text{-}5)$$

$$\bullet OH + \bullet OH \quad \longrightarrow \quad H_2O_2 \qquad\qquad k = 5.0 \times 10^9 \text{ M}^{-1} \text{ s}^{-1} \qquad\qquad (4\text{-}6)$$

Being the slowest reaction, the rate determining step is the first step involving the reaction of ozone with OH$^-$ (reaction 4-1). Therefore, changing the pH of the solution has a significant impact on the ozone decomposition, such that ozone decomposes faster with increasing pH (Staehelin and Hoigne, 1982). The superoxide ion ($O_2\bullet^-$) or its protonated counterpart, the hydroperoxyl radical (HO$_2\bullet$), acts as an enhancer of ozone decomposition. These radicals (HO$_2\bullet$/O$_2\bullet^-$) are both generated and consumed in the ozonation process. For example, the HO$_2\bullet$ decomposes to superoxide radical which, in turn, reacts with molecular ozone (reaction 4-3) (Staehelin and Hoigne, 1982).

The addition of inorganic and organic compounds to the solution may also affect the ozone decomposition. Hence, the addition of such compounds to reaction mixtures can be used to control the ozone or selected radical reactions. For example, carbonate (CO$_3^{2-}$) and bicarbonate (HCO$_3^-$) ions in aqueous solutions scavenge •OH (with the rates of 3.9×10^8 M^{-1} s^{-1} and 8.5×10^6 M^{-1} s^{-1}, respectively) (Buxton et al., 1988) to form oxidation products (i.e., bicarbonate/carbonate radicals: HCO$_3^\bullet$/CO$_3^{-\bullet}$) without producing superoxide radical; thus, increasing carbonate can slow down the overall rate of ozone decomposition (Elovitz et al., 2000). Organic scavengers such as *tert*-butyl alcohol (TBA) that react with •OH ($k_{\bullet OH} = 6.0 \times 10^8$ M^{-1} s^{-1}) (Buxton et al., 1988), but not with ozone ($k_{O3} \sim 3.0 \times 10^{-3}$ M^{-1} s^{-1}) (Hoigne and Bader, 1983), can be used to quench other

103

•OH reactions. Tetranitromethane [TNM; $C(NO_2)_4$] can also be used as an indicator of the radical reactions in ozonation process. TNM reacts with $HO_2^\bullet/O_2^{\bullet-}$ at a diffusion controlled rate (reactions 4-7 and 4-8) which produces the nitroform anion ($C(NO_2)_3$).

$$O_2^{\bullet-} + C(NO_2)_4 \longrightarrow C(NO_2)_3^- + NO_2 + O_2 \qquad k = 1.9 \times 10^9 \text{ M}^{-1} \text{ s}^{-1} \text{ (Bielski et al.,}$$

1985) (4-7)

$$HO_2^\bullet + C(NO_2)_4 \longrightarrow H^+ + C(NO_2)_3^- + NO_2 + O_2 \text{ (Henglein et al., 1959; Sutton,}$$

1975) (4-8)
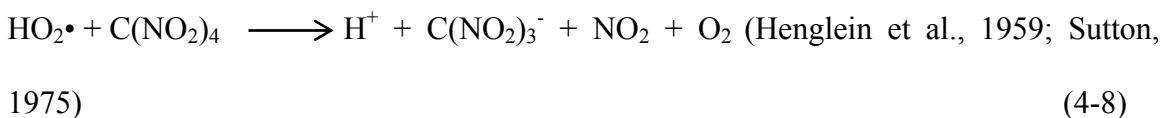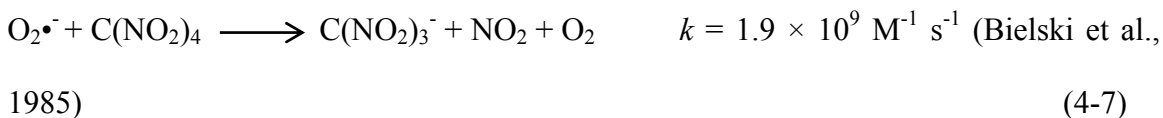
OSPW is a complex mixture of largely uncharacterized organic acids (saturated and un-saturated) and inorganic compounds (Mojelsky et al., 1992); therefore, model organic compounds have been used in many studies to predict the possible degradation mechanisms of the dissolved organic fraction of OSPW. Cyclic structures are prominent features of NA in OSPW (Headley and McMartin, 2004), and cyclohexanoic acid (CHA) has been previously selected as a model compound to study the mechanism of NA decomposition induced by •OH (Drzewicz et al., 2010) because of its simple structure (i.e., one ring and one carboxylic acid group). By using ultraviolet irradiation in the presence of hydrogen peroxide (UV/H_2O_2), it was shown that CHA underwent degradation through a peroxyl radical formation. The decay of the peroxyl radical led predominantly to the formation of 4-oxo-CHA, minor amounts of hydroxy-CHA, and later the oxo- and hydroxy-CHA further degraded to various dihydroxy-CHAs (Drzewicz

et al., 2010). To date, however, there is no study on the mechanism of CHA degradation in the ozonation process, albeit the structure reactivity of model NAs and preliminary work showing the significance of •OH radical pathway during the ozonation of OSPW NAs have been previously reported (Perez-Estrada et al., 2011).

The objective of the current study was to investigate the mechanism of CHA degradation and byproduct formation, in the ozonation process at pHs 3 and 9. The effect of inorganic constituents, such as carbonate ion, and the impacts of organic radical scavengers, such as TBA and TNM, on the performance of the ozonation treatment were also studied using the stoichiometric analysis approach (Gomez et al., 2008). Stoichiometric analysis approach involves estimating the relative reactivity of a compound towards an oxidant (e.g. NAs and ozone) without considering the time of the treatment.

4.2 Material and methods

4.2.1 Materials

The CHA used was of analytical grade (> 99% purity) and was purchased from TCI (Portland, OR, USA). A stock solution of CHA (250 mg/L) was prepared by dissolving appropriate amount of CHA in aqueous solution of phosphate or carbonate buffer and the pH was adjusted as desired. Carbonate (20 mM) and phosphate (4 mM) buffers were prepared using sodium bicarbonate ($NaHCO_3$) and monosodium phosphate (NaH_2PO_4) (Fisher Scientific Co., Canada), respectively. The pH of the solutions was

adjusted using 50% carbonate free sodium hydroxide (NaOH) (ACS purity) and 80% perchloric acid ($HClO_4$) solutions (Fisher Scientific Co., Canada). TBA, TNM, and potassium indigo trisulfonate were purchased from Sigma–Aldrich (Oakville, ON, Canada) and were used without further purification. The concentrations of TBA, TNM, carbonate, and phosphate used during the experiments were initially selected based on the literature; however, their concentrations were adjusted based on the conditions (i.e., ozone and CHA concentrations) of the specific experiment. The concentrations of TBA and TNM ranged from 5 to 20 mM and up to 10 mM, respectively.

Ammonium acetate, acetic acid, and methanol were purchased from Fisher Scientific (LC-MS grade). All analyte solutions were prepared in ultrapure water (resistivity = 18 MΩ × cm and total organic carbon (TOC) < 0.1 mg/L) obtained from a Millipore and Elga system equipped with an Elix UV lamp. All stock solutions were prepared using ozone-demand-free (ODF) water and the glassware used in experiments was cleaned and pre-treated with ODF water. Details of ODF water and ODF glassware preparation and are presented in Appendix A.

Hazards: TNM is strong poison and explosive in the presence of impurities. Precautions (wearing gloves and goggles, and using proper ventilation) must, therefore, be taken when working with TNM. Residual TNM in solution can be removed easily by strong alkali.

4.2.2   Ozonation apparatus and experiments

Ozone gas was produced by a corona discharge ozone generator (PCI-Wedeco, Model GLS-7, Water Technology, Herford, Germany) from extra dry high purity oxygen. For any specific experiment, ozone stock solution (being used in batch reactors) was prepared by bubbling ozone gas to a 1 L solution kept in an ice bath, in order to slow the ozone decomposition during the bubbling period. For ozonation at pH 9, the pH of 4 mM phosphate buffer or 20 mM carbonate buffer was adjusted to 9 using sodium hydroxide (NaOH) solution. The concentration of ozone stock solution during ozonation was monitored using a spectrometric method by measuring the absorbance of the solution in a quartz cuvette at 260 nm. After reaching the approximate desired concentration, the diffuser was removed from the bottle and the ozone concentration was measured using the indigo method as an accurate initial ozone measurement (APHA, 2005) (see Appendix A for details). The same procedure was followed for the experiments at pH 3, except that the pH was adjusted by the addition of $HClO_4$ solution.

Ozonation reactions were performed in 5-mL volumetric flasks with gas tight ground glass stoppers. Every set of ozonation experiments (e.g., ozonation of CHA at pH 9 in presence of carbonate and TBA) was completed in five volumetric flasks at different applied ozone doses. The procedure was as follows: 1 mL of CHA stock solution (250 mg/L) along with the scavenger and/or buffer was placed in each flask. TBA and TNM were added to the flasks according the ozone concentration, with the volumes of 68 to 218 µL stock solution (5% v/v) for TBA and 1.5 to 5 µL for pure TNM. The amount of

0.25, 0.5, 1, 2, and 3 mL of ozone stock solution was added to all 5 flasks and immediately the flasks were tightly closed and shaken for two minutes manually to ensure ozone gas was reacted in its entity; tested by measuring the ozone residual in the flask. To examine if ozone concentration was constant during the experiment, the concentration of ozone in the stock solution was measured after treatment by the indigo method after adding 3 mL of the stock ozone solution to the last flask. The flasks were filled with ODF water to the mark (5 mL line) to compensate for the differences in ozone solution volume added to each flask. A control flask was filled with 1 mL CHA and diluted to the mark with ODF water without the addition of any ozone to produce the final concentration of 50 mg/L. All the experiments were performed in triplicates and at room temperature (20 ± 2 °C).

4.2.3 Analytical methods

A high-pressure liquid chromatograph (HPLC) coupled to an ion trap mass spectrometer (Varian 500-MS) was used for the analysis of CHA and its degradation byproducts. A Phenomenex, C8, 5 μm, 250 mm × 3 mm column was used for separations of the target compounds. The chromatographic conditions were: A, 100% methanol, and B, 4 mM ammonium acetate with 0.01% acetic acid, gradient elution from 30% to 70% A over 30 min, injected volume 20 μL, flow 200 μL/min. Using these conditions, the detection limit of CHA was 20 μg/L (4 ng), and the retention time of CHA was around 40 min, whereas all the byproducts eluted before that.

4.3 Results and Discussion

4.3.1 Effect of pH on CHA degradation by ozone

The effect of pH on the extent of CHA degradation and byproduct formation in the ozonation process was investigated at pHs 3 and 9. The pKa of CHA is 4.9, thus at pH 3 CHA is mostly in its protonated form ($C_6H_{11}COOH$), whereas at pH 9 CHA is mostly in the anionic form ($C_6H_{11}COO^-$). As shown in Figure 4-1, for the degradation of one mole of CHA at pH 9, 0.9 ± 0.22 moles of ozone was utilized, whereas at pH 3, 1.7 ± 0.24 moles of ozone were utilized. Thus, the reactivity of CHA at pH 9, in which both ozone and •OH are present at high concentration, was higher than in a system with predominantly molecular ozone (i.e., pH 3). Previously, it was reported that the degradation rate of CHA in the UV/H_2O_2 process, in which •OH was the main oxidant, were not different at pHs 3 and 9. It was also found that the type and concentration of byproducts formed during the treatment were the same at the two studies pHs (Afzal et al., 2012). Thus, it is assumed that the proportion of protonated/anionic CHA does not affect the reaction, and all the observed changes in this study, therefore, are related mainly to contrasting ozone chemistries at pHs 3 and 9.
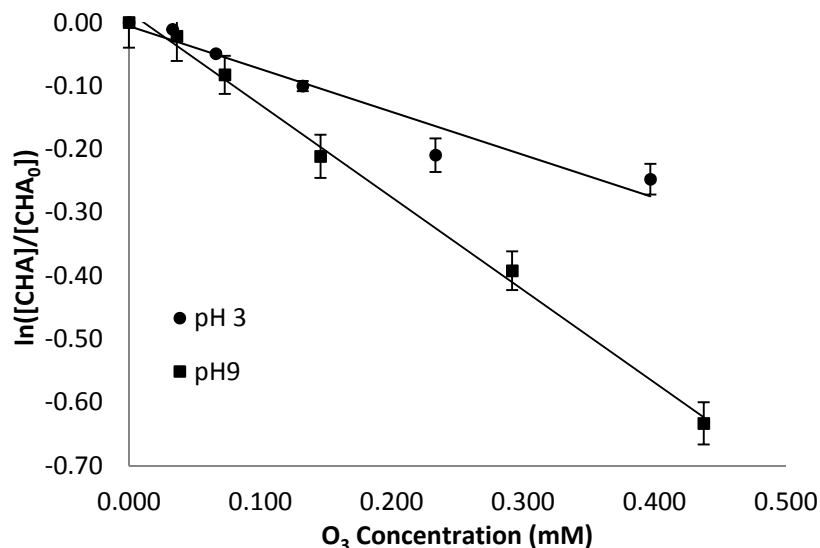
Figure 4-1. Stoichiometric analysis of CHA during ozonation process at pHs 3 and 9

Drzewicz et al. (2010) showed that three major byproducts were formed during the oxidation of CHA by •OH in the UV/H_2O_2 process: dihydroxy-CHA (*m/z* 159), oxo-CHA (*m/z* 141), and hydroxy-CHA (*m/z* 143). Contrary to the UV/H_2O_2 treatment of CHA, the byproduct *m/z* 159 was not observed here at either pH. As discussed by Drzewicz et al. (2010), the byproduct *m/z* 159 suggests the presence of dihydroxy-CHA, or heptadioic acid. This byproduct was either not formed in enough quantity to be detected, or could have been highly reactive toward molecular ozone by analogy to malonic acid (Hoigne and Bader, 1983).

4.3.2   Mechanism of CHA ozonation at pH 9

In the ozonation process, at pH 9, a byproduct with *m/z* 141 was observed (Figure 4-2). The presence of a peak at *m/z* 141 in the LC-MS/MS analysis suggests the

formation of oxo-CHA, but further confirmation for the presence of this product was reached through a product peak at m/z 97 (loss of 44 or CO_2), thereby confirming the presence of the carboxylate group. Drzewicz et al. (2010) previously described the formation of 4-oxo-CHA as a result of hydrogen abstraction via a carbon centered CHA radical (reaction 4-9) which reacts with oxygen to form a peroxyl-CHA radical (reaction 4-10) and then forms oxo-CHA by two recombination reactions (reactions 4-11 and 4-12).

(4-9)

(4-10)

$$(4\text{-}11)$$

$$(4\text{-}12)$$
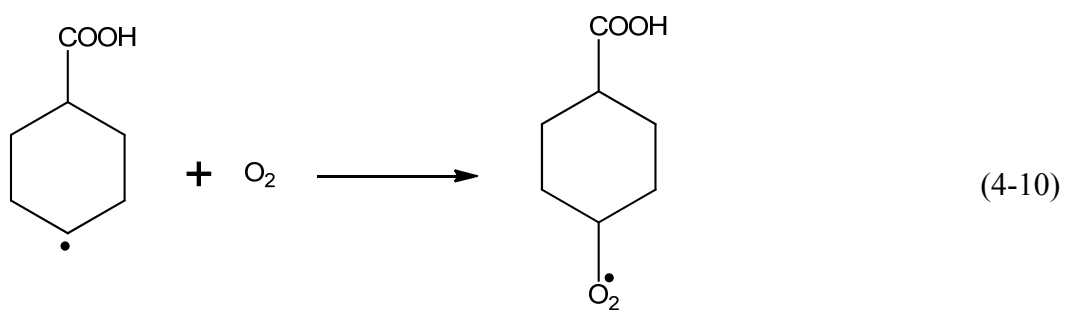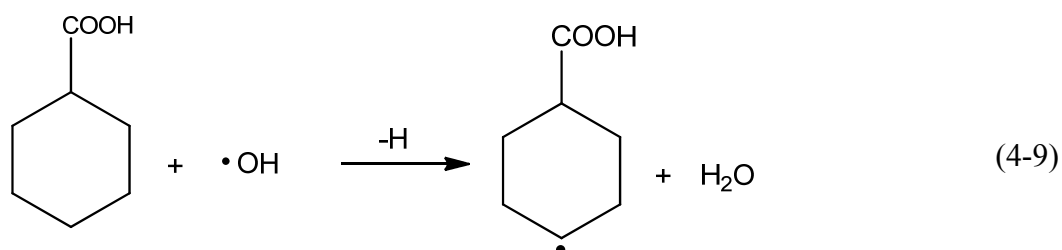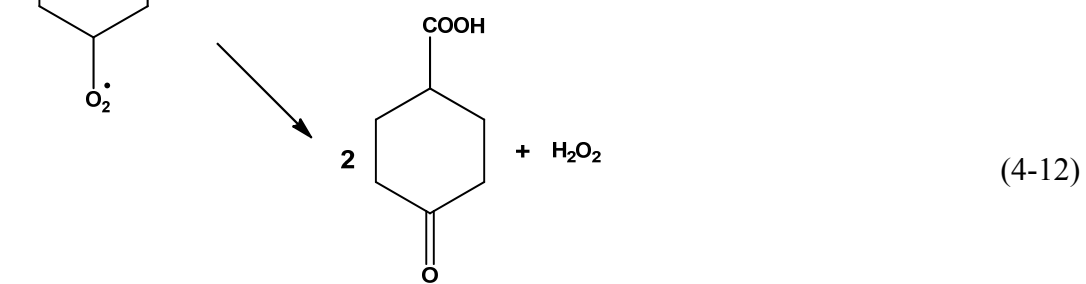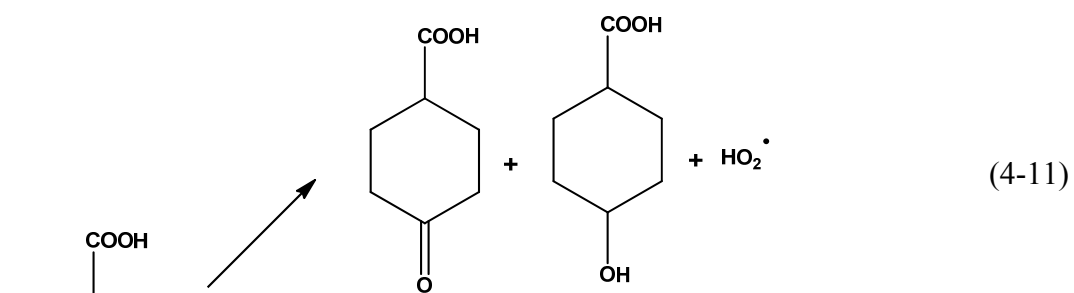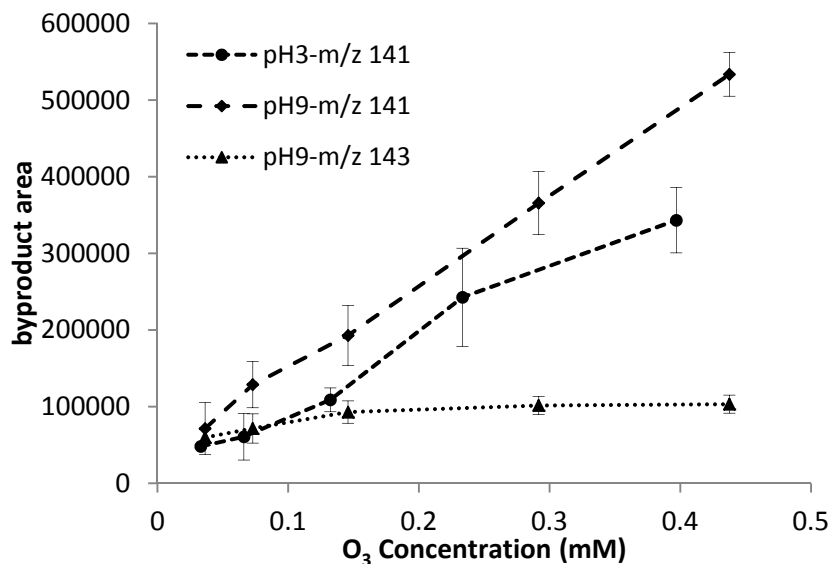
Figure 4-2. Byproduct formation during the ozonation of CHA at pHs 3 and 9.

The second byproduct, also previously shown to be formed from CHA in the UV/H_2O_2 process (*m/z* 143, hydroxy CHA), was observed at pH 9 in the ozonation process and had a characteristic MS/MS product ion at *m/z* 125 (neutral loss of m/z 18, or H_2O) (Drzewicz et al., 2010). The presence of the peak at *m/z* of 143 (at pH 9) suggests that the peroxyl-CHA radical may recombine to form hydroxyl-CHA (reaction 4-11), as described by Drzewicz et al. (2010).

4.3.3 Mechanism of ozonation of CHA at pH 3

At pH 3, the oxidation pathway is somewhat different from pH 9. The presence of a byproduct at *m/z* 141 in LC-MS/MS at this pH suggests the formation of oxo-CHA. The pathway in which this product is formed might be explained by the formation of CHA-

oxyl radical in the reaction of ozone with CHA along a molecular pathway (reaction 4-13) (Bailey, 1958).

(4-13)
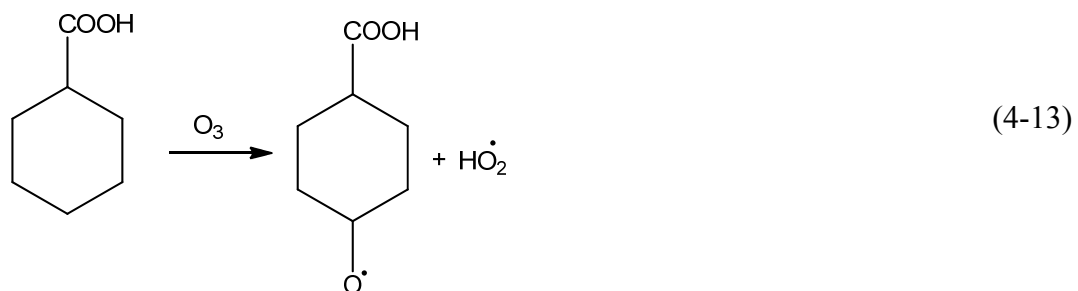
This unstable radical most likely rearranges through α hydrogen shift (reaction 4-14) to form hydroxyl-CHA radical, which further reacts with oxygen present in the solution to form a sterically unstable peroxyl radical (reaction 4-15) (Anbar et al., 1966; Bothe et al., 1978). This radical then loses hydroxyl anion or $HO_2^{\bullet}$ to form oxo-CHA, a thermodynamically stable compound (reaction 4-16) (Drzewicz et al., 2010).

(4-14)

114

$$(4\text{-}15)$$

$$(4\text{-}16)$$
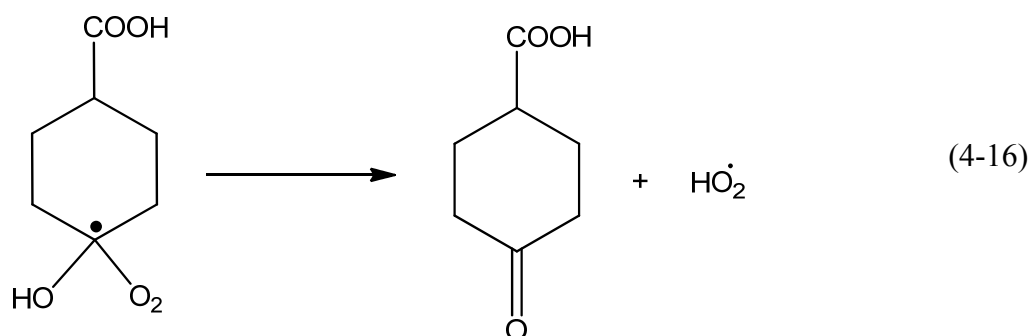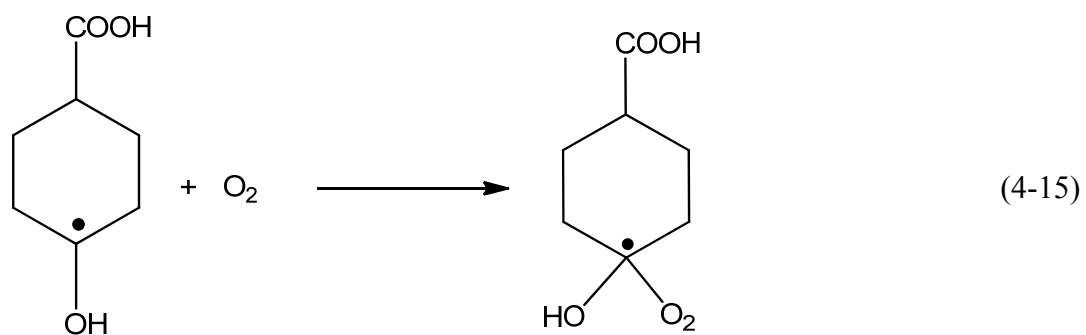
At pH 3, in which molecular ozone is the predominant oxidant, the hydroxy-CHA byproduct (*m/z* 143) was not observed, suggesting that reaction of ozone with CHA to form hydroxy-CHA (reaction 4-17) is not significant, or that any hydroxy-CHA reacts quickly with ozone to form oxo-CHA (reaction 4-18).

$$\text{(4-17)}$$

$$\text{(4-18)}$$
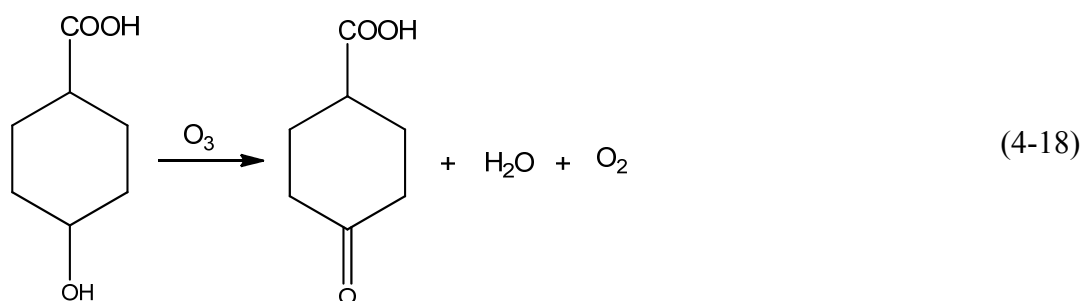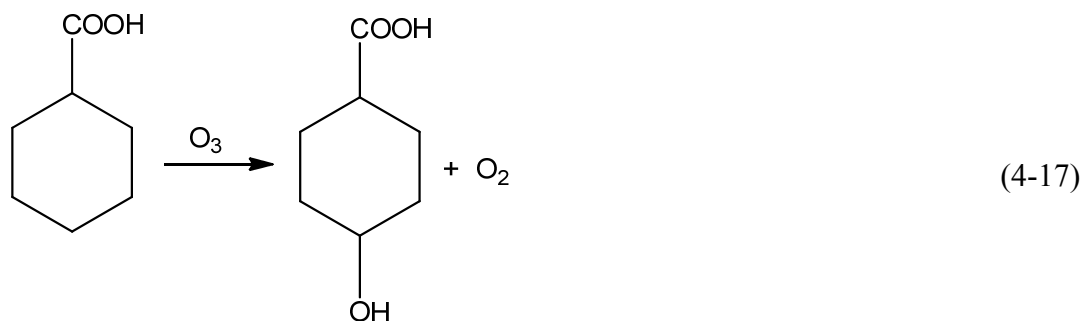
4.3.4 The effect of the presence of carbonate and TBA on the ozonation of CHA at pH 9

The presence of CO_3^{2-}/HCO_3^- is known to slow the ozone decomposition in water (Elovitz et al., 2000) and to also scavenge •OH (reactions 4-19 and 4-20) (Buxton et al., 1988; Gardoni et al., 2012). However, with increasing CO_3^{2-}/HCO_3^- there are diminishing returns on ozone stabilization (Tomiyasu et al., 1985). In the presence of high concentration of CO_3^{2-}/HCO_3^-, intermediate radicals ($HCO_3^\bullet$ and $CO_3^{\bullet-}$) become concentrated enough to react directly with ozone, and carbonate species then act as promoters of the ozone decomposition (Elovitz et al., 2000).

$$HCO_3^- + \cdot OH \longrightarrow OH^- + HCO_3 \cdot \qquad k_{OH} = 8.5 \times 10^6 \, M^{-1} \, s^{-1} \qquad (4\text{-}19)$$

$$CO_3^{2-} + \cdot OH \longrightarrow OH^- + CO_3^- \cdot \qquad k_{OH} = 3.9 \times 10^8 \, M^{-1} \, s^{-1} \qquad (4\text{-}20)$$

Results of the experiments at pH 9 showed that the presence of 20 mM carbonate did not change the CHA decomposition rate (Figure 4-3). For the decomposition of one mole of CHA at pH 9 in the presence of bicarbonate, 0.7 ± 0.28 moles of ozone was utilized that was not significantly different (based on the regression analysis with 95% confidence interval and p-value < 0.05) from that of the ozonation system without bicarbonate, in which 0.9 ± 0.22 moles of ozone was utilized for the one mole CHA decomposition. A possible explanation for this behaviour is that even though in a solution of bicarbonate, ozone is prevalent and $\cdot$OH may also form during the reaction of molecular ozone with CHA (reaction 4-21). Moreover, at pH 9 the prevalent species is bicarbonate, which has less reactivity towards $\cdot$OH than carbonate (Buxton et al., 1988). Additionally, the second-order rate constant of the reaction between CHA and $\cdot$OH is 5.5 $\times 10^9$ which is three orders of magnitude higher than that of bicarbonate (Drzewicz et al., 2010). Since the concentration of CHA was 0.4 mM and the bicarbonate level was 20 mM; the scavenger effect of bicarbonate, therefore, is expected to be minor.

$$\text{(4-21)}$$
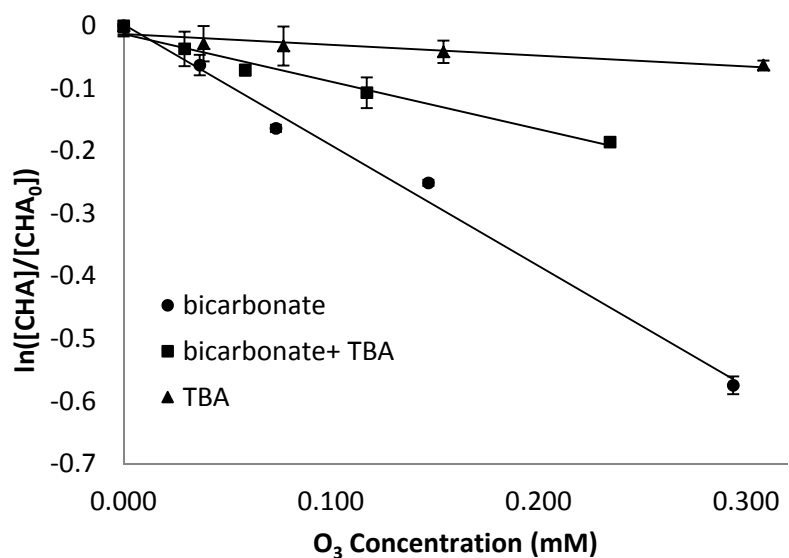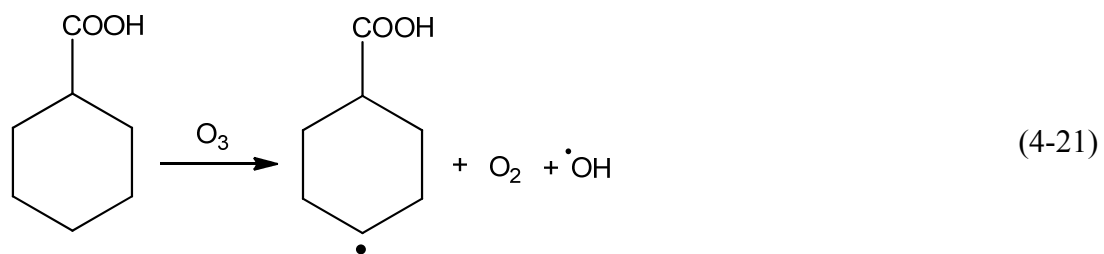
Figure 4-3. Stoichiometric analysis of CHA during the ozonation process at pH 9 in presence of 20 mM carbonate and TBA.

The only byproduct formed during the experiment in the presence of bicarbonate was m/z 141 (Figure 4-4). This species is characteristics of oxo-CHA based on the further confirmation through a product peak at m/z 97 (loss of 44 or CO_2). If in the presence of bicarbonate, the mechanism proposed in reaction 4-21 was likely, CHA radical and •OH

118

would be formed. The resulting radical may subsequently decay by one of the previously mentioned recombination reactions (reactions 4-11 and 4-12) to form oxo-CHA.

In the presence of bicarbonate and TBA, it is assumed that only ozone is available for reaction because •OH is scavenged by both TBA and bicarbonate. Therefore, the concentration of •OH is likely low, and a reactivity similar to CHA decomposition at pH 3 was expected. The results confirmed this hypothesis, as ozone utilization for CHA degradation at pH 3 (1.7 ± 0.24 mole of ozone per mole of CHA degraded) was not significantly different (based on the regression analysis with 95% confidence interval and p-value < 0.05) from that at pH 9 in presence of both TBA and bicarbonate (1.4 ± 0.22 mole of ozone per mole of CHA degraded).
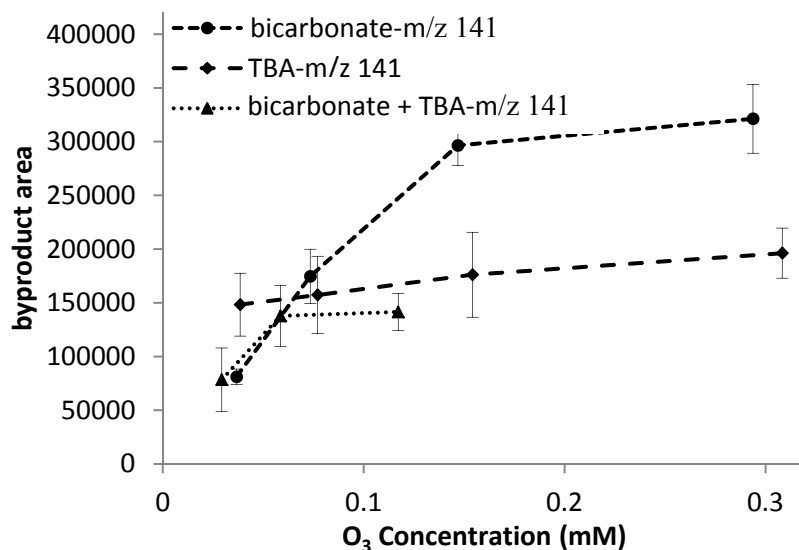
Figure 4-4. Formation of *m/z* 141 byproduct during the ozonation of CHA at pH 9 in presence of bicarbonate and TBA.

For CHA degradation in the presence of TBA alone (Figure 4-3), ozone utilization was significantly higher (5.8 ± 0.24 mole of ozone per mole of CHA degraded) than in the other two processes. As explained earlier, TBA is highly reactive towards •OH, and no species is present in the solution to cease ozone decomposition to •OH (i.e., carbonate); therefore, ozone utilization becomes very high.

The only byproduct formed in both processes involving TBA was *m/z* 141 (Figure 4-4), characteristics of oxo-CHA based on the MS/MS analysis. It is likely that the formation of oxo-CHA was due to the formation of CHA-oxyl radical in the reaction of ozone with CHA along a molecular pathway which consequently led to the formation of oxo-CHA as explained before (reactions 4-14 to 4-17).

4.3.5   The effect of the presence of TNM and carbonate/TNM on the ozonation of CHA at pH 9

The reaction between ozone and $HO_2^{\bullet}$ (chain carrier) is one of the possible pathways for the generation of •OH in the ozonation process (reactions 4-1 to 4-5) (Kwon and Lee, 2006). Superoxide radicals may form during the reaction of molecular ozone with either hydroxide ion (reaction 4-1) or CHA (reaction 4-14). Reduction of TNM to nitroform anion ($C(NO_2)_3^-$) through reaction with $O_2^{-\bullet}$ at a diffusion-controlled rate ($k = 1.9 \times 10^9$ M^{-1} s^{-1}) (reaction 4-7) has previously been used as an indicator of superoxide radicals in the ozonation process (Staehelin and Hoigne, 1982; Flyunt et al., 2003).

Figure 4-5 shows the degradation of CHA in the presence of TNM and bicarbonate in the ozonation process at pH 9. There is no significant difference (based on the regression analysis with 95% confidence interval and p-value < 0.05) between ozone utilization for CHA degradation in presence of TNM (2.0 ± 0.38 mole of ozone per mole of CHA degraded) and TNM/bicarbonate (2.5 ± 0.24 mole of ozone per mole of CHA degraded) at pH 9. However, the ozone utilization decreased significantly when bicarbonate alone was applied at the same pH (0.7 ± 0.28 mole of ozone was utilized per mole CHA degraded, based on the regression analysis with 95% confidence interval and p-value < 0.05). When TNM is added to the system, the superoxide radicals formed during ozone decomposition, are scavenged, resulting in a decrease of the •OH formation. As such, CHA may mostly undergo degradation through molecular ozone pathway rather than radical pathway. In both processes of the CHA ozonation in presence of TNM and TNM plus bicarbonate, the byproduct formed was m/z 141 (Figure 4-6), characteristics of oxo-CHA based on the MS/MS analysis.
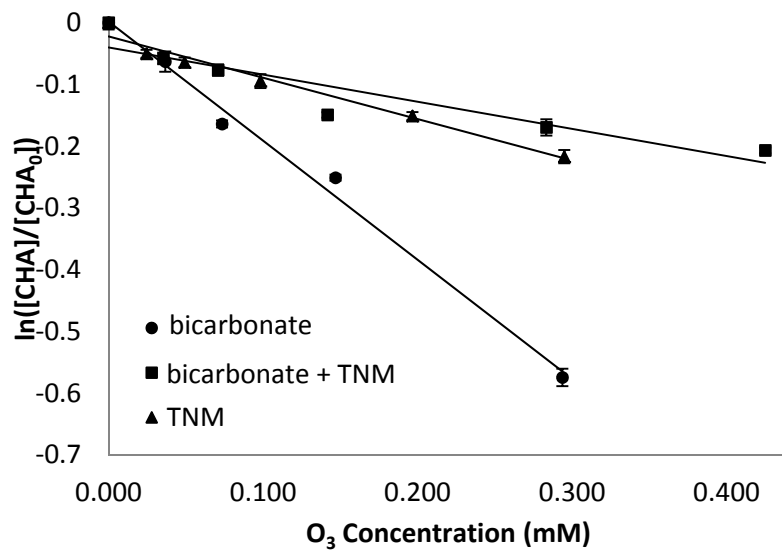
Figure 4-5. Stoichiometric analysis of CHA during its ozonation at pH 9 in presence of bicarbonate and TNM.
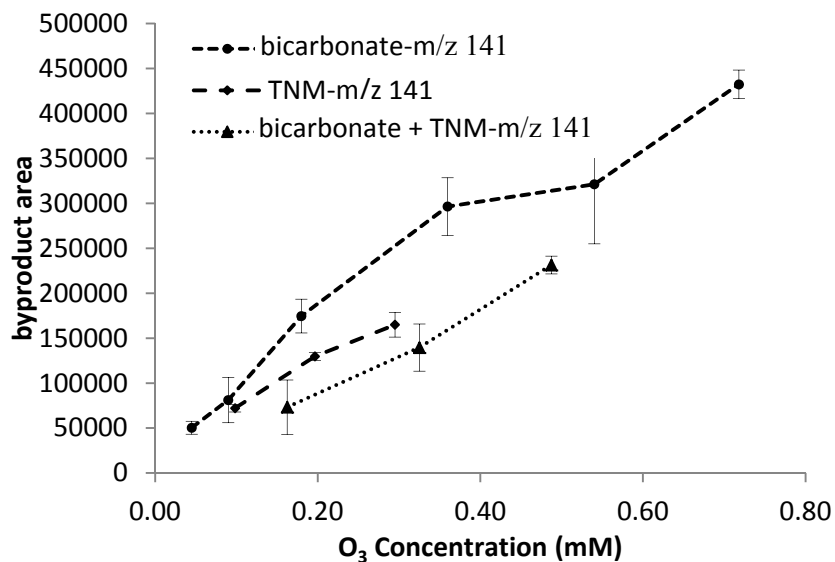
Figure 4-6. Formation of *m/z* 141 byproduct during the ozonation of CHA at pH 9 in presence of bicarbonate and TNM.

If the mechanism proposed in reaction 4-14 is likely, as explained earlier, the CHA-oxyl radical is formed. This radical product may undergo further peroxidation to shift the hydrogen (reaction 4-15) and consequently a peroxyl radical will form which further could decompose to oxo-CHA (reactions 4-16 and 4-17). Other products formed in these reactions are superoxide radicals. While TNM is scavenging these superoxide radicals, the formation of oxo-CHA is still prevalent (Figure 4-6).

4.4   Conclusions

The mechanism of degradation of CHA, a model NA compound, during ozonation at pHs 3 and 9 and in the presence of radical scavengers was investigated. The main conclusions of this study are as follows:

- The mechanism for the ozonation of CHA was different at pH 3 and pH 9.

- At pH 9, 4-oxo-CHA and 4-hydroxy-CHA were detected by LC-MS/MS, confirming the •OH pathway in which superoxide CHA radical might be an intermediate.

- The addition of bicarbonate to the reaction mixture at pH 9 did not have any effect on CHA ozonation; nevertheless, the addition of TBA and TNM to the same reaction decreased CHA degradation which further confirms the •OH pathway.

- At pH 3, the CHA ozonation follows different route. The presence of oxo-CHA but absence of hydroxy-CHA implies that the pathway is based on molecular ozonolysis of CHA rather than hydroxyl radical formation.
- The following mechanistic schemes (**A** and **B**) are proposed for both pHs.
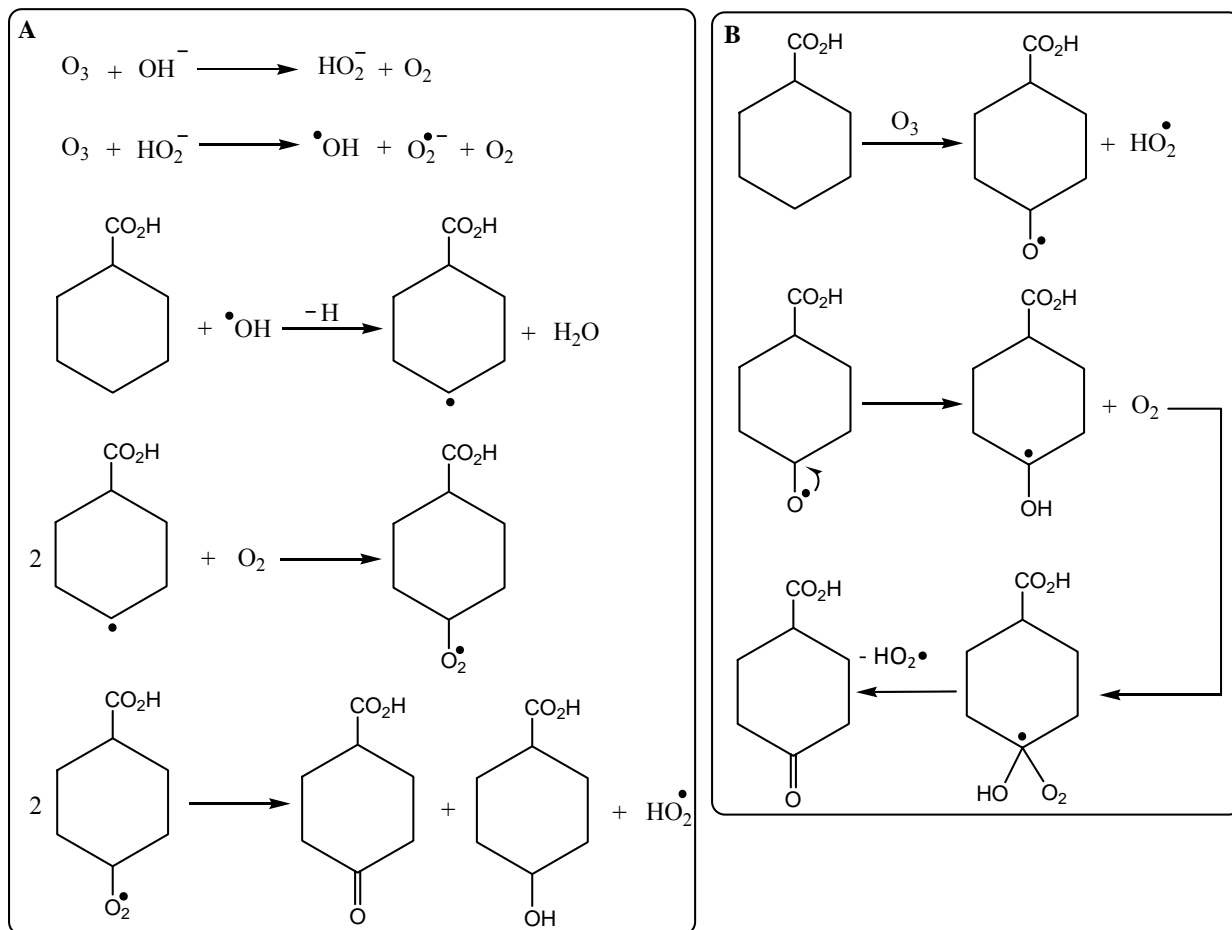
Scheme 4-1. Proposed mechanisms for the ozonation of CHA at pH 9 (**A**), and at pH 3 (**B**).

124

4.5 Recommendation

Since the presence of carbonate in the CHA solution at pH 9 did not show any significant effect on the ozonation treatment, it is recommended that the ozonation of OSPW NAs is applied for the real applications either without changing the pH of OSPW (i.e. slightly alkaline pH) or in presence of H_2O_2.

4.6 References

Afzal A, Drzewicz P, Martin JW, Gamal El-Din M. Decomposition of cyclohexanoic acid by the UV/H_2O_2 process under various conditions. Sci Total Environ 2012; 426:387-392.

Afzal A, Drzewicz P, Pérez-Estrada LA, Chen Y, Martin JW, Gamal El-Din M. Effect of molecular structure on the relative reactivity of naphthenic acids in the UV/H_2O_2 advanced oxidation process. Environ Sci Technol 2012;46:10727-10734.

Allen EW. Process water treatment in canada's oil sands industry: I. Target pollutants and treatment objectives. J Environ Eng Sci 2008;7:123-138.

Anbar M, Meyerste D, Neta P. Reactivity of aliphatic compounds towards hydroxyl radicals. J Chem Soc B 1966;8:742-747.

American Public Health Association (APHA), Standard methods for the examination of water and wastewater. 21st ed. Washington: American Water Works Association and Water Environment Federation; 2005.

Bailey PS. The reactions of ozone with organic compounds. Chem Rev 1985;58:925-1010.

Bielski BHJ, Cabelli DE, Arudi RL, Ross AB. Reactivity of HO_2/O^{2-} radicals in aqueous-solution. J Phys Chem Ref Data 1985;14:1041-100.

Bothe E, Schuchmann MN, Schultefrohlinde D, Vonsonntag CMN. HO_2 Elimination from alpha-hydroxyalkylperoxyl radicals in aqueous solution. Photochem Photobiol 1978;28:639-644.

Buxton GV, Greenstock CL, Helman WP, Ross AB. Critical-review of rate constants for reactions of hydrated electrons, hydrogen-atoms and hydroxyl radicals ($\bullet OH/\bullet O^-$) in aqueous-solution. J Phys Chem Ref Data 1988;17:513-886.

Canonica S and Tratnyek PG. Quantitative structure-activity relationships for oxidation reactions of organic chemicals in water. Environ Toxicol Chem 2003;22:1743-1754.

Chelkowska K, Grasso D, Fabian I, Gordon G. Numerical simulations of aqueous ozone decomposition. Ozone-Sci Eng 1992;14:33-49.

Drzewicz P, Afzal A, Gamal El-Din M, Martin JW. Degradation of a model naphthenic acid, cyclohexanoic acid, by vacuum UV (172 nm) and UV (254 nm) / H_2O_2. J Phys Chem A 2010;114:12067-12074.

Elovitz MS, von Gunten U, Kaiser HP. Hydroxyl radical/ozone ratios during ozonation processes: II. The effect of temperature, pH, alkalinity, and DOM properties. Ozone-Sci Eng 2000; 22:123-150.

Flyunt R, Leitzke A, Mark G, Mvula E, Reisz E, Schick R, von Sonntag C. Determination of •OH, O_2^-, and hydroperoxide yields in ozone reactions in aqueous solution. J Phys Chem B 2003;107:7242-7253.

Gamal El-Din M, Fu HJ, Wang N, Chelme-Ayala P, Perez-Estrada L, Drzewicz P, Martin JW, Zubot W, Smith DW. Naphthenic acids speciation and removal during petroleum-coke adsorption and ozonation of oil sands process-affected water. Sci Total Environ 2011;40:5119-25.

Garcia-Garcia E, Pun J, Pérez-Estrada LA, Gamal El-Din M, Smith DW, Martin JW, Belosevic M. Commercial naphthenic acids and the organic fraction of oil sands process water downregulate pro-inflammatory gene expression and macrophage antimicrobial responses. Toxicol Lett 2011;203:62-73.

Gardoni D, Vailati A, Canziani R. Decay of ozone in water: A review. Ozone-Sci Eng 2012;34:233-242.

Gomez AL, Lewis TL, Wilkinson SA, Nizkorodov SA. Stoichiometry of ozonation of environmentally relevant olefins in saturated hydrocarbon solvents. Environ Sci Technol 2008;42:3582-3587.

Hagen MO, Garcia-Garcia E, Oladiran A, Karpman M, Mitchell S, Gamal El-Din M, Martin JW, Belosevic M. The acute and sub-chronic exposures of goldfish to

naphthenic acids induce different host defense responses. Aquat Toxicol 2012;109:143-149.

Han XM, MacKinnon MD, Martin JW. Estimating the in-*situ* biodegradation of naphthenic acids in oil sands process waters by HPLC/HRMS. Chemosphere 2009;76:63-70.

Headley JV, McMartin DW. A review of the occurrence and fate of naphthenic acids in aquatic environments. J Environ Sci Heal A 2004;39:1989-2010.

Henglein A, Langhoff J, Schmidt G. Tetranitromethane as a radical scavenger in radiation chemical studies. J Phys Chem 1959;63:980-980.

Hoigné J, Bader H. Rate constants of reactions of ozone with organic and inorganic-compounds in water I. Non-dissociating organic-compounds. Water Res 1983;17:173-183.

Kwon BG and Lee JH. Determination of hydroperoxyl/superoxide anion radical $HO_2^•/O^{2-}$ concentration in the decomposition of ozone using a kinetic method. Bull Korean Chem Soc 2006;27:1785-1790.

Martin JW, Barri T, Han XM, Fedorak PM, Gamal El-Din M, Perez-Estrada L, Scott AC, Jiang JT. Ozonation of oil sands process-affected water accelerates microbial bioremediation. Environ Sci Technol 2010;44:8350-6.

Masliyah J, Zhou Z, Xu Z, Czarnecki J, Hamza H. Understanding water-based bitumen extraction from Athabasca oil sands. Can J Chem Eng. 2004; 82: 628–54.

Mojelsky TW, Ignasiak TM, Frakman Z, McIntyre DD, Lown EM, Montgomery DS, Strausz OP. Structural features of alberta oil sand bitumen and heavy oil asphaltenes. Energ Fuels 1992;6:83-96.

Pérez-Estrada LA, Han XM, Drzewicz P, Gamal El-Din M, Fedorak PM, Martin JW. Structure-reactivity of naphthenic acids in the ozonation process. Environ Sci Technol 2011;45:7431-7437.

Scott AC, Zubot W, MacKinnon MD, Smith DW, Fedorak PM. Ozonation of oil sands process water removes naphthenic acids and toxicity. Chemosphere 2008;71:156-60.

Staehelin J and Hoigne J. Decomposition of ozone in water - Rate of initiation by hydroxide ions and hydrogen-peroxide. Environ Sci Technol 1982;16:676-681.

Sutton HC. Reactions of hydroperoxyl radical (HO_2) with nitrogen-dioxide and tetranitromethane in aqueous-solution. J Chem Soc Faraday Trans 1975;71:2142-2147.

Tomiyasu H, Fukutomi H, Gordon G (1985). Kinetics and mechanism of ozone decomposition in basic aqueous-solution. Inorg Chem 1985;24: 2962-2966.

5 DECOMPOSITION OF CYCLOHEXANOIC ACID AND DECONTAMINATION OF OIL SAND PROCESS-AFFECTED WATER BY THE O_3/H_2O_2 ADVANCED OXIDATION PROCESS

5.1 Introduction

In Northern Alberta, oil sands industries extract bitumen from the oil sands using alkaline hot water in the surface mining process (Masliyah et al., 2004). The general term, naphthenic acid (NA), is used to describe a complex mixture of alkyl-substituted aliphatic cyclic and linear carboxylic acids that are naturally present in petroleum and bitumen. NAs have the general chemical formula of $C_nH_{2n+Z}O_2$, where n is the number of carbon atoms and Z is either 0 or an even negative integer representing the number of hydrogen lost as the structure becomes more cyclic or unsaturated (Headley and McMartin, 2004). The soluble fraction of NAs becomes concentrated in the oil sands process-affected water (OSPW), which is subsequently stored in large tailings ponds because of a zero discharge policy (Schramm et al., 2000). The reported range of NAs concentration in tailing ponds is between 25 and 125 mg NA/L (Allen, 2008; Pourrezaei et al., 2011) depending on the analytical method (Martin, et al., 2008). The toxicity of OSPW to aquatic organisms including rainbow trout, fathead minnows, Daphnia magna, and *Vibrio fisheri* (Clemente and Fedorak, 2005), as well as mice and midges has been

mainly related to organic content of OSPW including NAs (Headley and McMartin, 2004; Scott et al., 2005; Garcia-Garcia, 2011, Anderson et al., 2012; He et al., 2012). Thus, the NAs removal from OSPW has been one of the targets of studies since the 1980s (Allen, 2008). The current technology for the OSPW treatment is mostly based on the natural biodegradation, but this method is too slow to keep up with the fast industrial expansion.

The applications of advanced oxidation processes (AOPs) in water and wastewater treatments have been studied for years and have been shown to be very efficient for the removal of organic and recalcitrant pollutants (Parsons, 2004; Ikehata et al., 2008). AOPs rely on the formation of extremely reactive oxidizing agents (i.e. hydroxyl radicals; $\bullet$OH). Second to fluorine, the $\bullet$OH radical is the strongest known oxidant with a potential of 2.8 V versus standard hydrogen electrode. It is a non-specific oxidant that reacts with inorganic and organic compounds with rate constants ranging from 10^6 to 10^9 M^{-1} s^{-1} (Buxton et al., 1988). The combination of ozone/hydrogen peroxide (O_3/H_2O_2) is the most commonly applied AOP in drinking water treatment because conventional ozonation process can be adapted easily to an AOP by adding H_2O_2 to the system (Duguet et al., 1985; Glaze et al., 1987). The addition of H_2O_2 accelerates the O_3 decomposition to $\bullet$OH. However, this system is recommended for the solutions in which O_3 is relatively stable (i.e. water with high alkalinity and low organic matter content) (Acero and Von Gunten, 2001; Griffini and Iozzelli, 1996).

In the O_3/H_2O_2 (peroxone) process, •OH are formed through several reactions (5-1 to 5-6) (Acero and von Gunten, 2000).

$$H_2O_2 \longleftrightarrow H^+ + HO_2^- \tag{5-1}$$

$$O_3 + HO_2^- \longrightarrow \text{•OH} + O_2 + O_2\text{•}^- \tag{5-2}$$

$$H^+ + O_2\text{•}^- \longleftrightarrow HO_2\text{•} \tag{5-3}$$

$$O_3 + O_2\text{•}^- \longrightarrow O_3\text{•}^- + O_2 \tag{5-4}$$

$$O_3\text{•}^- + H^+ \longrightarrow HO_3\text{•} \tag{5-5}$$

$$HO_3\text{•} \longrightarrow \text{•OH} + O_2 \tag{5-6}$$

And the overall reaction is:

$$H_2O_2 + 2O_3 \longrightarrow 2\text{•OH} + 3O_2 \tag{5-7}$$

Therefore, the stoichiometric ratio is one mole of H_2O_2 to two moles of O_3. The theoretical mass ratio is 1 g of H_2O_2 to 2.82 g of O_3, or, 1 g of O_3 to 0.354 g of H_2O_2. Higher pH is preferential for the peroxone process because of the initiation reaction (Acero and von Gunten, 2000).

The presence of dissolved organic carbon in OSPW (i.e., other than NAs) may affect the decomposition of NAs in the peroxone process, as they compete for the •OH. Additionally, the presence of high concentration of inorganic anions such as bicarbonate

in OSPW could act as hydroxyl radical scavengers (Buxton and Elliot, 1986) in OSPW, further slowing the degradation of NAs.

To date, no investigation of the effect of O_3/H_2O_2 AOP on the OSPW and model NA compounds has been carried out (Allen, 2008). Since cyclic structures are a prominent feature of NA structures in OSPW (Headley and McMartin, 2004), cyclohexanoic acid (CHA) was previously selected as a simple model compound to study the mechanism of NA decomposition induced by •OH in ultrapure water (Drzewicz, et al., 2010; Afzal et al., 2012).

The objectives of this study were to assess:

- the reactivity of CHA in the O_3/H_2O_2 process under different O_3 to H_2O_2 ratios (stoichiometric ratio and commonly used ratios) and pH values,

- the degradation of OSPW NAs by using O_3 and O_3/H_2O_2 (three ratios similar to the CHA experiments) in a batch reactor (ozone stock solution is added to the reactor containing OSPW), and

- the removal of extractable organic acids (EOA) from OSPW using O_3 and O_3/H_2O_2 (three different ratios close to the ones in the batch system). In order to have the conditions similar to the real application of ozone in the industry, these experiments were performed in a semi-batch system. In the semi batch process, ozone gas is bubbled directly to the reactor containing OSPW.

5.2 Materials and methods

5.2.1 Chemicals and sample preparation

Cyclohexanoic acid (CHA, > 99% purity) was purchased from TCI (Portland, OR, USA). A stock solution (250 mg/L) of CHA was prepared in buffer solutions and the pH was adjusted as desired and stored at 4 °C; working solutions were prepared daily from this stock solution. The pH of the solutions was adjusted using 50% carbonate free sodium hydroxide (NaOH) (ACS purity) and 80% perchloric acid ($HClO_4$) solutions. Phosphate buffers (4 mM) were prepared using monosodium phosphate (NaH_2PO_4). An H_2O_2 stock solution (30% w/w) was used for the experiments. All stock solutions were prepared using ozone-demand-free (ODF) water and all the glassware used in experiments were cleaned and pre-treated with ODF water (details are presented in Appendix A).

Ammonium acetate, acetic acid, methanol (LC-MS grade) and all above mentioned chemicals were purchased from Fisher Scientific Co, Canada. All analytical solutions were prepared in ultrapure water (resistivity = 18 MΩ × cm and total organic carbon (TOC) < 0.1 mg/L). Other chemicals and reagents were of analytical grade and were used as received. Ultrapure water was obtained from a Millipore and Elga system equipped with an Elix UV lamp. The OSPW was supplied by Syncrude Canada Ltd. (Fort McMurray, AB, Canada) and kept at 4 °C until use. No pre-treatment was performed on

134

the OSPW before the ozonation experiments. Some of the OSPW characteristics are presented in Table 5-1.

Table 5-1. Some of the characteristics of OSPW (adapted from Pourrezaei et al., 2011)

Parameter	Average Value
TOC	51 mg/L
COD	240 mg/L
NAs	23.6 mg/L
Oxidized-NAs	31.6 mg/L
Extractable Organic acids	70.0 mg/L
pH	8.5
Turbidity	180 NTU
Alkalinity	630 mg/L
Conductivity	3750 µS/cm
Ammonium	22 mg/L
Chloride	515 mg/L
Sulfate	513 mg/L
Sodium	827 mg/L
Aluminum	8.5 mg/L
Iron	3.3 mg/L
Barium	0.35 mg/L
Vanadium	0.018 mg/L

5.2.2 Ozonation apparatus and O_3/H_2O_2 experiments

5.2.2.1 O_3/H_2O_2 of CHA in a batch system

Ozone gas was produced by a corona discharge ozone generator (PCI-Wedeco, Model GLS-7, Water Technology, Herford, Germany) from extra dry high purity oxygen. For any specific experiment, ozone stock solution (being used in batch reactors) was prepared by bubbling ozone gas to a 1 L solution. In order to perform the ozonation and O_3/H_2O_2 experiments at pH 9, the pH of the 4 mM phosphate buffer was adjusted to 9 with NaOH. The 1 L bottle was kept in an ice bath to slow down the ozone decomposition. The ozone concentration of the stock solution during the ozonation was monitored using spectrometric method by measuring the absorbance of the solution in a quartz cuvette at 260 nm (Bahnemann and Hart, 1982; Forni et al., 1982). After reaching the approximate desired concentration, the tube and diffuser were removed from the bottle and the ozone concentration was measured using the indigo method as an accurate initial ozone measurement (APHA, 2005) (details are presented in Appendix A). The same procedure was followed for the experiments at pH 3, except that the pH of 3 was adjusted using $HClO_4$.

Ozonation and O_3/H_2O_2 reactions were performed in 5 mL volumetric flasks with gas tight ground glass stoppers. All the experiments were performed in triplicates and at room temperature (20 ± 2 ℃). Every set of experiments was conducted in five volumetric flasks. In each flask a specific concentration of ozone was applied. The procedure was as follows: 1 mL of CHA stock solution (250 mg/L) along with the scavenger and/or buffer

136

was placed in each flask. The appropriate amount of H_2O_2 was also added to the flasks according to the ratio to O_3. 0.25, 0.5, 1, 2, and 3 mL of ozone stock solution was added into the according flasks, the flasks were closed immediately and shaken for a couple of minutes to make sure all ozone was consumed (this was tested by measuring the ozone residual in the flask). The ozone concentration in the stock solution was measured again by the indigo method after adding the stock ozone solution to the last flask to make sure the stock ozone concentration had not changed during the experiment. Flasks then were filled with ODF water to the line of 5 mL to compensate for the difference in ozone volume added to each flask. Parallel to each experiment, a blank/control was run. This control flask was filled with 1 mL CHA and 4 mL ODF water only, leading to a CHA concentration of 50 mg/L. The same procedure was applied to the treatment of OSPW by the O_3 and O_3/H_2O_2 in a batch system. However, no pH adjustment was applied and the OSPW was treated as received.

5.2.2.2 O_3/H_2O_2 of OSPW in a semi-batch system

An ozone generator (Wedeco, Model GSO-40, Water Technology, Herford, Germany) was used to produce ozone gas using extra dry, high purity oxygen. In order to achieve stable ozone concentration in the feed gas, the ozone generator was allowed to stabilize for 10 min before O_3 and O_3/H_2O_2 experiments. The feed gas was sparged into the liquid phase (OSPW) though a gas diffuser. The appropriate amount of H_2O_2 (to reach the desired concentration based on the ratio with O_3) was added to the reactor (a 4-L

Erlenmeyer flask) before bubbling ozone. Two ozone monitors (model HC-500 from Wedeco) were also used for the ozone measurements. Potassium iodine (KI) was used to calibrate the ozone monitors according to Standard Methods for the Examination of Water and Wastewater (APHA, 2005) (details are included in Appendix A).

5.2.3 Analytical methods

A high performance liquid chromatograph (HPLC) coupled to an ion trap mass spectrometer (Varian 500-MS) was used for the analysis of CHA. The chromatographic conditions were: A, 100% methanol, and B, 4 mM ammonium acetate with 0.01% acetic acid, gradient elution from 30% to 70% A over 30 min, flow 200 μL/min, injected volume 20 μL. A Phenomenex, C8, 5 μm, 250 mm × 3 mm column was used for separations.

Fourier transform infrared (FT-IR) spectroscopy was used (Scott, Young et al. 2008) to measure the extractable organic acids (EOA) concentration in the OSPW before and after treatment in the semi-batch system. Details of FT-IR measurements are presented in Appendix A. For the OSPW NAs measurement in the experiments in batch system, an ultra-pressure liquid chromatography-high resolution mass spectrometry (UPLC-HRMS) was used (details of the analytical procedure are listed in Appendix A).

5.3 Results and discussion

5.3.1 CHA degradation using O_3/H_2O_2 at pH 3 and 9 in a batch system

Figures 5-1 and 5-2 show the results of experiments performed to study the efficiency of the CHA degradation using O_3/H_2O_2 with different molar ratios along with the ozonation alone.
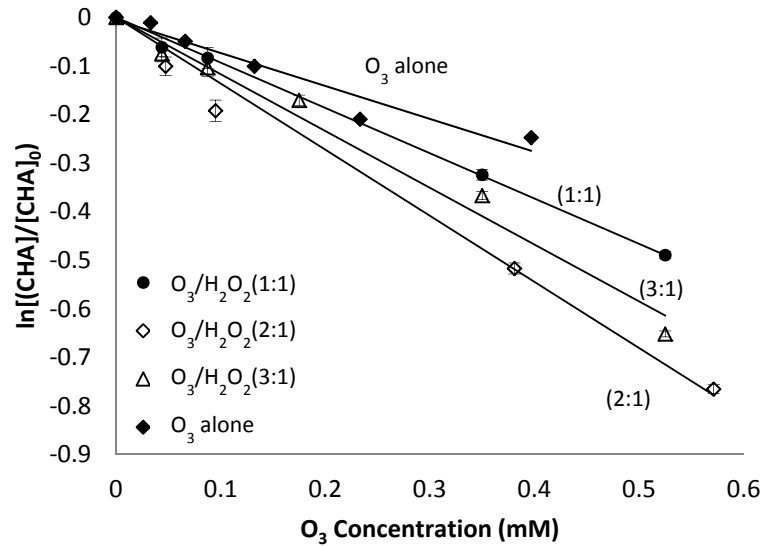
Figure 5-1. CHA degradation at pH 3 with different O_3 to H_2O_2 ratios; error bars are standard deviation of three replicates.
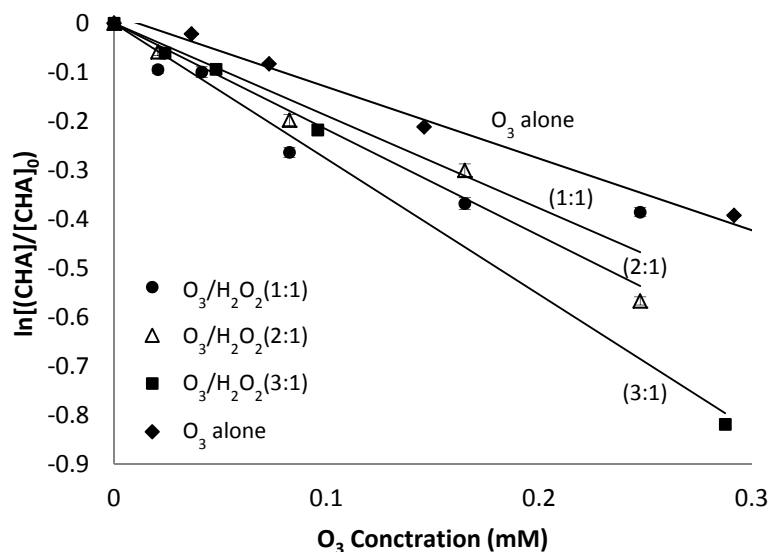
Figure 5-2. CHA degradation at pH 9 with different O_3 to H_2O_2 ratios; error bars are standard deviation of three replicates.

The results showed that at pH 3, CHA removal was significantly higher when using O_3 to H_2O_2 ratios of 2:1 (1.36 ± 0.08 mole CHA was removed by utilizing one mole ozone) and 3:1 (1.17 ± 0.12 mole CHA was removed by utilizing one mole ozone) comparing with the ratio of 1:1 (0.93 ± 0.05 mole CHA was removed by utilizing one mole ozone). However, the CHA degradation with the O_3 to H_2O_2 ratio of 2:1 and 3:1 were not statistically different. The removal efficiency of CHA in O_3/H_2O_2 treatment with all three ratios at pH 3 was higher compared with O_3 alone process at the same pH (Figure 5-1). As it is very well established, the removal efficiency of organic compounds in the O_3/H_2O_2 system depends on the degree of hydroxyl radical (•OH) generation. As

explained earlier, the •OH generation in this system is performed by the reaction 5-7 which is the overall result of several reactions.

The stoichiometry of reaction 5-7 suggests that the theoretical mole ratio of H_2O_2 to O_3 is 0.5 (or O_3 to H_2O_2 = 2:1) for an effective •OH generation. At its concentration below a certain level, the effect of H_2O_2 is insignificant in the O_3/H_2O_2 reaction (Brunet et al., 1984; Glaze and Kang, 1989; Kuo et al., 1999). Therefore, a molar ratio less than 0.5 will result in limited •OH radical generation. It should be noted that high concentration of H_2O_2 in the solution may act as radical scavenger as it is shown in the reaction 5-8 (Buxton et al., 1988).

$$H_2O_2 + •OH \longrightarrow HO_2• + H_2O \quad k_{OH} = 2.7 \times 10^7 \, M^{-1} \, s^{-1} \quad (5\text{-}8)$$

The results at pH 9, however, showed that, the removal of CHA was higher in the O_3 to H_2O_2 ratio of 3:1 (2.77 ± 0.07 mole CHA was removed by utilizing one mole ozone) comparing with the ratios of 1:1 (1.89 ± 0.23 mole CHA was removed by utilizing one mole ozone) and 2:1 (2.17 ± 0.15 mole CHA was removed by utilizing one mole ozone). The CHA degradations with the O_3 to H_2O_2 ratio of 2:1 and 1:1 were not statistically different. The removal efficiency of CHA in O_3/H_2O_2 treatment with all three ratios at pH 9 was higher compared with O_3 alone process at the same pH (Figure 5-2).

Comparing the overall results of the O_3/H_2O_2 process at pH 3 and 9, it was shown that the process is more effective at pH 9. In the O_3/H_2O_2 process, the O_3 decomposition

141

cycle is initiated mainly by HO_2^-. This is contrary to the conventional ozonation process in which OH^- initiates O_3 decomposition. However, at pH 9, the efficiency of the O_3/H_2O_2 treatment is higher because of both initiation reactions (Acero and Von Gunten, 2001).

5.3.2   Treatment of OSPW using O_3 and O_3/H_2O_2 in a semi-batch system

The degradation of OSPW by the O_3 and O_3/H_2O_2 process was studied in a semi-batch system. Figure 5-3 shows the percentage EOA removal from OSPW using 30 mg/L (0.625 mM) utilized O_3 dose and three O_3 to H_2O_2 ratios. The first column in figure 5-3 represents the EOA concentration in the raw OSPW, the other columns represent the EOA from OSPW treated with O_3 alone, and different molar ratios of O_3 to H_2O_2 (1:1, 2:1 and 1:2), respectively.
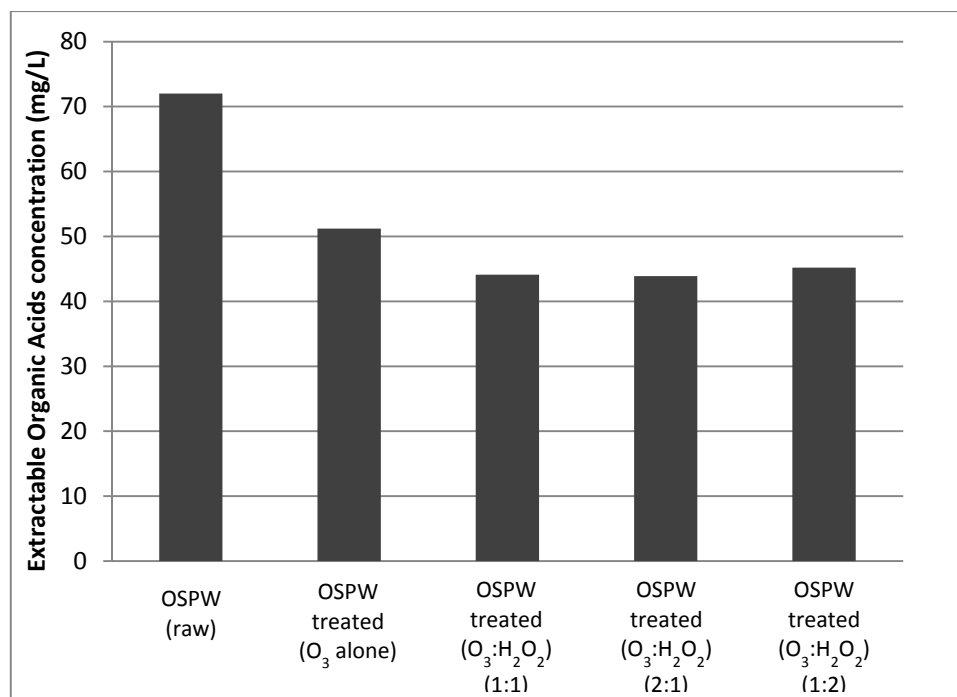
Figure 5-3. Treatment of OSPW using 30 mg/L utilized O_3 dose and three O_3 to H_2O_2 ratios in a semi-batch reactor.

In order to understand the effect of utilized ozone dose for the OSPW treatment, in the second set of experiments (Figure 5-4) the EOA removal from OSPW was investigated using 85 mg/L (1.77 mM) O_3. The first column in the figure represents the EOA concentration in the raw OSPW and the other columns present OSPW treated with O_3 alone, and different molar ratios of O_3 to H_2O_2 (2:1, 2.5:1 and 3:1), respectively.
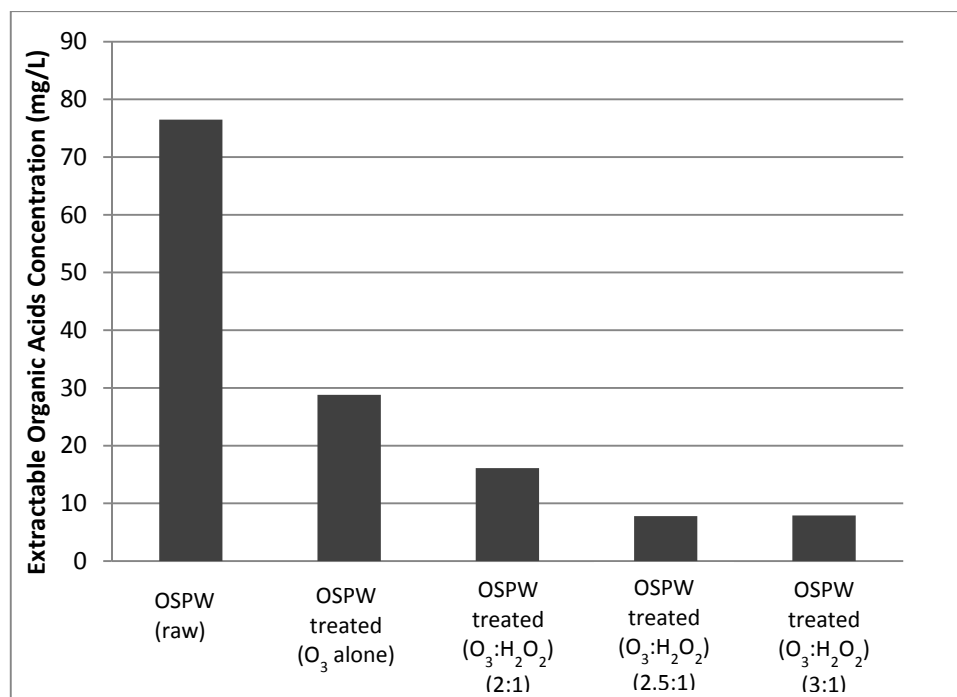
Figure 5-4. Treatment of OSPW using 85 mg/L utilized O_3 dose and three O_3 to H_2O_2 ratios in a semi-batch reactor.

Using 30 mg/L ozone (4 min ozone bubbling into a 4-L OSPW bottle), only 29% of EOA was removed. By adding H_2O_2 to the reactor with the ratio of 1:1 to ozone, the EOA removal increased to 39%. By changing the ratios from O_3 to H_2O_2 from an initial 1:1 to 2:1 and to 1:2, the removal of EOA did not change significantly (percentage removal was 39 and 37%, respectively). It should be noted that the chemistry of the products detected by FT-IR could be very different after each treatment as all the extractable acid products are analyzed using FT-IR. Therefore, it is not known in the O_3/H_2O_2 process what kinds of compounds were removed and what were formed. This means that the results are not necessarily related to NA removal.

144

The pH of OSPW is between 7.5 and 8.5 which means even in presence of ozone alone, there is a likely formation of •OH. However, the presence of radical scavengers in the OSPW reduces the efficiency of the ozonation treatment. As explained earlier, the addition of H_2O_2 increases the formation of •OH and consequently, the removal of EOA increases, but there is no significant difference if the molar ratios are 1:1, 2:1 or 1:2.

When using a 85 mg/L utilized ozone dose (15 min ozone bubbling into a 4-L OSPW bottle), 62.4% of EOA was removed (see figure 5-4) Although the presence of radical scavengers in OSPW decreased the efficiency of ozonation, at this high ozone concentration, the effect of radical scavengers is limited due to the presence of high ozone concentration in the system for its reaction with extractable organic acids of OSPW. By adding H_2O_2 to the reactor with the ratio of 1:2 to ozone, the EOA removal increased to 79%. By changing the H_2O_2 ratio, (decreasing the actual H_2O_2 concentration), the removal of EOA changed significantly (percentage removal with the O_3 to H_2O_2 ratios of 2.5:1 and 3:1 was approximately 90%). According to these two sets of experiments (Figures 5-3 and 5-4), it can be suggested that at low utilized ozone doses the addition of H_2O_2 has a negligible effect on the levels of EOA degradation. This might be due to the high scavenging content of the OSPW (see Table 5-1). When the concentration of O_3 and H_2O_2 is high, the amount of •OH generated in the solution is also high and even if a part of •OH is consumed by scavengers, there are radicals available for EOA removal. The process seems to be more efficient at O_3 to H_2O_2 rates of 2.5:1 and

3:1 than at higher O_3 to H_2O_2 ratios of 1:2. This might be due to a synergic scavenging effect of H_2O_2, inorganic and organic radical scavengers.

5.3.3 Treatment of OSPW using O_3 and O_3/H_2O_2 in a batch system

The degradation of OSPW by the O_3 and O_3/H_2O_2 process was also studied in a batch system. Table 5-2 shows the results of NAs degradation in the O_3 and O_3/H_2O_2 process. The best NAs removal was observed at the O_3 to H_2O_2 ratio of 0.6.

H_2O_2 concentration was measured after each experiment using I_3^- method (see Appendix A for details of the H_2O_2 concentration measurement). The results showed (Table 5-2) that in all the experiments, the H_2O_2 residual is high and close to the initial concentration applied. As explained in chapter 4.3.2, H_2O_2 is generated during the process where O_3 is used as oxidising agent. The hydrogen peroxide generation might be due to the reaction of peroxyl-NAs radicals with ozone. These peroxyl-NAs radicals may be produced via the reaction of NAs with Ozone (see reaction 4-12 in chapter 4).

Table 5-2. Concentration of O_3, H_2O_2, and NAs in O_3/H_2O_2 process in a batch system.

	O_3 concentration (mg/L)	H_2O_2 concentration (mg/L)	O_3 to H_2O_2 molar ratio	NA concentration (mg/L)	H_2O_2 concentration after treatment (mg/L)
OSPW	0	0	N/A	21.029	0
OSPW diluted[*] (1:5)	0	0	N/A	4.114	0
OSPW+O_3	12	0	N/A	0.477	0
OSPW + O_3/H_2O_2	12	2.38	3.5	0.113	1.46
OSPW + O_3/H_2O_2	12	3.57	2.4	0.192	3.06
OSPW + O_3/H_2O_2	12	7.14	1.2	0.243	6.66
OSPW + O_3/H_2O_2	12	14	0.6	0.070	12.76

The structure reactivity of NAs (both model NA compounds and real OSPW) with ozonation (Perez-Estrada et al., 2011) and UV/H_2O_2 (Afzal et al., 2012) has been studied before. It was shown in the ozonation process that NAs with a higher carbon number were favoured in the degradation due to the possibility for hydrogen abstraction and also NAs with more cyclic structures were depleted faster because of the higher reactivity of tertiary carbons present in the structure of the more cyclic compounds (Perez-Estrada et al., 2011). In the UV/H_2O_2 process, NAs with a higher carbon number were also favoured

in degradation, but more cyclic structures (or double bonds) seemed to have no impact onto the degradation (Afzal et al., 2012).

Figures 5-5 and 5-6 show the structural dependence (number of carbon atoms and Z number) of the detected NAs in the raw OSPW and the treated OSPW with O_3 and O_3/H_2O_2. Comparing Figure 5-5 A and 5-5 B confirms that compounds with a higher number of carbons and higher Z number (equivalent to number of rings or double bonds) were removed from the system. The experiments conducted with O_3 showed that the reactivity of certain NAs towards O_3. Some degradation products were formed during the treatment which had less Z (i.e. not cyclic or one ring). It should be noted that since the pH of OSPW is between 7.5 and 8.5, the OSPW NAs oxidation is due to both molecular O_3 and •OH not ozonolysis. Figures 5-5 C and 5-6 D to F show the OSPW NAs degradation using different O_3/H_2O_2 ratios. Comparing with O_3 treatment alone, the removal of NAs using O_3/H_2O_2 is higher due to the presence of both O_3 and •OH in the solution.
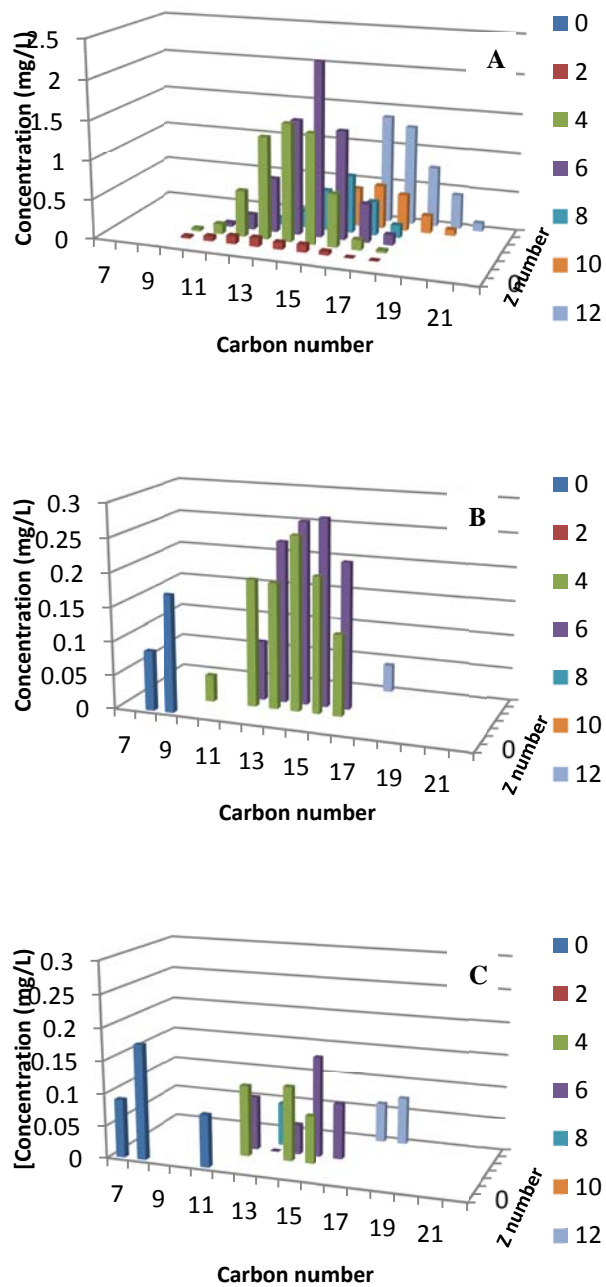
Figure 5-5. Initial concentration of NAs in raw OSPW (A), concentration after treatment with 12mg/L O_3 (B) and concentration after treatment with 12mg/L O_3 + H_2O_2 (1:1 ratio) (C).

149
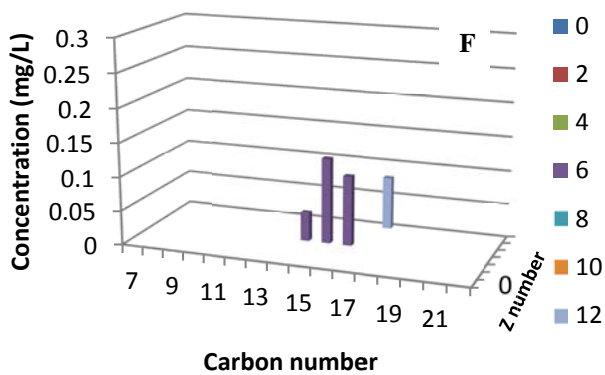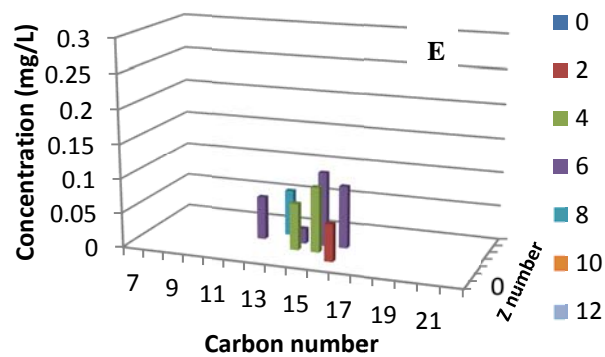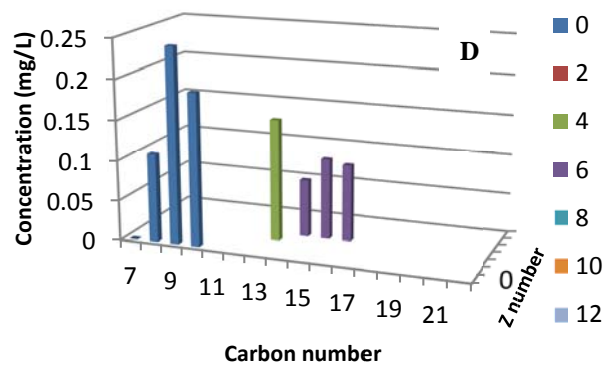
Figure 5-6. Concentration of NAs according to their carbon number and Z found in OSPW treated water with different O_3:H_2O_2 ratios. Initial O_3 concentration 12 mg/L. 2:1 ratio (D), 3:1 ratio (E), 1:2 ratio (F).

5.4 Conclusions

Cyclohexanoic acid (CHA) as a simple model NA compound and OSPW were treated by O_3 and O_3/H_2O_2 advanced oxidation process (AOP). The main conclusions of this study are as follows.

- The removal of CHA was higher in the O_3/H_2O_2 system than in O_3 alone independent of the tested pH values (3 and 9)

- At pH 3, the highest degradation of CHA with the O_3/H_2O_2 process was observed at the H_2O_2 to O_3 ratio of 0.3 and 0.5.

- At pH 9, the highest degradation of CHA with the O_3/H_2O_2 process was observed at the H_2O_2 to O_3 ratio of 0.3.

- In a batch system, 99% removal of OSPW NAs was achieved at the H_2O_2 to O_3 ratio of 0.6 without changing the pH of OSPW.

- In a semi-batch system, approximately 90% of extractable organic acids concentration of OSPW was removed with O_3/H_2O_2 process with 85 mg/L of ozone and O_3 to H_2O_2 ratio of 0.3.

5.5 Recommendation

Recommendations for the future works in this study are as follows:

- Microbial degradation of O_3/H_2O_2 treated OSPW should be investigated to examine the overall benefit of this treatment for real applications.

151

- Kinetic studies on the OSPW NAs degradation in O_3/H_2O_2 should be performed.

- For the kinetics experiments it is recommended to use a stopped-flow system in which NA degradation along with O_3 is considered.

- The O_3/H_2O_2 experiments are recommended to be optimized in terms of O_3 to H_2O_2 ratio for the real industrial applications.

5.6 References

Acero JL, von Gunten U. Influence of carbonate on the ozone/hydrogen peroxide based advanced oxidation process for drinking water treatment. Ozone-Sci Eng 2000;22:305-328.

Acero JL, Von Gunten U. Characterization of oxidation processes: ozonation and the AOP O_3/H_2O_2. J Am Water Works Ass 2001;93:90-100.

Afzal A, Drzewicz P, Martin JW, Gamal El-Din M. Decomposition of cyclohexanoic acid by the UV/H_2O_2 process under various conditions. Sci Total Environ 2012; 426:387-392.

Afzal A, Drzewicz P, Perez-Estrada L, Chen Y, Martin JW, Gamal El-Din M. Effect of molecular structure on the relative reactivity of naphthenic acids in the UV/H_2O_2 advanced oxidation process. Environ Sci Techno 2012;46:10727-10734.

American Public Health Association (APHA), Standard methods for the examination of water and wastewater. 21st ed. Washington: American Water Works Association and Water Environment Federation; 2005.

Anderson JC, Wiseman SB, Wang N, Moustafa A, Perez-Estrada L, Gamal El-Din M, Martin JW, Liber K, Giesy JP. Effectiveness of ozonation treatment in eliminating toxicity of oil sands process-affected water to chironomus dilutus. Environ Sci Technol 2012;46:486-493.

Bahnemann D, Hart EJ. Rate constants of the reaction of the hydrated electron and hydroxyl radical with ozone in aqueous solution. J Phys Chem 1982;86:252-255.

Brunet R, Bourbigot MM, Dore M. Oxidation of organic compounds through the combination ozone-hydrogen peroxide. Ozone-Sci Eng 1984;6:163-183.

Buxton GV, Elliot AJ. Rate constant for reaction of hydroxyl radicals with bicarbonate ions. Radiat Phys Chem 1986;27:241-243.

Buxton GV, Greenstock CL, Helman WP, Ross AB. Critical-review of rate constants for reactions of hydrated electrons, hydrogen-atoms and hydroxyl radicals (•OH/•O$^-$) in aqueous-solution. J Phys Chem Ref Data 1988;17:513-886.

Clemente JS, Fedorak PM. A review of the occurrence, analyses, toxicity, and biodegradation of naphthenic acids. Chemosphere 2005;60:585-600.

Drzewicz P, Afzal A, Gamal El-Din M, Martin JW. Degradation of a model naphthenic acid, cyclohexanoic acid, by vacuum UV (172 nm) and UV (254 nm) / H$_2$O$_2$. J Phys Chem A 2010;114:12067-12074.

Duguet JP, Brodard E, Dussert B, Mallevialle J. "Improvement in the effectiveness of ozonation of drinking water through the use of hydrogen peroxide. Ozone-Sci Eng 1985;7:241-258.

Forni L, Bahnemann D, Hart EJ. Mechanism of the hydroxide ion initiated decomposition of ozone in aqueous solution. J phys chem 1982;86:255-259.

Garcia-Garcia E, Pun J, Pérez-Estrada LA, Gamal El-Din M, Smith DW, Martin JW, Belosevic M. Commercial naphthenic acids and the organic fraction of oil sands process water downregulate pro-inflammatory gene expression and macrophage antimicrobial responses. Toxicol Lett 2011;203:62-73.

Glaze WH, Kang JW. Advanced oxidation processes- Test of a kinetic model for the oxidation of organic compoundswith ozone and hydrogen peroxide in a semibatch reactor. Ind Eng Chem Res 1989;28:1580-1587.

Glaze WH, Kang JW, Chapin DH. The chemistry of water treatment processes involving ozone, hydrogen peroxide and ultraviolet radiation. Ozone-Sci Eng 1987;94:335-352.

Griffini O, Iozzelli P. The influence of H_2O_2 in ozonation treatment: Experience of the water supply service of Florence, Italy. Ozone-Sci Eng 1996;18:117-126.

He YH, Wiseman SB, Wang N, Perez-Estrada LA, Gamal El-Din M, Martin JW, Giesy JP. Transcriptional responses of the brain-gonad-liver axis of fathead minnows exposed to untreated and ozone-treated oil sands process-affected water. Environ Sci Technol 2012;46:9701-9708.

Headley JV, McMartin DW. A review of the occurrence and fate of naphthenic acids in aquatic environments. J Environ Sci Heal A 2004;39:1989-2010.

Ikehata K, Gamal El-Din M, Snyder SA. Ozonation and advanced oxidation treatment of emerging organic pollutants in water and wastewater. Ozone Sci Eng 2008;30:21-26.

Kuo CH, Zhong L, Zappi ME, Hong AP. Kinetics and mechanism of the reaction between ozone and hydrogen peroxide in aqueous solutions. Can J Chem Eng 1999;77:473-482.

Martin JW, Han XM, Peru KM, Headley JV. Comparison of high- and low-resolution electrospray ionization mass spectrometry for the analysis of naphthenic acid mixtures in oil sands process water. Rapid Commun in Mass Sp 2008;22:1919-1924.

Masliyah J, Zhou Z, Xu Z, Czarnecki J, Hamza H. Understanding water-based bitumen extraction from Athabasca oil sands. Can J Chem Eng. 2004; 82: 628–54.

Pérez-Estrada LA, Han XM, Drzewicz P, Gamal El-Din M, Fedorak PM, Martin JW. Structure-reactivity of naphthenic acids in the ozonation process. Environ Sci Technol 2011;45:7431-7437.

Pourrezaei P, Drzewicz P, Wang YN, Gamal El-Din MG, Perez-Estrada LA, Martin JW, Anderson J, Wiseman S, Liber K, Giesy JP. The impact of metallic coagulants on the removal of organic compounds from oil sands process-affected water. Environ Sci Technol 2011;45: 8452-8459.

Scott AC, MacKinnon MD, Fedorak PM. Naphthenic acids in Athabasca oil sands tailings waters are less biodegradable than commercial naphthenic acids. Environ Sci Technol 2005;39:8388-94.

Scott AC, Zubot W, MacKinnon MD, Smith DW, Fedorak PM. Ozonation of oil sands process water removes naphthenic acids and toxicity. Chemosphere 2008;71:156-60.

6 GENERAL CONCLUSIONS AND RECOMMENDATIONS

6.1 Thesis overview

Oil sand process water generated during the extraction of bitumen from oil sands processes in Northern Alberta, Canada, is a complex alkaline mixture or organic and inorganic compounds together with a stable suspension of small. Because of a zero discharge policy, companies dealing with the oil sands are required to store OSPW in tailings ponds close to their sites. There are some environmental issues attributed to the OSPW storing including presence of NAs in surface waters surrounding the oil sands sites due to their leaching from the tailings ponds. Because of the presence of high concentration of refractory organic compounds such as NAs, OSPW becomes highly toxic. Various treatment technologies such as CFS, adsorption, biological treatment, membrane filtration, and AOPs have been studied for their efficiency in treating OSPW. Nevertheless, there exist significant research gaps related to the efficiency and applicability of these treatment technologies for the remediation of OSPW at a large industrial scale. For the release of OSPW into the environment, especially Athabasca River, the treated OSPW should meet the standard guidelines. Therefore, the removal of the inorganic and organic compounds including NAs should be the highest priority during OSPW treatment.

Based on these needs, the present research was focused on the elucidation of mechanisms and treatability of three types of advanced oxidation processes: UV/H_2O_2,

ozonation at alkaline pH, and O_3/H_2O_2. A simple one-ring NA model compound, cyclohexanoic acid (CHA), was selected and the effect of different system parameters (concentration of H_2O_2, power of the UV lamp, pH, presence of radical scavengers and OSPW constituents) on the reactivity of CHA in the UV/H_2O_2 AOP was investigated. The structure reactivity of several model NA compounds in the UV/H_2O_2 advanced oxidation process was also studied. The third part of the research was related to the study of the mechanism of CHA ozonation using different conditions including pH and presence of radical scavengers. Finally, the last part of this study was focused on the treatability of OSPW NAs using O_3/H_2O_2 process.

6.2 Conclusions

The following conclusions were drawn as a result of this research:

- Based on the results of the degradation of a model NA compound (CHA), increasing concentration of H_2O_2 increased the CHA degradation rate up to the optimal molar concentration ratio of 23 (ratio of H_2O_2 to CHA). It was also shown that pH did not have any significant effect on the CHA degradation rate and the byproducts formation in the ultrapure water. When carbonate and chloride ions were present in the solution at concentrations close to those in OSPW, CHA degradation rate decreased by 55% and 23%, respectively. Other organic and inorganic compounds present in OSPW competed with CHA for the reaction with •OH. Such

that the pseudo-first order rate constant for CHA degradation in raw OSPW was 81% lower than that in ultrapure water. However, the effectiveness of the UV/H_2O_2 process was higher after OSPW pre-treatment with the powdered activated carbon due to the removal of organic compounds, still remained significantly lower (62%) than its rate of degradation in ultrapure water.

- Relative rate measurements using mixtures of two model NA compounds confirmed that NAs with the higher number of carbons had higher reactivity in the UV/H_2O_2 process. It was also concluded that reactivity favoured NAs with one saturated ring, in comparison with the corresponding linear NAs. However, for the model compounds with the three saturated rings, no increased reactivity was observed in comparison with monocyclic NA.

- The findings of the structure-reactivity study using model NA compounds were further tested with the OSPW. It was confirmed that during the UV/H_2O_2 treatment of OSPW, the efficiency of degradation increased with increasing number of carbon atoms. However, no clear structure-reactivity dependence was observed by increasing the number of rings (or double bond equivalents).

- The mechanism of degradation of CHA in the ozonation process at pHs 3 and 9 and in the presence of radical scavengers showed that the

mechanism of CHA ozonation was pH dependent. At pH 9, 4-oxo-CHA and 4-hydroxy-CHA were detected by LC-MS/MS, thus confirming the •OH pathway in which the superoxide CHA radical might be an intermediate. The addition of carbonate ions to the ozonation system at pH 9 did not have any influence on CHA degradation. However, the addition of TBA and TNM decreased CHA degradation, which further confirmed the •OH degradation pathway.

- At pH 3, the oxo-CHA was observed as an intermediate, but no hydroxy-CHA was detected. This suggested that at pH 3 the pathway was likely based on the degradation of CHA by molecular ozonolysis rather than on •OH formation.

- Addition of H_2O_2 to the ozonation system at the ratio of 1:2 significantly increased CHA removal at both studied pHs.

- In a batch ozonation system, 99% removal of OSPW NAs was achieved at a H_2O_2 to O_3 ratio of 0.6 at a natural pH of OSPW. However, in a semi-batch system, approximately 90% of EOA of the OSPW was removed with O_3/H_2O_2 process when 85 mg/L of ozone was utilized in presence of H_2O_2 (O_3 to H_2O_2 ratio of 0.3).

6.3 Recommendations

Based on the results obtained in this study, the following recommendations can be drawn:

- Main focus in this research was on the model NA compounds. Even though the OSPW was also treated by the AOPs, there is still a research gap for the application of UV/H_2O_2 and O_3/H_2O_2 to OSPW treatment, especially with respect to the optimum pre-treatment strategy of OSPW. Therefore, it is recommended more research to be conducted in order to determine the best pre-treatment method in order to achieve the highest removal of contaminants prior to AOP application.

- The application of O_3/H_2O_2 for the removal of OSPW NAs has not been optimized. It is recommended to use the stopped-flow methods for kinetics study and treatment optimization.

- The economical evaluation of the two proposed advanced oxidation processes (UV/H_2O_2 and O_3/H_2O_2) for the real industrial application is also recommended. Estimation of the overall cost of the UV/H_2O_2 and O_3/H_2O_2 processes is important for upscaling the system.

- Microbial degradation studies should be conducted for the UV/H_2O_2 and O_3/H_2O_2 treated OSPW to examine the overall benefit of these treatments for the real applications.

APPENDICES

Appendix A: Experimental Procedures

A-1. UV/H$_2$O$_2$ Experiments

A-1-1. Determination of H$_2$O$_2$ residual concentration by the I$_3^-$ method:

Materials:

- ✓ Hydrogen peroxide (H$_2$O$_2$:35% certified)

- ✓ Sodium hydroxide (NaOH)

- ✓ Ammonium molybdate ((NH$_4$)$_6$Mo$_7$O$_2$·4H$_2$O)

- ✓ Potassium hydrogen phthalate (KHP)(C$_8$H$_5$KO$_4$)

- ✓ Ultrapure water

- ✓ 500-, 100-, and 10-mL volumetric flasks

- ✓ Spectrophotometer

Preparation of solution A:

Add 1.0 g of NaOH, 33 g of KI and 0.1 g of (NH$_4$)$_6$Mo$_7$O$_2$·4H$_2$O to a 500 mL volumetric flask and bring up to the mark with ultrapure water.

Preparation of solution B:

Add 10.0 g of potassium acid phthalate (KHP) to a 500 mL volumetric flask and bring up to the mark with ultrapure water.

Note: The density of the stock 34.8% H$_2$O$_2$ solution (actual assay) is 1.135 g/L. Therefore, H$_2$O$_2$ concentration of the stock solution = 1.135 g/L × 0.348 × 1000 ≈ 395,000 mg/L. The absorbance of the solution was measured at 351 nm in a 10 mm cell.

164

A-1-1-1. Preparation of H_2O_2 standards for high H_2O_2 concentrations and the absorbance determination:

Dilutions for H_2O_2 concentrations are prepared from approximately 29.6 mg/L to 118.5 mg/L as follows:

- Add 1 mL of the stock 35% H_2O_2 solution to a 100-mL volumetric flask and bring up to the mark with ultrapure water. The concentration of this solution is approximately 3,950 mg/L. This solution serves as a diluted stock solution.

- Prepare 118.5, 94.8, 59.2 and 29.6 mg/L H_2O_2 in 100-mL volumetric flasks. The addition of H_2O_2 from the diluted stock solution is 3.00 mL, 2.40 mL, 1.50 mL, and 0.75 mL, respectively.

The absorbance determination for H_2O_2 standards is as follows:

- Add 170 μL of each H_2O_2 standard solution, 4.9 mL of solution A and 4.9 mL of solution B to a series of 10-mL volumetric flasks (one flask for each H_2O_2 concentration), and bring it to the mark with ultrapure water.

- Wait for approximately 10 seconds until the solution becomes straw yellow and then measure the absorbance at 351 nm.

- Repeat the above steps for 2 replicates to achieve the average absorbance for each H_2O_2 concentration.

A-1-1-2. Preparation of H_2O_2 standards for low H_2O_2 concentrations and absorbance determination:

Dilutions for H_2O_2 concentrations are prepared from approximately 2.95 mg/L to 23.7 mg/L as follows:

- Prepare 23.70, 11.80, 5.90, and 2.95 mg/L H_2O_2 in 100-mL volumetric flasks. The addition of H_2O_2 from the diluted stock solution is 600 μL, 300 μL, 150 μL, and 75 μL, respectively.

The absorbance determination for H_2O_2 standards is as follows:

- Add 900 μL of each H_2O_2 standard solution, 4.9 mL of solution A and 4.9 mL of solution B to a series of 10-mL volumetric flasks (one flask for each H_2O_2 concentration), and bring it to the mark with ultrapure water.

- Wait for approximately 10 seconds until the solution becomes straw yellow and then measure the absorbance at 351 nm.

- Repeat the above steps for 2 replicates to achieve the average absorbance for each H_2O_2 concentration.

A-1-1-3. Procedure for H_2O_2 concentration determination in the samples:

- Prepare the standard calibration curve for the H_2O_2 standard solutions. One curve for high concentrations and one for low concentrations. Using linear trend line, determine the linear equation related to each standard calibration curve.

- Based on the background information (i.e. initial H_2O_2 concentration in the sample), either add 170 μL (for H_2O_2 concentrations between 25 to 120 mg/L) or

900 μL (for H_2O_2 concentrations between 2.5 to 25 mg/L) to a 10-mL volumetric flask.

- Add 4.9 mL of solution A and 4.9 mL of solution B to the flask.

- Wait for approximately 10 seconds and then measure the absorbance at 351 nm.

- Repeat the above steps for 2 replicates for quality control purposes.

- Put the absorbance in the linear equation and calculate the H_2O_2 concentration.

A-1-2. UV experiments:

Materials:

- ✓ Solutions of model NA compounds, OSPW

- ✓ H_2O_2 solution (diluted for the specific experiment)

- ✓ UV collimated beam apparatus (Model PSI-1-120, Calgon Carbon Corporation)

- ✓ Low-pressure (10 W) UV lamp

- ✓ Petri dish (reactor), stir bar, and magnetic stirrer

- ✓ Radiometer (Model IL 1400A with a SED240 Detector, International Light Inc.)

- ✓ Spectrophotometer, 10 mm quartz cuvette, pH meter

- ✓ Cary 50 UV-Vis spectrophotometer

Procedure:

- Solutions of the model NA compounds (CHA and other compounds in Chapter 3) are irradiated for various exposure times by using a UV collimated beam apparatus equipped with a 10W low-pressure UV lamp

167

- A radiometer is used to measure the UV irradiance at the center of the UV beam on the surface of the samples (the radiometer should be calibrated at 254 nm).

- H_2O_2 is added to the model NA compound solutions right before the UV exposure.

- The absorbance of the solution which is being exposed (i.e. model NA compound + H_2O_2) is measured using a regular spectrophotometer. In case of the OSPW, Varian Cary 50 (Varian, Palo Alta, CA, USA) spectrophotometer is used for scanning the OSPW solution which is being exposed (i.e. OSPW + H_2O_2) from 200 nm to 400 nm. A 10-mm path length quartz cuvette is used.

- Petri dishes (60-mm) are used in the experiments as reactors in batch mode.

- Open the nitrogen cylinder, plug the collimated beam apparatus, and turn on the UV lamp. It takes approximately 10 minutes for the device to stabilize.

- Using a radiometer, determine the UV irradiance at the centre of the sample position and also measure the irradiance across the center of the beam. These data is used for Petri factor estimation.

- Place the Petri dish (reactor) in the center of the UV beam.

- Measure the distance between the solution surface and the UV lamp.

- Place a stir bar into the Petri dish. This is necessary for the solution to receive equal fluence. Stirring should be slow to avoid making turbulence in the solution.

- Pour sample solution (normally 15 mL) into the Petri dish and start mixing.

- Open the shutter and at different time intervals, take around 150 μL sample and put them into the HPLC vials for the NA concentration measurements.

- For the OSPW, since 150 μL is not enough for analysis, prepare a series of Petri dishes and expose each dish to the UV light for appropriate amount of time.

- To make sure the irradiance was constant during the experiment, measure the irradiance again after the treatment.

- After finishing the experiment, close the shutter, turn off the UV lamp, close the nitrogen cylinder, and around 10 minutes after turning off the lamp, and unplug the apparatus.

Safety: Eye protection is an absolute requirement for using the UV collimated beam apparatus.

A-2. Ozonation Experiments

A-2-1. Ozone-demand-free water preparation:

Ozone-demand-free (ODF) water is used for preparation of all the buffers and solutions that is required for ozonation (and O_3/H_2O_2) experiments. Materials and method are as follows:

Materials:

- ✓ Ozone generator (PCI-Wedeco, Model GLS-7, Water Technology, Herford, Germany)

- ✓ Ultrapure water (resistivity = 18 MΩcm; TOC < 0.1 mg/L) obtained from a Millipore and Elga system equipped with an Elix UV lamp

- ✓ Glass bottle

- ✓ Ice bath container

Procedure:

- Using an ozone generator bubble ozone gas through glass bottle (could be a 4 L bottle) of ultrapure water (for a 4 L bottle at least 30 minutes).

- To achieve more than 20 mg/L O_3 in water, the ODF bottle is better to be kept and cooled in an ice bath during the procedure.

- The ozonated water is covered with aluminum foil and is left overnight.

- If ODF water is going to be used after one day, the water is boiled for at least 10 minutes to remove any ozone residual. Otherwise, the bottle can be kept for 2-3 days and the ozone residual is being removed gradually.

- The ODF glass containers is sealed and stored until needed.

A-2-2. Ozone-demand-free glassware preparation:

All the ozonation (and O_3/H_2O_2) experiments must be carried out using the ODF glassware to make sure no ozone is consumed for the removal of glassware contamination. Materials and method are as follows:

Materials:

- ✓ Ozone generator (PCI-Wedeco, Model GLS-7, Water Technology, Herford, Germany)

- ✓ Ultrapure water (resistivity = 18 MΩcm; TOC < 0.1 mg/L) obtained from a Millipore and Elga system equipped with an Elix UV lamp

- ✓ Glassware (pipettes, beakers, volumetric flasks)

- ✓ Oven (Fisher scientific)

Procedure:

- All the glassware such as pipettes, reactors, flasks, bottles, and stir bars are washed with tap water and detergent (Fisher Scientific) (lab dishwasher may be used for cleaning).

- The washed glassware is soaked in ozone saturated water (O_3 concentration 20 mg/L or more) and the container is covered with aluminum foil overnight or for 8 hours.

- The ozonated water then is poured out the next day.

171

- The glassware is dried in oven (100°C) until they it gets dry (around 2 hours).

- All the ODF glassware is capped with aluminum foil until needed (better not to keep ODF glassware for a long time).

A-2-3. Ozone residual determination:

Ozone in the liquid phase is measured using spectrophotometric methods either by direct measurement or by using indigo method.

A-2-3-1. Direct spectrophotometric method

Ozone absorbs light in the UV region at 260 nm. Ozone residual is measured using quartz cuvettes with 10 or 50 mm light path depending on the concentration. The ozone concentration can be estimated by the following equation:

$$[O_3] = \frac{AMU}{k_{260}} \times abs \times l \qquad\qquad (B-1)$$

where AMU is the ozone atomic mass unit (48000 mg/mol), k_{260} is the ozone molar absorption (3300 M^{-1} cm^{-1}), *abs* is absorbance of the solution at 260 nm, and *l* is length of the light passage through the quartz cell (10 mm). The ozone concentration is determined by the mg/L. An easy equation to be used for direct measurement is as follows:

$$[O_3] = 14.5 \times abs \qquad\qquad (B-2)$$

Materials:

✓ Ozone stock solution

✓ Spectrophotometer

✓ 10 mm quartz cuvette

Procedure:

In a 10 mm quartz cell (cuvette), put ozone stock solution and place it in the cell holder and read the absorbance at 260 nm (*abs*). Calculate ozone concentration using equation B-1 or B-2.

A-2-3-2. Indigo method:

The indirect spectrophotometric ozone concentration measurement, indigo method, involves the reaction of ozone with potassium indigo trisulfonate in acidic solution.

Materials:

- ✓ Potassium Indigo trisulfonate ($C_{16}H_7N_2O_{11}S_3K_3$)

- ✓ Sodium dihydrogen phosphate (NaH_2PO_4)

- ✓ Concentrated phosphoric acid (H_3PO_4)

- ✓ ODF water

- ✓ 1-L ODF volumetric flask

- ✓ Two 100-mL ODF volumetric flasks for each ozone measurement

Preparation of indigo stock solution

- Add about 500 mL ODF water and 1 mL concentrated phosphoric acid to 1-L volumetric flask.

- With stirring, add 770 mg potassium indigo trisulfonate to it.

- Fill to mark with ODF water.

173

- Put the stir bar. Cover the flask with aluminum and stir it for about 1 hour.

- Store the indigo stock solution in the dark or covered by aluminum foil.

Note: The indigo stock solution is stable for 4 months or more if kept in the dark.

Preparation of indigo reagent I

To a 1-L volumetric flask, add 20 mL indigo stock solution, 10 g NaH_2PO_4 (or 11.5 g $NaH_2PO_4 \cdot H_2O$), and 7 mL conc. H_3PO_4. Dilute to mark.

Preparation of indigo reagent II

To a 1-L volumetric flask, add 100 mL indigo stock solution, 10 g NaH_2PO_4 (or 11.5 g $NaH_2PO_4 \cdot H_2O$), and 7 mL H_3PO_4. Dilute to mark.

Checking indigo stock solution

- Prepare 1 mL stock indigo solution / 100 mL ODF water.

- Read the absorbance of the solution at 600 nm. The absorbance should be 0.20 ± 0.01 for fresh solution.

- The stock solution should be discarded when absorbance falls below 0.16.

Note: When the absorbance of indigo reagents I and II decreases to less than 80% of its initial value, prepare the fresh solution (this happens typically within two weeks).

Procedure:

a) **Concentration range 0.01 to 0.1 mg O$_3$/L**

➤ Add 10 mL indigo reagent I to each of two 100-mL volumetric flasks.

➤ Blank: fill one flask to mark with ODF water (90 mL ODF water should be added).

➤ Sample: add 1-90 mL of sample, in accordance to the ozone residual concentration, to the 10 mL of reagent I and then use the ODF water to bring the volume up to 100 mL.

➤ Using a 10 mm quartz cuvette, read the absorbance of both solutions at 600 nm.

b) **Concentration range 0.05 to 0.5 mg O$_3$/L**

➤ Add 10 mL indigo reagent II to each of two 100-mL volumetric flasks.

➤ Blank: fill one flask to mark with ODF water (90 mL ODF water should be added).

➤ Sample: add 1-90 mL of sample, in accordance to the ozone residual concentration, to the 10 mL of reagent I and then use the ODF water to bring the volume up to 100 mL.

➤ Using a 50 mm cell, read the absorbance of both solutions at 600 nm.

Note: Wait approximately 10 minutes for colour to be developed before reading the absorbance. However, the absorbance should be read within 4 hours.

c) **Concentration greater than 0.3 mg O$_3$/L**

➢ Proceed using indigo reagent II, but for this higher ozone concentrations use a correspondingly smaller sample volume.

➢ Dilute the mixture to 100 mL with ODF water.

➢ Use 10 mm cell to read the absorbance at 600 nm.

Calculation of ozone concentration:

The ozone concentration can be calculated using the following equation:

$$mg\frac{O_3}{L} = \frac{100 \times \Delta A}{f \times b \times V} \qquad (B-3)$$

In equation B-3, 100 (mL) is the flask volume, ΔA is the difference of absorbance of the blank and the sample (blank absorbance − sample absorbance), f equals 0.42, b (cm) is the path length of the cell, and V (mL) is the sample volume. The factor f is calculated based on a sensitivity factor of 20000/cm for the change of absorbance (600 nm) per mole of added ozone per liter.

Note: Minimum detectable concentration of ozone is 2 µg O$_3$/L (in theory). However, practical lower limit for residual measurement is 10 to 20 µg/L.

A-2-4. Ozonation process in a semi-batch system:

A-2-4-1. Procedure of calibrating the ozone monitor (HC-500 model):

➢ Dissolve 10g KI in 400 mL water, transfer the solution into a 500 mL wash bottle.

➢ Connect an HC-500 ozone monitor to another one in series and by-pass the flow meter.

➢ Connect the wet meter to the effluent of the wash bottle. Connect the monitor to wash bottle influent.

➢ Turn on the ozone generator and adjust the knob of ozone concentration to full.

➢ Wait for 10 min and let the monitora to be stabilized.

➢ Connect the tube between ozone monitor and the wash bottle. Disconnect the connection when roughly 3 L gas passes the wet meter (1 cycle).

➢ While the gas passes the wet meter, record two monitors readings every 5 seconds.

➢ Transfer the solution from the wash bottle into a 500 mL volumetric flask.

➢ Wash the wash bottle several times with water, then transfer the washed solution into the volumetric flask.

➢ Bring the solution in 500 mL flask to the volume with water and mix thoroughly.

➢ Repeat previous steps three times (in total) and change the ozone concentration knob to three different positions in order to produce three volumetric flasks of the solution (This is for having three ozone concentrations in the gas).

➤ transfer 50 mL solution from each volumetric flask to a 100 mL flask, add 2 mL H_2SO_4 (2 M). Titrate this solution with $Na_2S_2O_3$ (0.1 N). Record the volume of $Na_2S_2O_3$ used.

➤ According to the standard method (APHA, 2005), calibrate 0.1 N $Na_2S_2O_3$ solution.

➤ Prepare another solution by adding 1 mL H_2SO_4 (concentrated), 10 mL $KH(IO_3)_2$ (0.10 N) and 1 g KI to 80 mL water. Titrate this solution with Na_2SO_3 (0.1 N). Record the volume used in the titration. Calculate the normality of $Na_2S_2O_3$.

➤ Input the measurements in a Excel speardsheet to deduce the formula for converting the monitor readings into ozone concentration (W/W %). A linear regression is used for the relationship between the monitor readings and real weight percentages.

A-2-4-2. Ozone concentration measurement in a semi-batch system:

The flow rate of the ozone gas was measured by a calibrated flow meter (4 to 20 L/min and 0.5 to 2 L/min). The utilized ozone dose for this system was calculated by using the equation 5-1 (Gamal El-Din and Smith, 2002).

$$\Delta O_3 = \int_0^t \frac{(Q_{G,in} C_{G,in} - Q_{G,out} C_{G,out})}{V_L} \, dt - C_L \qquad (5-1)$$

Where ΔO_3 is the amount of the utilized ozone (mg/L), $C_{G,in}$ is the ozone concentration in the feed gas (mg/L), $C_{G,out}$ is the ozone concentration in the off gas (mg/L), C_L is the residual ozone concentration in the liquid phase (mg/ L), V_L is the effective reactor

volume (L), $Q_{G,in}$ is the feed gas flow rate (L/min), $Q_{G,out}$ is the off gas flow rate (L/min), and t is the ozone contact time (min). After the ozonation, the OSPW was purged by pure nitrogen for 10 min to strip the ozone residual and oxygen from the reactor.

A-3. Analytical techniques

A-3-1. Measurement of extractable organic acids fraction in OSPW using FT-IR:

Materials:

- ✓ OSPW

- ✓ Dichloromethane (DCM - CH_2Cl_2)

- ✓ sulfuric acid (H_2SO_4)

- ✓ Separatory funnels and funnel holder

- ✓ Beakers

- ✓ Laboratory glass tubes

- ✓ FT-IR spectrometer (PerkinElmer: Spectrum 100)

- ✓ 3 mm KBr cell

- ✓ Analytical balance

Extraction procedure:

- Filter 250 mL of NA solution (i.e. OSPW) through 45 µL polyvinylidene fluoride (PVDF) Millipore filter.

- Adjust the pH of the sample to 2 using H_2SO_4.

- Add 125 mL of DCM to the sample and pour the mixture into the separatory funnel.

- Mix the content so well by shaking the separatory funnel. Frequently, open the funnel let all the generated gases go out. Keep mixing for around 1 min.

- Let the mixture settle on a funnel holder for around 4 min.

- At this time all the extractable organic fraction including NAs has been dissolved in organic phase (the phase which is at the bottom of the funnel).

- Open the funnel valve and transfer the organic phase to a beaker.

- Try to avoid entering the aqueous phase to the beaker by closing the valve before reaching the border of organic and aqueous phase.

- Repeat all the above mentioned steps using another 125 mL of DCM to make sure all the extractable fraction of OSPW including NAs extract from solution.

Note 1: The extraction can be performed at once using 250 mL DCM; but it is recommended to do it in two steps for better accuracy.

Note 2: The amount of the solution can be adjusted based on the initial amount of OSPW. For instant if there is only 50 mL of OSPW available for the analysis, the extraction can be performed in a smaller funnel in two steps of adding 25 mL DCM.

- Transfer the beaker's content (i.e. DCM + organic phase) to a lab tube under the fume hood and use an evaporation unit with low flow until DCM is completely dried out. This usually takes overnight.

Analysis procedure:

- Place a beaker on an analytical balance and put the lab tube containing dried sample inside the beaker, then set the balance to zero. Dried samples are dissolved

in about 7.0 g of the organic solvent (DCM) and the exact weight of the solvent added is recorded for the calculation purpose.

- 3 mm KBr cell used for the FT-IR analysis is rinsed with DCM optima before the analysis. FT-IR spectrometer (PerkinElmer: Spectrum 100)

- Run the FT-IR spectrometer and save the chromatogram. EOA quantification is based on the absorbance of wavelengths 1743 and 1706 cm^{-1} for monomer and dimmer carboxylic acids, respectively.

- The actual concentration of the sample is calculated based on the mass of DCM optima and the volume of the original sample.

Safety: Using eye protection, wearing appropriate mask, wearing lab gloves, and working under the fume hood are absolute requirements for working with DCM in the lab.

A-3-2. Measurement of OSPW NA concentration using UPLC/HRMS:

Materials:

- ✓ OSPW

- ✓ tetradecanoic acid-1-^{13}C (internal standard)

- ✓ 10 mM ammonium acetate, Methanol, and acetonitrile (Optima-grade)

- ✓ Waters Acquity UPLC® System

- ✓ HR Synapt G2 HDMS MS equipped with an ESI source

- ✓ Centrifugal device

✓ UPLC Phenyl BEH chromatographic column (1.7 μm, 150 mm × 1 mm)

Analysis procedure:

For analysis of OSPW NAs:

- samples (5 mL) were centrifuged for 10 min at 10,000 RPM and 500 μL of the supernatant was placed in a 2 mL glass vial with 450 μL of methanol and 50 μL of an internal standard solution (tetradecanoic acid-1-^{13}C); final concentration of internal standard was 200 ng/mL.

- A Waters Acquity UPLC® System (Milford, MA, USA) was employed for efficient and rapid chromatographic separation of the NAs and oxidized products.

- Chromatographic separations were run on a Waters UPLC Phenyl BEH column (1.7 μm, 150 mm × 1 mm) using a mobile phase of: A, 10 mM ammonium acetate solution prepared in Optima-grade water, and B, 10 mM ammonium acetate in 50% methanol 50% acetonitrile, both Optima-grade. Gradient elution was as follows: 1% B for the first 2 min, then ramped to 60% B by 3 min, to 70% B by 7 min, to 95% B by 13 min, followed by a hold until 14 min and finally returned to 1% B, followed by a further 5.8 min re-equilibration time. The flow was constant at 100 μL/min and column temperature was kept at 50 °C, while samples were maintained at 4 °C.

- Detection was performed with a high resolution Synapt G2 HDMS mass spectrometer equipped with an electrospray ionization source operating in negative ion mode.

- The system was controlled using MassLynx® ver. 4.1.

- Tuning and calibration were performed using standard solutions of lucine enkaphenlin and sodium formate, respectively, provided by Waters Corporation (Milford, MA, USA).

- TargetLynx® ver. 4.1 was used for data analysis of the target compounds, and the relative ratio of the chromatographic peak area of each analyte to that of the internal standard was calculated for subsequent analysis.

Appendix B: Calculations

B-1. UV calculations

B-1-1. The estimation of photon efficiency:

The light energy of one photon at 253.7 (~ 254) nm is:

$$U = hcN_A / \lambda = (6.6 \times 10^{-34} \text{ J s} \times 2.99 \times 10^8 \text{ m s}^{-1} \times 6.02 \times 10^{23} \text{ mol}^{-1}) / (253.7 \times 10^{-9} \text{ m}) =$$

$$471528 \text{ J mol photon}^{-1}.$$

Where the average irradiance of UV lamp is 0.11 m W cm^{-2}, the incident photon flow on the Petri dish (6 cm diameter) is:

$$N = E \times \text{area} / U_\lambda = (0.11 \times 10^{-3} \text{ W cm}^{-2} \times \pi \times 3^2) / (471528 \text{ J mol photon}^{-1}) =$$

$$6.6 \times 10^9 \text{ mol photon s}^{-1}.$$

For 80 min irradiation time, this photon will be:

$$6.6 \times 10^9 \text{ mol photon s}^{-1} \times 60 \text{ min/s} \times 80 \text{ min} = 3.168 \times 10^{-5} \text{ mol photon}.$$

On the other hand, based on the pseudo-first order rate constants (Table 2-1 in Chapter 2), the mole CHA degraded in 80 min UV exposure time (depending of H_2O_2 concentration) are as follows (calculated based on the 0.078 mM initial CHA concentration):

$$H_2O_2 = 20 \text{ mg/L; } 0.029 \text{ mM CHA was degraded;}$$

$$H_2O_2 = 40 \text{ mg/L; } 0.050 \text{ mM CHA was degraded;}$$

$$H_2O_2 = 60 \text{ mg/L; } 0.065 \text{ mM CHA was degraded;}$$

$$H_2O_2 = 80 \text{ mg/L; } 0.068 \text{ mM CHA was degraded.}$$

Then, mol CHA degraded/mol photon entering depending of H_2O_2 concentration are as follows:

$H_2O_2 = 20$ mg/L; mol CHA degraded/mol photon entering $= 0.92$

$H_2O_2 = 40$ mg/L; mol CHA degraded/mol photon entering $= 1.58$

$H_2O_2 = 60$ mg/L; mol CHA degraded/mol photon entering $= 2.05$

$H_2O_2 = 80$ mg/L; mol CHA degraded/mol photon entering $= 2.15$

B-1-2. UV dose calculations:

To estimate the fluence rate in a UV collimated beam apparatus, several corrections must be made. For monochromatic light, the averaged fluence rate (E'_{avg}) can be estimated by the following equation:

$$E'_{avg} = E_0 \times PF \times RF \times WF \times DF \qquad (A-1)$$

where E_0 is the radiometer reading at the center of the Petri dish, PF is the Petri factor, RF is the reflection factor, WF is the water factor, and DF is the divergence factor.

Reflection factor (RF):

RF accounts for the light incident on the solution that is reflected at the solution/air interface. RF can be estimated by:

$$RF = 1 - \frac{(n_1 - n_2)^2}{(n_1 + n_2)^2} \qquad (A-2)$$

where n_1 and n_2 are the refractive indices of the two media traversed by the light.

Petri factor (PF):

PF accounts for the differences for the radiation field across the Petri dish. PF can be estimated by:

$$PF = \frac{\text{Averaged Incident Irradiance}}{\text{Incident irradiance at the Centre of Petri Dish}} \qquad (A-3)$$

Water factor (WF):

WF accounts for the decrease of the incident irradiance due to the water absorption in the irradiated column. WF can be estimated by:

$$WF = \frac{1 - 10^{-a \times l}}{a \times l \times \ln(10)} \qquad (A-4)$$

where a is the absorption coefficient of the solution (m^{-1}) at the wavelength of irradiation and l is the path length (m).

Divergence factor (DF):

DF accounts for the beam divergence that can be estimated by the following equation:

$$DF = \frac{L}{L + l} \qquad (A-5)$$

where L is the distance from the top of the solution to the UV lamp.

The fluence (H′) in J m^{-2} in a UV collimated beam apparatus is given by:

$$H' = E'_{p\,(avg)} \times RF \times PF \times WF \times DF \times t \qquad (A-6)$$

where $E'_{p\,(avg)}$ is the average photon fluence rate throughout the solution.

B-2. Theoretical second-order rate constant estimations

B-2-1. Anbar et al. (1966) method for rate estimation:

In Anbar et al. (1966) method, the rates are calculated by the summation of the partial specific reactivities of H atoms at different positions in the molecule structure. Based on this method, H atoms at different positions have different reactivities as follows:

- ✓ Each H atom on a primary carbon (CH_3) at α position to the carboxylate group ($CH_3CO_2^-$) reacts with the rate of $0.14 \times 10^8 \ M^{-1} s^{-1}$.

- ✓ Each H atom on a secondary (RCH_2) carbon at α position to the carboxylate group ($RCH_2CO_2^-$) reacts with the rate of $1.75 \times 10^8 \ M^{-1} s^{-1}$.

- ✓ Each H atom on a tertiary (R_2CH) carbon at α position to the carboxylate group ($R_2CHCO_2^-$) reacts with the rate of $5.3 \times 10^8 \ M^{-1} s^{-1}$.

- ✓ Each H atom on a primary carbon in other positions react at $0.36 \times 10^8 \ M^{-1} s^{-1}$

- ✓ Each H atom on a secondary carbon in other positions react at $3.0 \times 10^8 \ M^{-1} s^{-1}$

- ✓ Each H atom on a tertiary carbon in other positions react at $8.4 \times 10^8 \ M^{-1} s^{-1}$

Examples of rate calculation:

For the compounds octanoic acid (OA; $C_8H_{16}O_2$) and 2-methylheptanoic acid (2meHPA; $C_8H_{16}O_2$), the rate is calculated as follows:

OA:

OA structure: CH_3-CH_2-CH_2-CH_2-CH_2-CH_2-CH_2-COOH

- Number of the H atoms at α position to the carboxylate group: 2 secondary atoms; partial reactivity of each of these 2 atoms: $1.75 \times 10^8 \, M^{-1} s^{-1}$.

- Number of H atoms at other positions: 10 secondary atoms and 3 primary atoms; partial reactivity of each of 10 atoms: $3.0 \times 10^8 \, M^{-1} s^{-1}$, and partial reactivity of each of 3 atoms: $0.36 \times 10^8 \, M^{-1} s^{-1}$.

- The overall reactivity of OA based on these partial reactivities:

  $[(2 \times 1.75) + (10 \times 3) + (3 \times 0.36)] \times 10^8 \, M^{-1} s^{-1} = 3.458 \times 10^9 \, M^{-1} s^{-1}$

2meHPA:

2meHPA structure: CH_3- CH_2-CH_2-CH_2-CH_2-CH-COOH

$$|$$
$$CH_3$$

- Number of the H atoms at α position to the carboxylate group: 1 tertiary atom; partial reactivity of this atom: $5.3 \times 10^8 \, M^{-1} s^{-1}$.

- Number of H atoms at other positions: 8 secondary atoms and 6 primary atoms; partial reactivity of each of 8 atoms: $3.0 \times 10^8 \, M^{-1} s^{-1}$, and partial reactivity of each of 6 atoms: $0.36 \times 10^8 \, M^{-1} s^{-1}$.

- The overall reactivity of OA based on these partial reactivities:

  $[(1 \times 5.3) + (8 \times 3) + (6 \times 0.36)] \times 10^8 \, M^{-1} s^{-1} = 3.146 \times 10^9 \, M^{-1} s^{-1}$

The ratio of the reactivity of OA and 2meHPA:

2meHPA/OA = $(3.146 \times 10^9) / (3.458 \times 10^9) = 0.91$

B-2-2. Minakata et al. (2009) method for rate estimation:

In the group contribution method (GCM) of Minakata et al. (2009), the overall reaction rate constants are calculated assuming H-atom abstraction mechanism. In this method, the reactivity of each individual C-H bond depends on the functional groups around it. For example, the presence of COOH, an electron-withdrawing group, decreases the rate of abstraction at the C-H bond α to the COOH group by a factor of 0.043.

In this method, group rate constants (for example Table B-1) and group contribution factors (for example Table B-2) are applied for the rate estimations.

Table B-001. Examples of group rate constants

Group rate constant ($\times 10^{-8}$ M^{-1}s^{-1})	
k^0_{prim}	1.18
k^0_{sec}	5.11
k^0_{tert}	19.9
k_{OH}	1.00
k_{COOH}	0.007

Table B-2. Examples of group contribution factor

Group contribution factor, X	
-CH$_3$	1.120
-CH$_2$, >CH-, >C<	1.174
->C-(oxygenated)-	0.6810
-OH	0.5780
-O-	0.5510
-CO-	0.1540
-CHO	0.6016
=O	0.3600
-COO, -COOH	0.0430

As explained in the Supporting Information of the paper by Minakata et al. (2009), an excel spread sheet has been developed for the rate estimations. In the excel spread sheet, $*k_{overall}$ is estimated by manually inputting group contribution factors and number of functional groups that are accommodated in the molecule of interest. All is needed to do is to put group contribution factors and # of functional groups from the Tables B-1 and B-2 (in case of carboxylic acids). The molecule required to be fragmented based on the group contribution method (GCM) explained in the main paper by Minakata et al. (2009).

Examples of rate calculation:

For the compounds octanoic acid (OA; $C_8H_{16}O_2$) and 2-methylheptanoic acid (2meHPA; $C_8H_{16}O_2$), the rate is calculated as follows:

OA:

OA structure: CH_3-CH_2-CH_2-CH_2-CH_2-CH_2-CH_2-COOH

Table B-3 shows the rate calculations for OA using the GCM and H-atom abstraction mechanism. In the Table B-3, the cells with the light green colour are filled using the data related to the group rate constant (Table B-1), the cells with the light orange colour are filled using the data related to the group contribution factor (Table B-2), and the cells with the light blue colour are filled automatically in the excel spread sheet by the summation of the factors in each section. Finally, the k_{abs}, which is the $k_{overall}$ in this case, is calculated by the summation of the rates in each section. As a result, the rate constant of the OA is $7.44 \times 10^9 \ M^{-1} s^{-1}$.

Table B-3. Rate calculation of OA using H-atom abstraction mechanism in a GCM.

k_{abs} ($k_{overall}$)	7.44E+09					
k^0_{prim}	1.18E+08					
k_{CH3R1}	4.14E+08					
X_{R1}	1.174	0	0	0	0	0
k^0_{sec}	5.11E+08					
$k_{CH2R1R2}$	7.03E+09					
X_{R1}	1.12	1.174	1.174	1.174	1.174	1.174
X_{R2}	1.174	1.174	1.174	1.174	1.174	0.043
k^0_{tert}	1.99E+09					
$k_{CHR1R2R3}$	0.00E+00					
X_{R1}	0	0	0	0	0	0
X_{R2}	0	0	0	0	0	0
X_{R3}	0	0	0	0	0	0
k_{COOH}	7.00E+05					
# of -COOH functional group	1					

2meHPA:

2meHPA structure: CH_3- CH_2-CH_2-CH_2-CH_2-CH-COOH
|
CH_3

Table B-4 shows the rate calculations for 2meHPA using the GCM and H-atom abstraction mechanism. The same procedure is applied in this Table and as a result, the rate constant of the 2meHPA is 6.51×10^9 M^{-1} s^{-1}. The ratio of the reactivity of OA and 2meHPA:

2meHPA/OA = (6.51×10^9) / (7.44×10^9) = 0.87

Table B-4. Rate calculation of 2meHPA using H-atom abstraction mechanism in a GCM.

k_{abs}	6.51E+09			
k^0_{prim}	1.18E+08			
k_{CH3R1}	8.28E+08			
X_{R1}	1.174	1.174	0	0
k^0_{sec}	5.11E+08			
$k_{CH2R1R2}$	5.57E+09			
X_{R1}	1.12	1.174	1.174	1.174
X_{R2}	1.174	1.174	1.174	1.174
k^0_{tert}	1.99E+09			
$k_{CHR1R2R3}$	1.13E+08			
X_{R1}	1.12	0	0	0
X_{R2}	0.043	0	0	0
X_{R3}	1.174	0	0	0
k_{COOH}	7.00E+05			
# of -COOH functional group	1			

Appendix C: Naphthenic Acid Speciation: Tables and Figures

Table C-1. Concentration of NA species in OSPW control sample (OSPW-filtered with 0.45 μm nylon filter as a function of the carbon number (*n*) and the cyclicity (-*Z*).

n	-Z=0	-Z=2	-Z=4	-Z=6	-Z=8	-Z=10	-Z=12
8	0	0	0	0	0	0	0
9	0	0.009	0.022	0	0	0	0
10	0	0	0.068	0	0	0	0
11	0	0	0.239	0	0	0	0
12	0	0	1.005	0	0	0	0
13	0	0.173	2.514	1.396	0.073	0	0
14	0	0.069	3.16	2.233	0.298	0	0
15	0	0	2.081	2.844	0.069	0.35	0
16	0	0	0.849	1.766	0.822	0.621	0
17	0	0	0.171	0.517	0.491	0.74	1.463
18	0	0	0	0.128	0.204	0.523	1.287
19	0	0	0	0.039	0.059	0.226	0.696
20	0	0	0	0	0.011	0.081	0.128
21	0	0	0	0	0	0.017	0
22	0	0	0	0	0	0	0.019
sum	27.461	mg/L					

Table C-2. Concentration of NA species in OSPW + UV(5 min)/H_2O_2 (250 mg/L) as a function of the carbon number (*n*) and the cyclicity (-*Z*).

n	-Z=0	-Z=2	-Z=4	-Z=6	-Z=8	-Z=10	-Z=12
9	0	0.011	0.025	0	0	0	0
10	0	0	0.06	0	0	0	0
11	0	0	0.199	0.008	0	0	0
12	0	0	0.781	0	0	0	0
13	0	0.083	2.076	1.096	0.074	0	0
14	0	0	2.519	1.696	0.228	0	0
15	0	0	1.555	2.124	0	0.288	0
16	0	0	0.609	1.373	0.586	0.47	0
17	0	0	0.124	0.4	0.366	0.545	0.996
18	0	0	0	0.089	0.148	0.363	0.937
19	0	0	0	0.028	0.034	0.187	0.497
20	0	0	0	0	0.006	0.049	0.027
21	0	0	0	0	0	0.014	0
22	0	0	0	0	0	0	0.015
sum	20.686	mg/L					

Table C-3. Concentration of NA species in OSPW + UV(10 min)/H_2O_2 (250 mg/L) as a function of the carbon number (n) and the cyclicity (-Z).

n	-Z=0	-Z=2	-Z=4	-Z=6	-Z=8	-Z=10	-Z=12
9	0	0.002	0.025	0	0	0	0
10	0	0	0.056	0	0	0	0
11	0	0	0.175	0.049	0	0	0
12	0	0	0.61	0	0	0	0
13	0	0.063	1.787	0.911	0.05	0	0
14	0	0	2.118	1.302	0.2	0	0
15	0	0	1.306	1.82	0	0.241	0
16	0	0	0.529	1.149	0.495	0.387	0
17	0	0	0.099	0.321	0.3	0.46	0.858
18	0	0	0	0.065	0.127	0.319	0.793
19	0	0	0	0.022	0.03	0.128	0.416
20	0	0	0	0	0.005	0.033	0
21	0	0	0	0	0	0.013	0
22	0	0	0	0	0	0	0.012
sum	17.276	mg/L					

Table C-4. Concentration of NA species in OSPW + UV(20 min)/H_2O_2 (250 mg/L) as a function of the carbon number (n) and the cyclicity (-Z).

n	-Z=0	-Z=2	-Z=4	-Z=6	-Z=8	-Z=10	-Z=12
8	0	0	0	0	0	0	0
9	0	0.006	0.023	0	0	0	0
10	0	0	0.046	0	0	0	0
11	0	0	0.134	0.065	0	0	0
12	0	0	0.4	0	0	0	0
13	0	0	1.348	0.681	0.048	0	0
14	0	0	1.551	0.849	0.145	0	0
15	0	0	0.959	1.276	0	0.172	0
16	0	0	0.375	0.829	0.339	0.294	0
17	0	0	0.065	0.218	0.214	0.334	0.615
18	0	0	0	0.035	0.088	0.24	0.538
19	0	0	0	0.014	0.019	0.107	0.289
20	0	0	0	0	0.007	0.027	0
21	0	0	0	0	0	0.006	0
sum	12.371	mg/L					

Table C-5. Concentration of NA species in OSPW + UV(30 min)/H_2O_2 (250 mg/L) as a function of the carbon number (n) and the cyclicity (-Z).

n	-Z=0	-Z=2	-Z=4	-Z=6	-Z=8	-Z=10	-Z=12
9	0	0.011	0.029	0	0	0	0
10	0	0	0.05	0	0	0	0
11	0	0	0.107	0.053	0	0	0
12	0	0	0.4	0	0	0	0
13	0	0	1.348	0.529	0.032	0	0
14	0	0	1.551	0.634	0.132	0	0
15	0	0	0.959	0.984	0	0.141	0
16	0	0	0.375	0.669	0.277	0.239	0
17	0	0	0.055	0.126	0.197	0.253	0.431
18	0	0	0	0.036	0.065	0.183	0.405
19	0	0	0	0.011	0.016	0.077	0.226
20	0	0	0	0	0.002	0.009	0
21	0	0	0	0	0	0.008	0
22	0	0	0	0	0	0	0.006

sum   10.628   mg/L

Table C-6. Concentration of NA species in OSPW + UV(30 min)/H_2O_2 (250 mg/L) as a function of the carbon number (n) and the cyclicity (-Z).

n	-Z=0	-Z=2	-Z=4	-Z=6	-Z=8	-Z=10	-Z=12
9	0	0	0.026	0	0	0	0
10	0	0	0.038	0	0	0	0
11	0	0	0.07	0.053	0	0	0
12	0	0	0.075	0	0	0	0
13	0	0	0.655	0.318	0.001	0	0
14	0	0	0.755	0.184	0.069	0	0
15	0	0	0.462	0.579	0	0.094	0
16	0	0	0.145	0.414	0.137	0.134	0
17	0	0	0.03	0.066	0.116	0.145	0.248
18	0	0	0	0.008	0.039	0.113	0.239
19	0	0	0	0.005	0	0.052	0.119
20	0	0	0	0	0	0.002	0
21	0	0	0	0	0	0.002	0
22	0	0	0	0	0	0	0.004

sum   5.397   mg/L

Table C-7. Concentration of NA species in OSPW + UV(40 min)/H_2O_2 (250 mg/L) as a function of the carbon number (n) and the cyclicity (-Z).

n	-Z=0	-Z=2	-Z=4	-Z=6	-Z=8	-Z=10	-Z=12
7	0	0.001	0	0	0	0	0
8	0	0	0	0	0	0	0
9	0	0.008	0.029	0	0	0	0
10	0	0	0.04	0	0	0	0
11	0	0	0.003	0.051	0	0	0
12	0	0	0	0	0	0	0
13	0	0	0.349	0.119	0	0	0
14	0	0	0.379	0	0.021	0	0
15	0	0	0.206	0.19	0	0.035	0
16	0	0	0.039	0.191	0.048	0.064	0
17	0	0	0	0	0.056	0.063	0.099
18	0	0	0	0	0.003	0.056	0.088
19	0	0	0	0.004	0	0.02	0.058
20	0	0	0	0	0	0	0
21	0	0	0	0	0	0	0
22	0	0	0	0	0	0	0.001
sum	2.221	mg/L					

Table C-8. Concentration of NA species in OSPW + UV(60 min)/H_2O_2 (250 mg/L) as a function of the carbon number (n) and the cyclicity (-Z).

n	-Z=0	-Z=2	-Z=4	-Z=6	-Z=8	-Z=10	-Z=12
9	0	0	0.022	0	0	0	0
10	0	0	0.027	0	0	0	0
11	0	0	0	0.035	0	0	0
12	0	0	0	0	0	0	0
13	0	0	0.095	0	0	0	0
14	0	0	0.102	0	0	0	0
15	0	0	0.076	0	0	0	0
16	0	0	0	0.059	0	0.019	0
17	0	0	0	0	0.012	0.022	0.017
18	0	0	0	0	0	0.022	0.031
19	0	0	0	0	0	0.004	0.012
20	0	0	0	0	0	0	0
21	0	0	0	0	0	0	0
22	0	0	0	0	0	0	0
sum	0.555	mg/L					
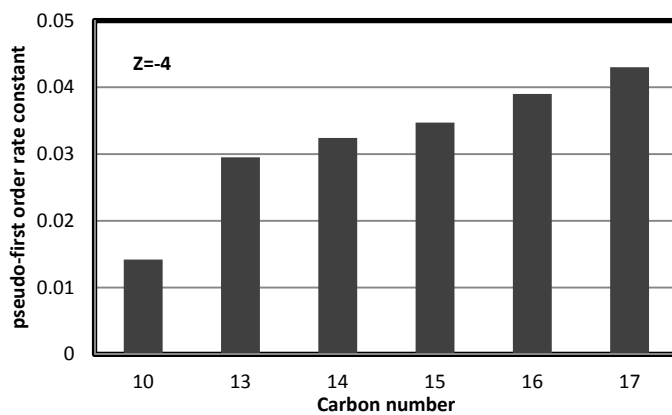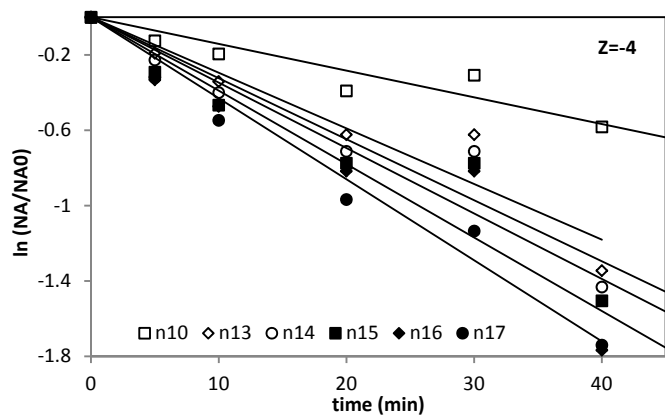
Figure C-1. Pseudo-first order kinetics of the OSPW in UV/H$_2$O$_2$ process for the NAs with Z=-4
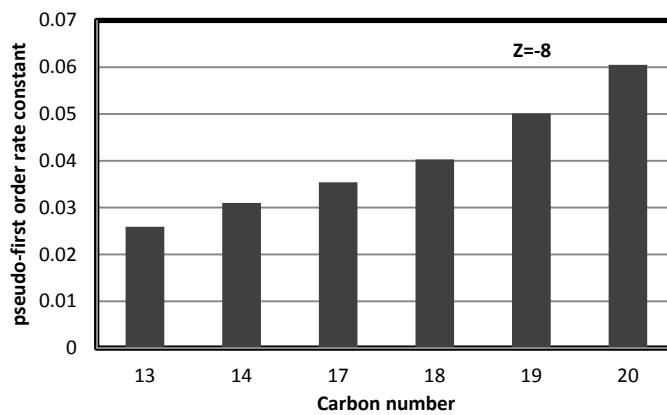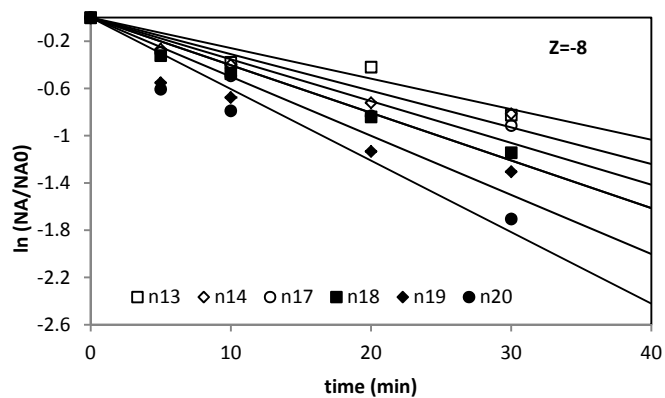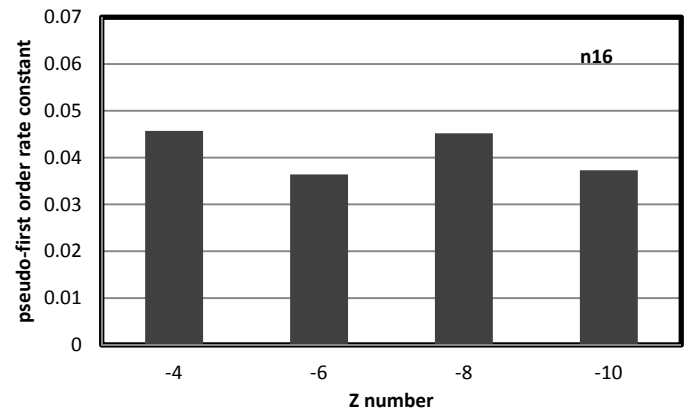

Figure C-2. Pseudo-first order kinetics of the OSPW in UV/H$_2$O$_2$ process for the NAs with Z=-8
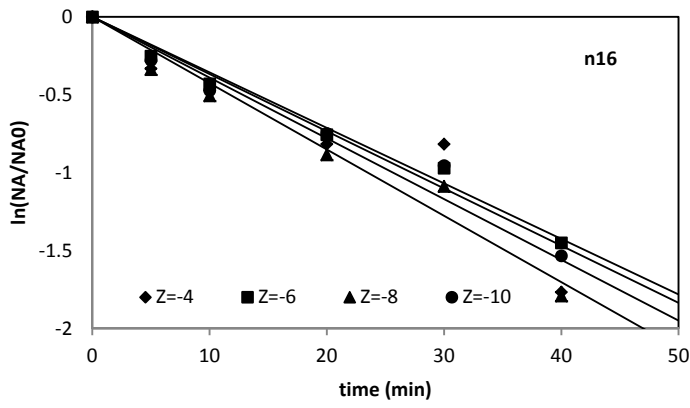
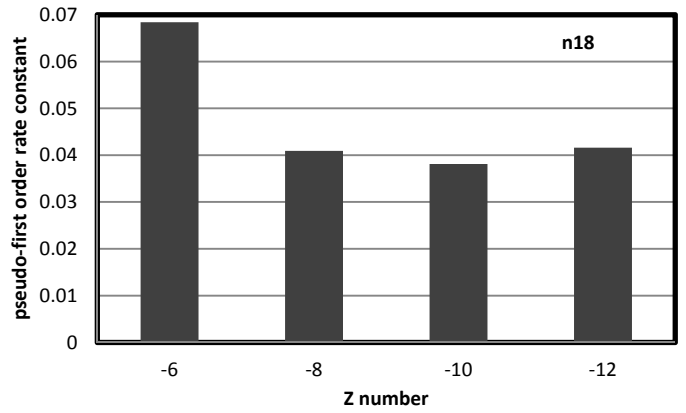**Figure C-3.** Pseudo-first order kinetics of the OSPW in UV/H$_2$O$_2$ process for the NAs with n=16
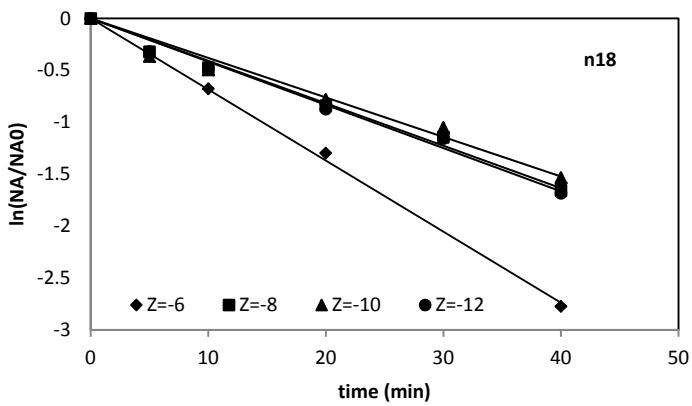
Figure C-4. Pseudo-first order kinetics of the OSPW in UV/H$_2$O$_2$ process for the NAs with n=18

203

Title:	Decomposition of cyclohexanoic acid by the UV/H2O2process under various conditions
Author:	Atefeh Afzal,Przemysław Drzewicz,Jonathan W. Martin,Mohamed Gamal El-Din
Publication:	Science of The Total Environment
Publisher:	Elsevier
Date:	1 June 2012
	Copyright © 2012, Elsevier

License Number	3083821056632
License date	Feb 07, 2013
Licensed content publisher	Elsevier
Licensed content publication	Science of The Total Environment
Licensed content title	Decomposition of cyclohexanoic acid by the UV/H2O2process under various conditions
Licensed content author	Atefeh Afzal,Przemysław Drzewicz,Jonathan W. Martin,Mohamed Gamal El-Din
Licensed content date	1 June 2012
Licensed content volume number	426
Number of pages	6
Type of Use	reuse in a thesis/dissertation
Portion	full article
Format	electronic
Are you the author of this Elsevier article?	Yes
Will you be translating?	No
Order reference number	
Title of your thesis/dissertation	Application of Advanced Oxidation Processes for Treatment of Naphthenic Acids in Oil Sands Process Water
Expected completion date	Mar 2013
Estimated size (number of pages)	210
Elsevier VAT number	GB 494 6272 12
Permissions price	0.00 USD
VAT/Local Sales Tax	0.00 USD
Total	0.00 USD

)

205